NOCTURNIN REGULATES METABOLIC FLUX THROUGH MAINTENANCE OF POLY(A) TAIL LENGTH DYNAMICS

APPROVED BY SUPERVISORY COMMITTEE

_____
Carla, Green, Ph.D.

_____
Joel, Elmquist, Ph.D., DVM

_____
David, Mangelsdorf, Ph.D.

_____
Joseph, Takahashi, Ph.D.

Dedication

This dissertation and the physical and mental effort necessary for its completion are dedicated to my family, specifically Tom, Virginia and Nathaniel. Without their continual support and encouragement this work would not have been possible.

NOCTURNIN REGULATES METABOLIC FLUX THROUGH MAINTENANCE OF POLY(A) TAIL LENGTH DYNAMICS

JEREMY JOSEPH STUBBLEFIELD

DISSERTATION / THESIS

Presented to the Faculty of the Graduate School of Biomedical Sciences

The University of Texas Southwestern Medical Center at Dallas

In Partial Fulfillment of the Requirements

For the Degree of

DOCTOR OF PHILOSOPHY

The University of Texas Southwestern Medical Center at Dallas

Dallas, TX

August, 2016

NOCTURNIN REGULATES METABOLIC FLUX THROUGH MAINTENANCE OF POLY(A) TAIL LENGTH DYNAMICS

JEREMY JOSEPH STUBBLEFIELD, Ph.D.

The University of Texas Southwestern Medical Center at Dallas, August 2016

CARLA BETH GREEN, Ph.D.

Abstract: Cyclic processes in both behavior and physiology are aligned to the external environment through the circadian clock. *Nocturnin* (*Noc*) is a rhythmically expressed gene regulated in part by the circadian clock and intimately linked to the metabolic state of an organism. Loss of *Nocturnin* ($Noc^{-/-}$) in mice results in resistance to diet-induced obesity. Encoding a deadenylase, NOC protein is thought to regulate mRNA turnover through its ability to remove Poly(A) tails from mRNA transcripts. Though NOC has been linked with lipid and glucose metabolism, its specific targets have not been identified. I explored NOC's role in metabolism by exposing Wildtype (WT) and $Noc^{-/-}$ mice to nutrient challenges consisting of High Fat Diet (HFD) and fasting/refeeding. I demonstrated that *Noc* can be acutely reduced with a fast and induced with refeeding in WT mice. Hepatic *Noc* expression oscillates in WT mice fed a High Fat Diet (HFD) but with increased amplitude. I performed mRNA-seq from livers of Wildtype (WT) and $Noc^{-/-}$ mice and identified significant upregulation of both cholesterol and bile acid synthesis genes in $Noc^{-/-}$ mice under basal and nutrient-challenged conditions. This dysregulation results in $Noc^{-/-}$ mice having significantly increased gallbladder volumes during times of fasting. I subjected WT and $Noc^{-/-}$ to hyperinsulinemic-euglycemic clamps and found that HFD-fed $Noc^{-/-}$ mice develop more severe insulin resistance than HFD-fed WT mice. Under

insulin-stimulated (clamped) conditions, HFD-fed *Noc*$^{-/-}$ mice fail to suppress endogenous glucose production and have reduced whole-body glucose turnover. Additionally, regular chow (RC) fed *Noc*$^{-/-}$ mice exhibit insulin resistance only during the dark phase. This deficit in glucose/insulin sensitivity can be partially rescued in *Noc*$^{-/-}$ mice through transgenic overexpression of WT NOC, but not a catalytically dead mutant NOC that cannot function as a deadenylase. The deadenylase activity of NOC is thus important for these metabolic phenotypes and I found that genes associated with bile acid, cholesterol and glucose metabolism have altered Poly(A) tail length regulation in *Noc*$^{-/-}$ mice and thus represent possible targets of NOC. This new understanding of the relationship between *Nocturnin*, the circadian system and metabolism will help guide the treatment of conditions such as obesity and diabetes.

Table of Contents

Prior Publications

1. **Stubblefield, JJ** and Green, CB. (2016*)* Mammalian Circadian Clocks and Metabolism: Navigating Nutritional Challenges in a Rhythmic World. In: Gumz, M (ed) Recent Advances in Physiology: Role of the Circadian Clock in Health and Disease. **The American Physiological Society and Springer**. ISBN 978-1-4939-3450-8 (ebook); 978-1-4939-3448-5 (hardcover)

2. Sephton, CF, Tang, AA, Kulkarni, A, West, J, Brooks, M, **Stubblefield, JJ**, Liu, Y, Zhang, MQ, Green, CB, Huber, KM, Huang, EJ, Herz, J, Yu and Yu, G. (2014). Activity-dependent FUS dysregulation disrupts synaptic homeostasis. **PNAS**. 111(44):E4769-78.

3. Yu, X, Rollins, D, Ruhn, KA, **Stubblefield, JJ**, Green, CB, Kashiwada, M, Rothman, PB, Takahashi, JS and Hooper, LV. (2013). T_H17 Cell Differentiation Is Regulated by the Circadian Clock. **Science**. 342(6159), 727-730.

4. **Stubblefield, JJ**, Terrien, J and Green, CB. (2012). Nocturnin: at the crossroads of clocks and metabolism. **Trends Endocrinol Metab**. 23(7), 326-333.

5. Mickman, CT, **Stubblefield, JJ**, Harrington, ME and Nelson, DE. (2008). Photoperiod alters phase difference between activity onset in vivo and mPer2::luc peak in vitro. **Am J Physiol Regul Integr Comp Physiol**. 295(5), R1688-R1694.

List of Figures

Chapter/Figure (continued) **Page**

Chapter I: Introduction

(Portions of this introduction appear in 1. Stubblefield, JJ and Green, CB. 2016. APS and Springer. ISBN 978-1-4939-3450-8 (ebook); 978-1-4939-3448-5 (hardcover) and 2. Stubblefield, JJ et al. 2012. Trends Endocrinol Metab.

Nocturnin: At the Crossroads of Clocks and Metabolism

The Circadian Clock

The daily environment presents organisms with a constant flux of energetic challenges. Navigating these challenges and efficiently utilizing energy both in times of activity and rest is vital to an organism's survival. Meal timing is of utmost importance in nearly every form of life; so too is the type of food being consumed. Coordinating internal processes with the external environment may seem challenging, but fortunately, most organisms have developed an internal timekeeping system that helps synchronize the energetic needs of their various organ systems.

The internal clock is known as the *circadian system* due to the near 24h rhythmicity of its own cycling as well as most of the processes that it governs. Behavioral processes such as sleep/wake cycles and feeding are under circadian control. Physiological processes such as body temperature, blood pressure and nutrient metabolism also occur with a daily rhythmicity. These 24h rhythms are generated by a molecular oscillator consisting of a series of interlocked transcription/translation feedback loops whereby certain core "clock" genes are transcribed and their protein products build up and inhibit their own transcription (reviewed in (Ko and Takahashi, 2006)). These core rhythms are self-sustained, cell-autonomous, and take approximately 24h to complete, thus making them circadian (about a day).

In mammals, this molecular oscillator exists in nearly every tissue of the body including liver, pancreas, muscle and lung (Yamazaki et al., 2000, Yoo et al., 2004, Marcheva et al., 2010). The diversity of tissues and organ systems requires some form of synchronization to maintain

coordinated rhythmicity. Synchronization is achieved in large part due to the hypothalamic Suprachiasmatic Nucleus (SCN). Located immediately dorsal to the crossing of the optic nerves at the optic chiasm, the SCN is a bi-nucleated structure whose cells receive direct light information via the retinohypothalamic tract (reviewed in (Mohawk and Takahashi, 2011). Within the SCN, this light information is the primary *Zeitgeber* (time-giver) serving as an entraining agent to coordinate molecular oscillations with the external light:dark (LD) cycle through induction of immediate early genes, including *Period* 1 (*Per1*) and *Per2*, core components of the clock (reviewed in (Reppert and Weaver, 2002)). *Per* feeds into and is part of the core mechanism that generates 24h rhythms. Within the core oscillator the transcription of *Per* genes (*Per1*, *Per2*, *Per3*) and *Cryptochrome genes* (*Cry1 and Cry2*) occurs via binding of the CLOCK:BMAL1 protein heterodimer to E-box enhancer elements of these genes. NPAS2 is a functional homologue of CLOCK and also regulates transcription by interacting with BMAL1. PER and CRY protein products then accumulate in the cytoplasm as PER:CRY complexes that translocate back into the nucleus and repress the activity of the CLOCK:BMAL1 heterodimer, thus inhibiting their own transcription (Figure 1). Timed PER and CRY protein degradation also contributes to the 24h molecular rhythm generation (reviewed in (Mohawk et al., 2012)). CLOCK:BMAL1 also induces *Rev-erb* (α and β) and *ROR* (α and ɣ) gene expression as part of an interlocking feedback loop that increases the robustness of the core clock machinery. The REV-ERB proteins inhibit, whereas RORα/ɣ induce expression of *Bmal1* (Preitner et al., 2002, Sato et al., 2004, Akashi and Takumi, 2005).

These molecular oscillations within the SCN are vital to rhythmic behavior, as animals with an SCN lesion have arrhythmic sleep, activity and feeding (reviewed in (Moore, 2013)).

The SCN is thus referred to as the "master pacemaker" within mammals, though the core clock machinery exists in peripheral tissues as well. The CLOCK:BMAL heterodimer, in addition to driving the core clock feedback loop, also regulates expression of thousands of genes, many of those involved in metabolism. Thus, the components of this "core" oscillator do not operate independently of the cellular environment in which they reside. In addition to light and body temperature, they receive inputs from molecules such as hormones, nuclear receptors and nutritional metabolites. These metabolic inputs help shape the resulting rhythms and oscillations. Nutritional challenges impacting the energetic state of an organism are important to study as they provide metabolic input that helps shape molecular rhythms in peripheral tissues.

My graduate studies have focused on a part of the clock output involving the gene *Nocturnin* (*Noc*, official gene symbol *Noct*). The circadian clock employs a variety of mechanisms for the regulation of metabolism in peripheral tissues. Rhythms in posttranscriptional gene regulation are emerging as an important regulatory layer for the circadian clock and metabolism (Kojima et al., 2012). As will be described in the following text and chapters, *Noc* encodes the protein NOCTURNIN (NOC) which acts as a deadenylase and regulates mRNA stability through the posttranscriptional regulation of Poly(A) tail length. *Noc* expression is controlled in part by the circadian clock, but it can also be influenced by the nutrient status of an organism. My work has revealed a temporal mechanism in which NOC is necessary for proper metabolic responses to nutrient (diet, metabolite) challenges.

Nocturnin is a circadian deadenylase

At a time when little was known of the components comprising the vertebrate circadian clock, *Noc* was discovered using a differential display screen in a search for cycling transcripts in retinal photoreceptors of *Xenopus laevis* (Green et al., 1996, Green and Besharse, 1996). *Noc* mRNA displays high amplitude, rhythmic expression in isolated *Xenopus* eye cups in cyclic light (light:dark) and constant (light:light or dark:dark) conditions (Green and Besharse, 1996). Significant sequence similarity is found between *Noc* and the yeast transcription factor *Carbon catabolite repressor 4* (*yCCR4*) and thus its official gene name was originally *carbon-catabolite repressor 4-like* (*Ccrn4l*) but was recently changed to *Noct* (Green and Besharse, 1996, Garbarino-Pico et al., 2007). yCCR4 is a multifunctional protein that is part of large transcriptional complexes in yeast, and has deadenylase activity confined to its C-terminal domain. *Nocturnin* lacks the N-terminal activation domains and leucine-rich repeat region necessary for yCCR4's interaction with transcription complexes (Green and Besharse, 1996). However, conserved in the *Noc* sequence is a C-terminal Mg^{2+}-dependent endonuclease-like domain, which was found in yCCR4 to be required for proper Poly(A)-specific mRNA degradation, implicating it as a functional deadenylase (Dupressoir et al., 2001). Deadenylation is one type of post-transcriptional modification occurring with mRNA transcripts whereby their 3' Poly(A) tails are removed, thus destabilizing the transcript and leading to its degradation or silencing. The ability of Nocturnin to function as a deadenylase and remove 3' adenosine residues from mRNA transcripts was confirmed in cell-based assays both with *Xenopus* (xNOC) and mouse (mNOC) Nocturnin protein (Baggs and Green, 2003, Garbarino-Pico et al., 2007).

While first discovered in *Xenopus*, *Noc* homologues were found in other species with a high degree of similarity in coding sequence. *xNoc* is 66% identical to human *Noc* (*hNoc*) and 65% identical to *mNoc* (Wang et al., 2001). *Noc* mRNA levels are highly rhythmic with peak amplitude occurring in the early evening, both in *Xenopus* and mouse (Green and Besharse, 1996, Wang et al., 2001). In mouse, *Noc* is expressed rhythmically in almost every tissue but with a particularly high amplitude rhythm in the liver (Wang et al., 2001). In Huh7 cells, a human hepatoma cell line, luciferase assays demonstrated that *Noc* is transcriptionally regulated by the CLOCK/BMAL1 heterodimer (Li et al., 2008). Li and colleagues also found that *Noc* has E-boxes upstream of its transcription start site and chromatin immunoprecipitation (ChIP) revealed direct binding of the CLOCK/BMAL1 heterodimer to these sequences (Li et al., 2008). The rhythmic profile of *Noc* is regulated by additional mechanisms beyond CLOCK/BMAL1 transcription. For example, recent evidence has demonstrated an important role for the liver-specific microRNA (miRNA) miR-122 in the proper shaping of rhythmic *Noc* expression (Kojima et al., 2010).

Noc is not critical for rhythm generation by the core clock, as mice deficient for *Nocturnin* ($Noc^{-/-}$) do not have overt circadian phenotypes (Green et al., 2007). More importantly, *Nocturnin's* circadian profile remains rhythmic in $Clock^{\Delta 19}$ animals, though with damped amplitude, suggesting that other signals or factors also exert control over *Noc's* expression (Oishi et al., 2003). Similarly, Kornmann and colleagues utilized transgenic mice in which the liver clock could be conditionally inactivated while the remainder of the clocks throughout the body remained unaffected. In these animals lacking a local liver clock, *Nocturnin* was among a small group of genes that remained rhythmic in the liver (Kornmann et al., 2007).

This further supports a role for systemic cues, potentially those arising from feeding and nutrient metabolism, in effecting *Noc* expression. Although NOC is not directly involved in regulating core clock gene expression, it does have functions in mediating its rhythmic output. Because many of the rate-limiting enzymes in metabolic reactions are under circadian control, gene expression must be tightly controlled and post-transcriptional mechanisms such as deadenylation play an important part in this process (Garbarino-Pico and Green, 2007, Sahar and Sassone-Corsi, 2012, Kojima et al., 2012). NOC, as a *circadian* deadenylase, is poised to play an important role in post-transcriptional regulation of metabolic genes under circadian control (Garbarino-Pico and Green, 2007).

Noc$^{-/-}$ mice are resistant to diet-induced obesity (DIO) and hepatic steatosis

As previously mentioned, *Noc* is expressed rhythmically throughout the body, including many tissues vital for metabolism, such as intestine and liver (Dupressoir et al., 1999, Wang et al., 2001, Douris et al., 2011). *Noc*$^{-/-}$ mice exhibit several metabolic phenotypes when challenged with a High Fat Diet (HFD) (Green et al., 2007), with the pronounced phenotype being that *Noc*$^{-/-}$ mice remain lean compared to their wildtype (WT) littermates. This "leanness" manifests itself peripherally, and a reduction in epididymal fat pad weight and hepatic lipid accumulation is observed (Green et al., 2007). However, these mice are not more active and do not consume less food than WT littermates. Additionally, their oxygen and carbon dioxide production/consumption is not altered and the *Noc*$^{-/-}$ mice exhibit a lower body temperature. Interestingly, their respiratory exchange ratio is slightly elevated, indicative of an altered utilization of lipid as an energy source. Hepatic expression levels of several genes associated

with lipid metabolism is significantly lower in *Noc*$^{-/-}$ mice. If NOC acts on these lipid-associated transcripts directly, one expectation would be that these transcripts are more stable in the absence of deadenylation, potentially leading to higher levels. However, the opposite is observed suggesting that NOC may be acting indirectly on other targets that in turn mediate the expression of these genes, or that it may have deadenylase-independent functions. This is a major mechanistic question that when answered will help in understanding the lean phenotype of *Noc*$^{-/-}$ mice and the role NOC plays in lipid metabolism. The ubiquitous expression of *Nocturnin* also confounds the interpretation of where NOC is acting and whether it has tissue-specific functions.

Noc responds acutely to external stimuli

Noc is unique among deadenylases in that it is an immediate early gene and responds to various stimuli such as the phorbol ester 12-O-tetradecanoylphorbol-13-acetate TPA and serum in cell culture (Garbarino-Pico et al., 2007). Given that TPA and serum are known factors capable of synchronizing clocks in cultured fibroblasts (Balsalobre et al., 1998, Tsuchiya et al., 2003), these results show that Nocturnin can be acutely regulated by physiological cues, thus suggesting that it plays a role in regulating responses to external signals in addition to its circadian role. In normal *ad libitum* (*ad lib*) feeding conditions, *Noc* expression peaks in the early evening in the small intestine (Douris et al., 2011), consistent with other tissues examined. This peak occurs concomitantly with peak food intake by mice. However, a daytime bolus of lipid given at a time when *Noc* expression is normally low and only modest quantities of food are consumed, acutely upregulates *Nocturnin* in the small intestine (Douris et al., 2011). This may reflect a role for NOC in the processing of lipid at this abnormal time of consumption.

Alignment of *Noc* expression with food intake, as well as its acute responsiveness to various stimuli including lipid, supports the idea that NOC might function to regulate nutrient metabolism, i.e. ingestion, trafficking and distribution of nutrients, with possible specificity for lipids.

Nutrient excess is linked with obesity through the development of increasing intracellular and systemic lipid products such as free fatty acids (FFA) and diacylglycerol (DAG) (Prentki and Madiraju, 2008). This results in a need to process and store these extra metabolites, and expansion of adipose tissue is one mechanism facilitating lipid storage, and seen with increasing lipid intake. Kawai and colleagues found that *Noc* is highly upregulated in 3T3-L1 cells undergoing adipogenesis (Kawai et al., 2010a, Kawai et al., 2010b), and similarly, mice chronically exposed to a HFD exhibit increased expression of *Noc* in epididymal white adipose tissue (eWAT) (Massiera et al., 2010b). Under *ad lib* feeding conditions on a standard chow diet *Noc* expression is not rhythmic in eWAT (Gilbert et al., 2011). However, when access to food is restricted to a narrow window during the daytime, *Noc* expression in eWAT becomes rhythmic, and fasting animals following this restricted feeding paradigm significantly induces *Noc* expression in eWAT (Gilbert et al., 2011). Coordination of *Noc* expression with the time of food intake implies a critical role for NOC in the regulation of metabolism.

Animals maintain metabolic homeostasis when fasted, in part, through upregulation of gluconeogenesis and mobilization of glucose, both of which help preserve proper blood glucose levels and prevent hypoglycemia. One of the key players involved in activation of gluconeogenic genes during fasting is the forkhead box (FoxO) family of transcription factors (Altarejos and Montminy, 2011). Paik *et al.* found that *Nocturnin* is one of the most highly downregulated

genes in liver endothelial cells from a *FoxO 1/3/4* conditional knockout mouse model (Paik et al., 2007). Knockdown of the *FoxOs* via shRNA also significantly reduces expression of *Nocturnin*. The *Noc* gene sequence was found to have conserved FoxO binding elements and FoxO binding to these sites has been confirmed by ChIP (Paik et al., 2007). While these findings demonstrate that *Noc* expression levels in the endothelium are affected by FoxO, the overall rhythmicity of mRNA and protein both here and in other tissues still needs to be assessed. When animals end their fast, they must likewise shut down gluconeogenesis and peripheral tissues such as liver and muscle take up glucose for utilization and storage (Samuel et al., 2010). Kubota and colleagues found that impairment of insulin signaling in endothelial cells is associated with reduced glucose uptake in skeletal muscle of mice (Kubota et al., 2011). With loss of *FoxO* in hepatic endothelial cells affecting *Noc* expression levels, NOC may play a role in regulating the metabolic response to the fed/fasting states. $Noc^{-/-}$ mice given a bolus of glucose, following an overnight fast during a glucose tolerance test, show significantly higher blood glucose values compared to WT littermates and they take longer to return to baseline levels (Green et al., 2007). This indicates a possible deficit in the processing of glucose levels in $Noc^{-/-}$ mice. Taken together, these findings imply a role for NOC in glucose/insulin signaling, an area that needs further study.

Diabetes, Obesity and the Clock

Diabetes is on the rise worldwide and so too are increasing levels of obesity (Chen et al., 2012). While genetic factors certainly contribute to these conditions, increasing evidence for their development through lifestyle and dietary choices leads one to consider the interesting

juxtaposition of the circadian clock with metabolism. Jet-lag and shift work present interesting cases in which energy intake in the form of feeding become misaligned or occur at inconsistent times in relation to the body's internal clock. The increased consumption of high calorie "western" diets also has links with circadian disruption.

The importance of proper alignment of metabolic processes has been demonstrated through studies of several clock mutant mice (Turek et al., 2005, Rudic et al., 2004, Lamia et al., 2008). The *Clock*$^{\Delta 19}$ mutant mouse produces a truncated form of the CLOCK protein that can dimerize with its partner BMAL1 and bind to E-boxes, but cannot activate transcription and thus acts in a dominant-negative fashion. The *Clock*$^{\Delta 19}$ mouse gains significantly more weight than wildtypes when fed a Regular Chow (RC) diet and becomes significantly more obese than wildtype (WT) littermates when fed a HFD (Turek et al., 2005). The increase in body weight on a RC diet is a result of increased energy intake and increased fat mass. Feeding patterns in these mice are altered such that they decrease their evening food intake while increasing the amount consumed during the day. Additionally, these animals have several risk factors associated with the metabolic syndrome including elevated serum levels of glucose, triglyceride, cholesterol and leptin.

PER2 also has important effects on adiposity in mice. Adult mice with a targeted disruption of the *Per2* gene (Bae et al., 2001) were found to have significantly lower body weight under regular chow conditions that resulted from decreased epididymal white adipose tissue (eWAT) weight and lower total fat mass in whole-body composition analysis (Grimaldi et al., 2010). A critical role for PER2 in adipose tissue was found in this study through interaction between PER2 and the lipid sensor and transcriptional regulator peroxisome proliferator-

activated receptor ɣ2 (PPARɣ2). PPARɣ2 belongs to the PPAR family of nuclear receptors and is a master regulator of lipid metabolism (Tontonoz and Spiegelman, 2008). PER2 was found to inhibit PPARɣ2-dependent transcription of key metabolic genes and this resulted in increased adipogenesis in vitro, but enhanced fat oxidation in vivo (Grimaldi et al., 2010). The interaction of PER2 with PPARɣ2 occurred independently of CRY proteins and other core clock factors, indicating a unique role for PER2 in regulating fat metabolism outside of its canonical role within the circadian machinery.

Obesity is not the only metabolic perturbation seen in clock mutant animals. *Clock*, *Bmal1* and *Cry1/2* all contribute to proper maintenance of glucose homeostasis (Turek et al., 2005, Lamia et al., 2008, Marcheva et al., 2010, Zhang et al., 2010a, Rudic et al., 2004, Lamia et al., 2011) and their contributions in this realm will be discussed in greater depth elsewhere in this chapter (see ***Glucose and Insulin Homeostasis***). To better understand how the clock (and its disruption) can have such profound metabolic consequences; one must more closely examine the diversity of rhythmic metabolic processes as well as the metabolic inputs that influence clock function.

Metabolic Rhythmicity:

Circadian Output: -omics

CLOCK and BMAL1 are transcription factors with thousands of binding sites within the genome, many of which reside on genes encoding rate-limiting enzymes of key metabolic pathways within the liver (Koike et al., 2012, Vollmers et al., 2012, Le Martelot et al., 2012). Indeed, it is estimated that ~10% of the hepatic transcriptome cycles (Panda et al., 2002, Storch

et al., 2002, Koike et al., 2012, Le Martelot et al., 2012, Vollmers et al., 2012, Menet et al., 2012). Cycling RNA transcripts are only part of the story however as post-transcriptional and post-translational factors also influence molecular rhythms (Kojima et al., 2012). As such, ~20% of the proteome in liver was found to have circadian rhythmicity, with many of these being enzymes important for vital liver functions, such as urea formation, and energetics, such as carbohydrate metabolism (Reddy et al., 2006, Robles et al., 2014).

Knowing that many rate limiting metabolic enzymes are cycling both at the RNA and protein level, recent studies have sought to determine the rhythmicity of the liver metabolome and lipidome. Examining different metabolites across the circadian cycle in mice on a regular chow (RC) diet revealed an accumulation of xenobiotic and amino acid metabolites peaking around mid-to-late evening with carbohydrate and lipid metabolites peaking mid-to-late daytime (Eckel-Mahan et al., 2012, Eckel-Mahan et al., 2013, Adamovich et al., 2014). Cycling xenobiotic metabolites is consistent with earlier observations that mRNA transcripts encoding proteins important for detoxification are under clock control (Gachon et al., 2006). Plasma metabolomes have also been examined in mice (Minami et al., 2009) and humans (Kasukawa et al., 2012) with the phasing of the identifiable metabolites being used to approximate internal body time and potentially diagnose circadian rhythm disorders.

Light is the major *Zeitgeber* for molecular oscillations within the SCN, but these rhythms are also self-sustaining. Therefore, removing light and placing animals in constant conditions such as constant darkness (DD), helps reveal a more direct role for the clock in governing behavioral and physiological rhythms. Analysis of the hepatic lipidome in ad libitum (ad lib) fed mice in DD conditions revealed that ~17% of the identifiable lipids could be classified as having

a circadian rhythm (Adamovich et al., 2014). The majority of these cycling lipids were triacylglycerol (TAG) species. Most of the oscillating lipids peaked during the subjective light phase, consistent with the need to liberate stored fat when energy intake is low, in order to maintain metabolic homeostasis. Indeed, gene expression of many of the biosynthetic and catabolic enzymes for TAG metabolism displays circadian rhythmicity in the mouse liver. This same study examined the role of the clock in lipid cycling by performing a similar lipidomic analysis of ad lib fed *Per1*$^{-/-}$/*Per2*$^{-/-}$ mouse liver from DD conditions. Surprisingly, a similar fraction of lipids had significant oscillations and of these, TAG species were again prominent. The peak phasing however was nearly opposite that found in wildtype animals. Thus, lipid oscillation itself may be clock-independent, but an intact clock helps dictate the phase.

The temporal aspect of food ingestion is a major behavioral output of the circadian system and this contributes to the cycling of metabolites. Meal timing will be discussed later in this review, but first we will focus on the metabolic sensors both responding to peripheral clocks and informing them of the cellular energetic status as this will help to better understand the molecular links between nutrient metabolism and rhythmic gene expression.

Metabolic Crosstalk

Trying to define circadian inputs becomes difficult as many "inputs" are factors that respond to the metabolic state of an organism, tissue or cell type. That state is often determined by the temporal energetic condition (fasting versus feeding), which is in turn dictated by the clock. Nicotinamide adenine dinucleotide (NAD^+) is a coenzyme in redox reactions and is linked to energetic processes within the cell. NAD^+ synthesis is controlled by the rate limiting enzyme nicotinamide phosphoribosyltransferase (NAMPT) and *Nampt* gene expression is under

clock control (Ramsey et al., 2009, Nakahata et al., 2009). Redox state is important to the core clock mechanism as NAD cofactors can influence CLOCK:BMAL1 and NPAS2:BMAL1 DNA binding (Rutter et al., 2001). There is additional feedback by NAD^+ through the action of SIRT1, an NAD^+-dependent deacetylase which associates with the CLOCK:BMAL1 complex and modulates its function. NAD^+ thus provides a direct link for circadian clock-mediated transcription with the energetic state of a cell (Asher et al., 2008, Nakahata et al., 2008, Rutter et al., 2001). Interestingly, SIRT1 protein and activity both cycle, yet *Sirt1* RNA remains relatively constant. Thus, post-transcriptional mechanisms must contribute to the circadian accumulation of SIRT1 protein. NAD^+ synthesis is under clock control and NAD^+ levels show cycling under ad lib and fasting conditions (Ramsey et al., 2009, Peek et al., 2013); so it would follow that SIRT1 activity would cycle due to its NAD^+ dependence. Not only is this an important feedback cycle for the clock itself, but this rhythmic production of NAD^+ also drives rhythms in mitochondrial function (Peek et al., 2013). Another NAD^+-dependent enzyme, poly(ADP-ribose) polymerase 1 (PARP1) also contributes to proper circadian gene expression. In the liver of mice PARP1binds to CLOCK:BMAL1 heterodimers and poly(ADP-ribosyl)ates CLOCK which reduces the DNA-binding activity of the heterodimer (Asher et al., 2010). PARP1 not only contributes in this manner to rhythmic transcription, but it also contributes to the phase shifting kinetics of clock genes in the liver when mice are subjected to daytime restricted feeding (Asher et al., 2010).

Metabolic flux within a cell also results in alternating ratios of AMP/ATP. The adenosine monophosphate (AMP)-activated protein kinase (AMPK) can respond to these altered ratios by phosphorylating CRY1 proteins, leading to their destabilization and reduced inhibition

of CLOCK:BMAL1 (Lamia et al., 2009). Two isoforms α1 and α2 exist for the catalytic subunit of AMPK. Mice deficient for the α1 isoform (*AMPKα1*$^{-/-}$) have specific deficits in circadian behavior; however *AMPKα2*$^{-/-}$ mice do not (Um et al., 2011). The α1 isoform is expressed predominantly in adipose and brain, whereas the α2 isoform is predominant in muscle. Loss of each isoform individually has differential effects on clock-gene expression in a tissue-specific manner. While overt behavioral rhythmicity is maintained in both the *AMPKα1*$^{-/-}$ and *AMPKα2*$^{-/-}$ mice, the impairments that *AMPKα1*$^{-/-}$ mice exhibit help support a role for AMPK in shaping the molecular oscillations of the core clock in vivo.

Recently, another molecular link between glucose metabolism and core clock components was revealed. The protein *O*-GlcNAc transferase (OGT), which mediates protein glycosylation, was found to contribute to both CLOCK:BMAL1 transcriptional activity and post-translational modification of PER2 (Kaasik et al., 2013, Li et al., 2013). Glycosylation catalyzed by OGT utilizes UDP-GlcNAc, a by-product of glucose metabolism via the hexosamine pathway. Overexpression of OGT was found to stabilize CLOCK proteins while decreasing ubiquitination of both CLOCK and BMAL1, leading to increased expression of their target genes *Per2* and *Cry1* in vitro (Li et al., 2013). *O*-GlcNAcylation also competes with phosphorylation of human PER2 protein on serine residues whose regulation is important for overt circadian behavior, as their mutation results in familial advanced sleep-phase disorder (Kaasik et al., 2013, Toh et al., 2001). Mice with a liver-specific loss of OGT have disruptions in plasma glucose rhythmicity and overall glucose metabolism (Li et al., 2013). OGT activity cycles and is regulated in part by glycogen synthase kinase 3β (GSK3β) (Kaasik et al., 2013). This regulation

is important for proper behavioral rhythmicity as inhibition of GSK3β in mice alters circadian wheel-running activity (Kaasik et al., 2013).

Another metabolic sensor impacting circadian behavior is FGF21 (Bookout et al., 2013). FGF21 can act as an endocrine hormone and mediates metabolic responses to both fasting and refeeding (reviewed in (Potthoff et al., 2012, Owen et al., 2015). The effects of FGF21 on the circadian system occur through regulation of clock output rather than the central pacemaker as the patterning of wheel-running behavior, but not circadian period, is altered in transgenic mice overexpressing FGF21 (Bookout et al., 2013). This is similar to a starvation response in mice and requires expression of the FGF21 receptor β-Klotho in the hypothalamus. Taken together, these findings further expand the role of metabolic sensors in fine-tuning clock function.

Nuclear Receptors Impact the Clock

Nuclear receptors (NRs) are metabolic sensors that regulate the transcription of a variety of genes in a ligand-dependent manner. These ligands are comprised mainly of hormones and nutrient metabolites. Transcripts under their control include key players in metabolic signaling cascades. Many nuclear receptors show clear patterns of rhythmic expression globally and in a tissue-specific manner (Yang et al., 2006). Among them are two components of the core circadian feedback loop REV-ERBα and RORα. As previously described, these two orphan nuclear receptors contribute to proper *Bmal1* transcription. A *Rev-erbβ* isoform also exists and has been shown to repress *Bmal1* transcription as well (Guillaumond et al., 2005). *Rev-erbα*$^{-/-}$ mice exhibit a significantly shorter free running period in constant darkness, though *Rev-erbβ*$^{-/-}$ do not show significant alterations. A recent report utilizing an inducible cre/lox system found

that inducible double knockout of both *Rev-erbα* and *Rev-erbβ* (iDKO) in adult mice resulted in a free-running period shorter even than that seen in *Rev-erbα*$^{-/-}$ mice alone. Additionally, these iDKO animals displayed fasting hypoglycemia and hypotriglyceridemia (Cho et al., 2012). When the double knockout of *Rev-erbα* and *Rev-erbβ* was restricted to the liver using the albumin-cre driver, this significantly disrupted the cycling of many genes associated with key metabolic pathways such as insulin signaling and the Tricarboxylic Acid (TCA) cycle (Cho et al., 2012). The nuclear receptor coactivator PGC-1α provides an additional layer of metabolic regulation of peripheral clock function by regulating *Bmal1* and *Rev-erbα* expression through coactivation of the ROR family of nuclear receptors (Liu et al., 2007).

The peroxisome proliferator-activated receptor α (PPARα) also forms a significant metabolic feedback loop with the core clock machinery. PPARα was shown to directly bind to PPAR response elements in the promoters of both *Bmal1* and *Rev-erbα* (Canaple et al., 2006). The PPAR family of nuclear receptors are important lipid sensors that transcriptionally regulate lipid processing through utilization and storage (Evans et al., 2004). PPARα gene expression is regulated by the circadian clock and cycles in vivo (Oishi et al., 2005). Several different PPAR isoforms exist (PPARα, PPARɣ and PPARδ) with tissue-specific expression. As mentioned previously, Nocturnin has also been shown to regulate proper nuclear receptor functioning through its regulation of hepatic *PPARɣ* expression under HFD conditions (Green et al., 2007). It has also been shown to participate in nuclear shuttling of PPARɣ in vitro in 3T3-L1 cells (Kawai et al., 2010b).

The retinoic acid receptor α (RARα) and retinoid x receptor α (RXRα) exist in complexes that respond to retinoic acid as a ligand and *RARα* mRNA cycles in multiple tissues (Yang et al.,

2006). In the presence of their hormonal ligand, both RARα and RXRα associate with CLOCK and NPAS2 and reduce transcriptional activation by CLOCK:BMAL1 and NPAS2:BMAL1 (McNamara et al., 2001). A screen looking for potential entraining agents in rat fibroblasts stably transfected with an *mPer2*-luc reporter revealed that several forms of retinoic acid can significantly affect rhythm entrainment (Nakahata et al., 2006). Additionally, administration of all-*trans*-retinoic acid in mice significantly phase-shifts *Per2* rhythms in the heart (McNamara et al., 2001). RXRα also forms a heterodimer with PPARɣ and thus contributes to the transcriptional program of lipid metabolism (Tontonoz and Spiegelman, 2008).

Corticosterone is the major murine glucocorticoid and this hormone cycles with robust rhythmicity. While expressed in most metabolic tissues, the glucocorticoid receptor (GR) is only rhythmic in white and brown adipose tissue under ad lib RC conditions (Yang et al., 2006). Glucocorticoids are used as entraining agents in cultured cells due to their induction of clock gene transcripts and they elicit phase shifts in clock gene expression in peripheral tissues upon injection (Balsalobre et al., 2000a, Balsalobre et al., 2000b). However, they were also found to inhibit the restricted-feeding phase shifting of clock gene expression in peripheral tissues in a GR-dependent manner (Le Minh et al., 2001). Corticosterone is secreted rhythmically by the adrenal gland and adrenalectomized mice displayed much faster phase resetting of clock gene expression in liver and kidney (Le Minh et al., 2001). While glucocorticoids may play important roles in tissue synchronization under ad lib conditions, they do not appear to be the primary *Zeitgeber* for peripheral tissues under restricted feeding conditions. In a restricted feeding paradigm, the liver receives nutrient signals dictated by the feeding time, yet signals such as glucocorticoids are still being driven in part by the master pacemaker within the SCN. Thus,

glucocorticoid interference in peripheral clock shifting highlights the opposing actions of the central clock in the SCN and the peripheral clocks in response to altered feeding regimens. Still, Cry1 associates with the GR and represses glucocorticoid-induced transcriptional activation, meaning that the core clock components contribute to glucocorticoid regulation of metabolic processes, if not entrainment (Lamia et al., 2011).

Feeding Cycles and Diet Influence Peripheral Clocks

Feeding: When you eat matters

For animals in the wild, meal timing is often more restricted than the ad lib conditions of the laboratory setting. Providing the mice with free access to food has allowed researchers to examine the roles of light:dark (LD) cycles, constant conditions such as constant dark (DD) and constant light (LL), as well as the clock itself on feeding behavior. Understanding the role of the clock in feeding requires consideration of both central and peripheral clocks. Althought the central clock makes important contributions to feeding-centers in the brain (reviewed in (Marcheva et al., 2013)) I will focus here on the effects of particular feeding regimens on peripheral clocks.

Feeding is an important entraining agent for peripheral circadian clocks, especially the liver. When either rats or mice experience temporal restricted feeding, where their access to food is limited to a few hours during the light phase, clock gene expression shifts in peripheral tissues (Damiola et al., 2000, Stokkan et al., 2001). The kinetics of this shift are tissue-specific as the liver shifts fairly rapidly compared with kidney, heart and pancreas (Damiola et al., 2000).

Of note, clock gene expression within the SCN remains unaffected by the restricted feeding, implicating a greater importance of nutrient signals in the entrainment of oscillators in the periphery and an uncoupling of the central pacemaker with peripheral tissues in altered feeding conditions.

While restricted feeding can uncouple the central and peripheral clocks, determining the role of the master pacemaker in peripheral entrainment under ad lib conditions can be difficult. As light is the major *Zeitgeber* for the master pacemaker in the SCN, removal of light as an input by placing animals in DD has been used to assess the autonomous nature of the clock in behavioral and physiological rhythms. As previously mentioned, animals put in DD were found to have oscillations in a large number of liver mRNAs and proteins. Mice in DD maintain rhythmic feeding, however, and so the cycling of many of these transcripts could still be a result of the feeding rhythm and not directly the local peripheral clock.

To help tease apart the different contributions of food versus the clock, Vollmers and colleagues examined transcriptional changes in the livers of both wildtype and *Cry1*$^{-/-}$/*Cry2*$^{-/-}$ mice in response to fasting, refeeding and temporal restricted feeding (Vollmers et al., 2009). Food availability for only 8h during the light phase was able to shift expression of many of the transcriptional targets of key metabolic regulators such as CREB, AKT, SREBP1/2 and ATF6. While many of these transcripts were arrhythmic under ad lib feeding in *Cry1*$^{-/-}$/*Cry2*$^{-/-}$ livers, they gained rhythmicity following the temporal restricted feeding. If food was removed altogether and hepatic gene expression assessed during 24h of fasting, it was found that more than 80% of the genes found to cycle under ad lib conditions ceased to oscillate. A small percentage maintained rhythmicity, and contained within this group were the components of the

core clock. This is yet further evidence that rhythms in peripheral transcriptomes are heavily influenced by the metabolic state of the organism, namely the timing of food ingestion.

Analysis of transcriptomes and proteomes is only part of the metabolic landscape. Determining actual metabolite levels in various tissues will help fill out the picture of how the clock and feeding cycles impact overt physiology. As previously mentioned, Asher and colleagues conducted a comprehensive analysis of the hepatic lipidome in wildtype and *Per1*$^{-/-}$*/Per2*$^{-/-}$ mice fed either ad lib or restricted to the dark phase (Adamovich et al., 2014). Their findings showed that a substantial fraction of lipids cycled in both WT and *Per1*$^{-/-}$*/Per2*$^{-/-}$ mice under ad lib conditions (~17%), yet the oscillating species in *Per1*$^{-/-}$*/Per2*$^{-/-}$ were mostly distinct from those in WT. While total daily food intake did not differ between the genotypes, *Per1*$^{-/-}$*/Per2*$^{-/-}$ mice lost their temporal consolidation of food intake to the dark phase and instead ate relatively equal amounts throughout the day. This unique oscillating population of lipids in ad lib *Per1*$^{-/-}$*/Per2*$^{-/-}$ mice thus represents a fraction of lipids whose control is not mediated entirely by the feeding pattern or the clock. A clear mechanism for their regulation is an area open for investigation. Temporal food restriction to the night phase altered the phasing of TAG accumulation with peaks around CT12 in both genotypes, corresponding with the presentation of food. Surprisingly, the oscillating TAG species now showed a clear overlap between WT and *Per1*$^{-/-}$*/Per2*$^{-/-}$ animals, indicating that meal timing can dictate the phasing of certain TAGs in the absence of a functional clock. Another important finding was that feeding restricted to the night phase lowered the total hepatic TAG levels by ~50% in WT animals compared to ad lib feeding. This reduction in lipid content of the liver is consistent with other recent findings that temporal restriction of food intake can improve metabolic parameters such as hepatic steatosis (Hatori et

al., 2012). Taken together, these data show that both the clock and feeding patterns can have significant impacts on both transcript and metabolic cycling, with important impacts on overall physiology, while also impacting one another.

Diet: What you eat matters

While the timing of nutrient intake is important, the type of nutrients taken in during feeding directly influences the clock as well. HFD feeding can change not only behavioral rhythms, but also molecular and metabolite oscillations (Kohsaka et al., 2007, Pendergast et al., 2013, Adamovich et al., 2014). As mice are progressively exposed to a HFD (containing 45% kcal from fat), their daytime locomotor activity increases, as does their food consumption during the light phase (Kohsaka et al., 2007). This is accompanied by alterations in clock gene expression in both hepatic and adipose tissue with a general trend toward damping of oscillations. Transcript levels of many key metabolic regulators of fat metabolism also display altered patterns with tissue-specific effects. Additionally, circulating hormones that normally oscillate under a RC diet are altered with HFD, though hypothalamic clock gene expression remains largely unaffected.

If one looks broadly at the effects of diet on the liver transcriptome and metabolome, a significant reorganization of molecular oscillations by high fat energy consumption is seen. Ten weeks of HFD consumption (60% kcal from fat) results in obesity, hepatic steatosis, hypertriglyceridemia and impaired glucose tolerance (Eckel-Mahan et al., 2013). After HFD feeding, there was a significant change in cycling metabolites such that some which were previously rhythmic lost their cycling and others which previously did not cycle became

rhythmic, while some remained unchanged. A similar alteration was seen in cycling transcripts in the liver. The circadian clock genes remained rhythmic in RC and HFD conditions, again highlighting the importance of nutrient and feeding cues on peripheral clocks. While the clock genes maintaining rhythmicity, HFD was found to alter the ability of CLOCK:BMAL1 to bind to target gene promoters. These effects of diet began to manifest with only 3 days of HFD exposure in mice and, remarkably, began to reverse when HFD animals were shifted back to RC feeding for two weeks.

The type and timing of food consumption both have profound effects independently on the circadian clock and rhythmic metabolic profile. It should not be surprising then that the combined effects of these two metabolic signals could have important effects on energy metabolism. Mice with time-restricted feeding (tRF) of a HFD to the night phase were found to be protected from DIO and many of the negative effects of ad lib HFD feeding. These animals had improvements in factors important for glucose metabolism (including phosphorylated cAMP response element-bind protein CREB (CREB) and hepatic AMP levels), as well as fat oxidation (including phosphorylated acetyl-CoA carboxylase), compared to their ad lib fed HFD counterparts (Hatori et al., 2012). . The tRF mice that were fed HFD only during the night were better able to utilize fat as an energy source as reflected in their improved respiratory exchange ratio and energy expenditure. Both hepatic steatosis and glucose metabolism were improved in the tRF HFD animals as well. While tRF in RC animals did not improve metabolic processes to the same extent, the marked improvements in the HFD animals can be an important guide in studying the temporal consequences of feeding.

Nutrient Uptake

When considering the temporal aspect of food consumption, nutrient uptake must also be considered. When fed ad lib, mice consume around 70% of their daily caloric intake in the evening hours (Kohsaka et al., 2007, Adamovich et al., 2014). Indeed, even though feeding behavior per se appears under the control of the circadian system, the uptake of the resulting nutrients is also gated by the clock. Due to the near ubiquitous nature of clock genes in different cell types, it is not surprising that the core clock machinery exists in cells of both the small intestine and colon (Pan and Hussain, 2009, Hoogerwerf et al., 2007). Clock gene rhythmicity in the colon persists in both the absence of LD cycles (in DD) and in vagotomized mice (Hoogerwerf et al., 2007), indicating a functional, local clock within the digestive tract. The small intestine is the major site of nutrient absorption and investigations into the temporal efficiency of nutrient absorption revealed that carbohydrates, peptides, lipids and cholesterol all show a time-dependent variance in their uptake (Pan and Hussain, 2009, Pan and Hussain, 2007). Absorption was higher during the middle of the dark phase compared to those during the middle of the light phase. This can likely be attributed to the rhythmic expression of many of the key transporters of these nutrients within the intestine (Pan et al., 2004, Pan et al., 2002, Pan and Hussain, 2007). It is still not clear whether the clock components directly regulate the expression of all of these transporters, as they too respond to different feeding regimens by altering their expression. Still, it remains clear that the intestine is primed to optimally absorb nutrients at certain times of day.

To help address the role of the clock, Pan and Hussain also investigated *Clock*$^{\Delta 19}$ mutant mice, which develop obesity, and found them to have equal absorption of nutrients during both

the day and night hours, consistent with the loss of temporal partitioning of their food intake (Turek et al., 2005, Pan and Hussain, 2009). The *Clock*$^{\Delta 19}$ mutant mice used in this study were whole-body mutants. It will be interesting to examine the effects of the local clock on nutrient absorption using the more selective conditional knockout animals that are now available. Investigations into complete loss of *Clock* in *Clock*$^{-/-}$ mice, which do not show the same severity of metabolic abnormalities with HFD as the *Clock*$^{\Delta 19}$ model, have disrupted fat absorption (Oishi et al., 2006). This disruption is thought to occur through improper lipid digestion in the stomach due to reduced daytime release of lipase. It should also be noted that the *Clock*$^{\Delta 19}$ and *Clock*$^{-/-}$ mice in each of these studies were on different genetic backgrounds (Turek et al., 2005, Oishi et al., 2006). *Noc*$^{-/-}$ mice also show deficits in lipid and cholesterol flux through intestinal enterocytes (Douris et al., 2011). This helps explain their resistance to DIO (Green et al., 2007), though a specific mechanism remains to be elucidated.

Bile Acid Metabolism

Rhythmic feeding creates a cycle of nutrient flux throughout the enterohepatic system. The uptake and processing of lipids is aided in part through bile acids (BAs). Primary BAs are synthesized in the liver and stored in the gallbladder where, upon nutrient ingestion, they are released into the proximal small intestine (duodenum) where they facilitate the solubilizing and uptake of lipid (reviewed in (Russell, 2003)). BAs are recycled in the distal small intestine (ileum) where they enter the circulation and can act as signaling molecules through interaction with Farnesoid X-activated Receptor (FXR) in the liver (Parks et al., 1999, Makishima et al.,

1999) or TGR5 in a variety of tissues (e.g. liver, gallbladder, intestine) ((Maruyama et al., 2002, Kawamata et al., 2003) and reviewed in (de Aguiar Vallim et al., 2013)).

Circadian disruption either through genetic manipulation of the core clock (Le Martelot et al., 2009) or through dissociation of the central and peripheral oscillators through temporal restricted feeding (Ma et al., 2009) significantly alters BA production and cycling. BAs exist as a variety of distinct species and these too exhibit circadian cycling (Zhang et al., 2011). Different BAs show differential activation of FXR (Parks et al., 1999, Makishima et al., 1999) and alterations to the BA pool composition can have dramatic effects on metabolism, namely glucose and lipid homeostasis ((Haeusler et al., 2012) and reviewed in (Kuipers et al., 2014)). It is therefore important that different mechanisms whereby the circadian clock regulates BA synthesis and metabolism be explored.

Glucose and Insulin Homeostasis

The temporal pattern of feeding results in a majority of caloric intake at certain times of day. Thus, nutrients taken in and not immediately used are stored for utilization during the intervening periods in order to maintain metabolic homeostasis. During times of fasting, the liver is the main site of glucose and ketone body production via gluconeogenesis (reviewed in (Previs et al., 2009)) and ketogenesis (reviewed in (Cotter et al., 2013)), respectively. Fasting is an important process that itself is influenced by the circadian system. In mammals, blood glucose is a critical parameter that must be maintained within strict margins (euglycemia), even when energy intake is restricted. Blood glucose values cycle throughout the day in mammals and proper circadian alignment contributes to this rhythmicity (Scheer et al., 2009). Importance

of maintaining proper glucose rhythmicity is evidenced with diabetic patients who often lose this control (Polonsky et al., 1988). Additionally, genetic disruption of clock components leads to altered ad lib and fasting glycemia (Turek et al., 2005, Lamia et al., 2008).

Since meal timing can vary throughout the day, organisms must contend with large influxes of nutrients and maintain euglycemia. A normal physiological response to a bolus of glucose is for the pancreas to secrete insulin which signals to the liver for a shutdown of gluconeogenesis and ketogenesis as well as to other peripheral tissues to take up glucose from the blood. One way of assessing insulin sensitivity is the glucose tolerance test, in which a bolus of glucose is administered and an animal's response as measured by blood sugar levels indicates their ability to regulate glucose homeostasis (Ayala et al., 2010). Clock mutant animals have illuminated a critical role for the circadian clock in mediating these physiological responses. *Clock*$^{\Delta 19}$ animals have altered glucose metabolism as displayed by hyperglycemia in the ad lib state (Turek et al., 2005). The *Clock*$^{\Delta 19}$ and *Bmal1*$^{-/-}$ mice have altered plasma glucose responses to an injection of insulin during the day and night (Rudic et al., 2004). Additionally, animals consuming a RC diet display a trend towards decreased glucose tolerance in the early morning which is exacerbated by HFD consumption (Rudic et al., 2004). A similar study found the day-night difference in glucose tolerance of animals fed a HFD to be somewhat blunted (Prasai et al., 2013), though glucose dose, age and dietary fat content were somewhat different than the experiments conducted by Rudic and colleagues, and these factors have been shown to critically influence glucose disposal (Ayala et al., 2010). Chronic feeding of a HFD leads to decreased daytime glucose tolerance, but remarkably, if the HFD feeding is restricted to 8h during the dark phase, daytime glucose tolerance returns to levels seen in regular chow, ad lib fed animals

(Hatori et al., 2012). Surprisingly, the *Noc*$^{-/-}$ mouse which is resistant to DIO has reduced daytime glucose tolerance but increased insulin sensitivity under RC conditions (Green et al., 2007). Interestingly, HFD feeding produces insulin resistance in both WT and *Noc*$^{-/-}$ mice, thus making the *Noc*$^{-/-}$ mouse an interesting model for studying the effect of diet on a diabetic phenotype independent of obesity.

A closer examination of glucose metabolism in *Clock*$^{\Delta 19}$ and *Bmal1*$^{-/-}$ revealed an important role for the circadian clock in regulating pancreatic function. Importantly, the pancreas contains a functional clock with oscillations of core clock genes in vivo and *Per2*^{Luc} in vitro (Marcheva et al., 2010). The hyperglycemia reported in *Clock*$^{\Delta 19}$ animals is due to elevated blood glucose during both the light and dark phases and this is accompanied by decreased insulin levels in the dark phase (Marcheva et al., 2010). Probing glucose tolerance, *Clock*$^{\Delta 19}$ animals had a subtle phenotype of reduced glucose tolerance, again accompanied with reduced insulin levels in response to an intraperitoneal glucose injection. Studying isolated pancreatic islets from *Clock*$^{\Delta 19}$ animals revealed that these clock mutants have decreased insulin release as a result of reduced insulin exocytosis. This defect is not limited to the *Clock*$^{\Delta 19}$ mutant, as *Bmal1*$^{-/-}$ mice display similar pancreatic deficits. Importantly, the local pancreatic clock is vital to proper pancreatic function as *PdxCreBmal1*$^{flx/flx}$ mice, which have a pancreas-specific clock disruption, recapitulate the phenotypes seen in the whole-body *Bmal1*$^{-/-}$ mutants with decreased glucose tolerance and reduced insulin exocytosis.

The glucose phenotype seen in whole-body *Bmal1*$^{-/-}$ mutants is due, at least in part, to loss of *Bmal1* in the liver, since conditional knockout of *Bmal1* specifically in the liver (*L-Bmal1*$^{-/-}$) resulted in disrupted cycling of key regulatory genes important for glucose homeostasis

(Lamia et al., 2008). Some of these genes retained their rhythmicity, though with altered phasing of expression. Of note, the major hepatic glucose transporter *Glut2* was expressed at very low levels and no longer cycled at either the RNA or protein level in *L-Bmal1*$^{-/-}$ mice. Additionally, these *L-Bmal*$^{-/-}$ mice displayed hypoglycemia only during the light phase of activity (when food intake is reduced) and a similar, though blunted response to insulin. These results, combined with those discussed above from pancreas-specific *Bmal1*$^{-/-}$ knockout (Marcheva et al., 2010), highlight the complex interplay of clocks within different peripheral tissues.

CREB is an important mediator of the gluconeogenic program (Altarejos and Montminy, 2011) and its activity-dependent phosphorylation was found to cycle (Vollmers et al., 2009). During fasting, gluconeogenesis is high and this is regulated in part through glucagon stimulation of CREB (Altarejos and Montminy, 2011). Administration of glucagon induced the key gluconeogenic genes *G6pc* and *Pck1* to a greater extent in the early part of the dark phase as compared to the early part of the light phase following a fast (Zhang et al., 2010a). This induction was significantly reduced in mice with adenoviral overexpression of CRY1 and these mice also had fasting-induced hypoglycemia. Conversely, RNAi-mediated knockdown of hepatic *Cry1* and *Cry2* in vivo resulted in increased mRNA expression of *G6pc*, the gene that encodes the catalytic subunit of Glucose-6-phosphate, and *Pck1*, which encodes the cytosolic form of phosphoenolpyruvate carboxykinase. Importantly, adenoviral overexpression of CRY1 in the genetically obese *db/db* mice significantly improved glucose tolerance. Loss of either *Cry1* or *Cry2* results in significant loss of glucose tolerance during the daytime. Combined loss of *Cry1* and *Cry2* in *Cry1*$^{-/-}$/*Cry2*$^{-/-}$ mice results in an even more severe loss of glucose tolerance during the light phase (Lamia et al., 2011). This is thought to act through increased

corticosterone production (an important mediator of gluconeogenesis) and loss of CRY interaction with the GR, resulting in increased *Pck1* expression. Together, these loss- and gain-of-function studies provide compelling evidence for the importance of the circadian clock in regulation of glucose homeostasis.

Overview

The circadian clock is vital to coordinating metabolic rhythms in mammals and disruptions to the circadian system can have profound impacts on health, specifically glucose, lipid and bile acid metabolism. The work that I will describe in the following chapters provides a new mechanistic layer to this circadian regulation of metabolism through my work with Nocturnin. I used a variety of molecular techniques (mRNA-seq, TAIL-seq), combined with phenotypic observations in WT and *Noc*$^{-/-}$ mice to identify potential targets of NOC that are regulated at the posttranscriptional level in order to maintain proper metabolic flux both basally and during nutrient-challenged conditions. Moving forward, this new understanding of the relationship between Nocturnin, the circadian system and metabolism will help guide the treatment of conditions such as obesity and diabetes.

Chapter II: Altered bile acid dynamics in mice lacking Nocturnin

Introduction:

Many processes in both physiology and behavior are cyclic. This is due in large part to the rhythmic environment in which organisms live. Temporal partitioning of food intake and rest allow for optimal survival and energy utilization. Thus it is not surprising that a system has evolved to predict the changes in environment associated with changes in energy state and food availability. The circadian system coordinates these rhythms with a near 24h periodicity in nearly every tissue of the mammalian body.

The master clock is located within the ventral hypothalamus and consists of a bi-nucleated structure known as the suprachiasmatic nucleus (SCN). The SCN is located just dorsal to the optic chiasm and can receive direct light information from the eyes via the retino-hypothalamic tract. Molecular transcription-translation feedback loops exist within cells of the SCN and consist of positive elements that initiate transcription of negative elements, which feedback and inhibit their own transcription (reviewed in (Ko and Takahashi, 2006). This process takes roughly 24 h and thus drives the circadian (circa~, meaning about and ~dian meaning daily) rhythms in the core clock. This core clock, or master pacemaker, is able to entrain the clocks in peripheral tissues via hormonal and chemical outputs.

Peripheral oscillators in tissues such as the liver and adipose tissue are responsive to the core clock within the SCN, but are also sensitive to nutritional cues. Indeed, peripheral and central clocks can become dissociated when food availability is restricted to the rest period of an organism such as mice (Damiola et al., 2000). Additional elements of the core clock oscillator

within peripheral tissues are directly nutrient responsive and can help shape the cycling of the clock within these tissues.

While the clock is useful for predicting cyclic changes in energy states, it is also important to consider that organisms living outside the carefully controlled environment of the laboratory might not regularly consume food. They would presumably have to forage and search out their food and thus would need to have a system generally tuned to a specific time of day, but which could maintain responsiveness to the intake of food and still allow for optimal metabolism upon nutrient influx. Components of the core clock are able to regulate cycling changes in gene expression, but the regulation of cycling genes and enzymes does not occur strictly at the level of transcription. Posttranscriptional and posttranslational mechanisms also exist and help fine-tune the overall cycling of different components intracellularly and between tissues at the whole-body level.

The protein Nocturnin (NOC), encoded by the *Nocturnin* (*Noc*) gene (official gene symbol *Noct*), is an exonuclease belonging to a class of enzymes known as deadenylases, which regulate mRNA stability and translatability through removal of the Poly(A) tail at the 3' end of mRNA transcripts (Green and Besharse, 1996, Garbarino-Pico et al., 2007). Poly(A) tail length is known to correlate with translation efficiency (Zhang et al., 2010b, Weill et al., 2012). NOC appears to have a critical metabolic function as mice lacking *Nocturnin* ($Noc^{-/-}$, KO) are resistant to diet-induced obesity (DIO) and hepatic steatosis upon High Fat Diet (HFD) feeding (Green et al., 2007). Because of this, I wanted to explore NOC's metabolic function and began by first determining its responsiveness to nutrient status. To do this I employed a combination of diet

and fasting/refeeding paradigms to examine how *Nocturnin* expression changes during metabolic challenge. Given NOC's deadenylase function, I explored changes in gene expression and Poly(A) tail length by mRNA-seq and TAIL-seq across the circadian cycle and in response to nutritional challenges in Wildtype (WT) and *Noc*$^{-/-}$ mice. I combined this molecular data with physiological measurements of metabolites in each condition and, taken together, the results described in this chapter have revealed potential targets of Nocturnin and the temporal and nutrient-specific conditions in which NOC regulates metabolic flux.

Methods:

Mice: WT and *Noc*$^{-/-}$ C57BL/6 mice were individually housed in light-tight environmental chambers under Green LED lighting on a 12:12 Light:Dark (LD) cycle with ZT0 defined as the time of lights on and ZT12 defined as the time of lights off. Specific time of lights on and lights off was variable, depending on the experiment, but all LD cycles maintained the LD 12:12 ratio and animals were allowed a minimum of 2 weeks to entrain to the specific LD cycle once placed in the environmental chambers. Animals on Regular Chow (RC) were fed Harlan Teklad diet 2918. Animals receiving High Fat Diet (HFD) were fed Research Diets D12492i (60 % kcal fat). HFD-fed mice were allowed to feed *Ad Libitum* (*Ad Lib*) for 3 weeks beginning at 6-8 weeks of age. Animals were 9-12 weeks of age at the time of tissue collection. Mice were sacrificed via decapitation for terminal blood collection followed by tissue harvest. Mice sacrificed at time corresponding to lights off were sacrificed under dim red light. All animal studies were conducted in accordance with IACUC regulations and guidelines.

Fast/Refed: Mice were placed in a fresh cage with woodchip bedding and water, but no food at the start of their fasting period. At the time of refeeding, the food (either RC or HFD) that was removed from each mouse was returned for the specified amount of time (1h or 4h) prior to the mouse being sacrificed for blood and tissue collection.

mRNA-seq: mRNA-seq libraries were created according to procedures outlined in (Takahashi et al., 2015) and sequenced on a HiSeq Sequencing System (Illumina) in the UT Southwestern Medical Center McDermett NGS Core. For mRNA-seq of HFD samples, the average read depth for all samples was 40 million reads. On average, 90% of the raw reads were mapped to the mouse genome (MM9). After QC filtering, an average of 28 million reads for each sample remained and of these, 77% were mapped to the MM9 genome and used for statistical comparisons by differential expression analsysis. For mRNA-seq of RC samples, a total of 16 samples was pooled (n=1/genotype/timepoint) and went through two rounds of sequencing. Each round yielding an average sequencing depth of 14 million reads per sample and the two rounds of sequencing were combined for each sample to achieve and average read depth of 28 million reads per sample. A second set of biological replicates (n=1/genotype/timepoint) was sequenced in a similar manner. An average of 97% of the total 28 million reads per sample was mapped to the mouse genome (MM10).

qPCR: Flash-frozen tissue was ground into powder under liquid nitrogen using a mortar and pestle. Tissue powder (50-100 mg) was homogenized in 1 mL TRIzol in a 2 mL tube using a Polytron mechanical homogenizer. Tissue homogenate was spun for at 10,000 RCF for 10 min at 4˚C. the supernatant was placed in a fresh 1.5 mL Eppendorf tube and Total RNA extracted by TRIzol. One ug total RNA was converted to cDNA using the ABI Reverse Transcription Kit. cDNAs were diluted 1:5 in ddH_2O and amplified using Power SYBR Green Master Mix (ABI) and gene-specific primers. mRNA relative quantities were determined using the ΔΔCT method.

Cycling of genes was determined either with Two-way ANOVA looking at the effect of time or by utilizing the Metacycle package within the R statistical computing software.

Gallbladder volume quantitation: Gallbladders were harvested from animals and punctured in a 1.5 mL Eppendorf tube and spun two times at 3000 RPM for 10 min. After each centrifugation the volume was pipetted in 10, 1.0, 0.5 and 0.25 uL increments and recorded.

Metabolite Analysis: Blood glucose was measured from tail vein using a OneTouch Ultra Mini glucometer and glucose test strips. Trunk blood was collected into EDTA-coated tubes (BD Falcon) and placed on ice. Whole blood was spun for 10 min. at 4000 RCF and plasma was removed and flash-frozen in liquid nitrogen. Plasma cholesterol was measured by the Metabolic Phenotyping Core at UT Southwestern Medical Center. Liver was harvested and immediately flash frozen. Liver cholesterol was also measured by the Metabolic Phenotyping Core at UT Southwestern Medical Center.

TAIL-seq and Poly(A) tail length quantitation: Tail-seq was performed by Dr. Peng Gao in my lab according the methodology outlined by V. Narry Kim and colleagues (Chang et al., 2014). Briefly, Total RNA was isolated from flash-frozen liver samples using TRIzol. Total RNA was rRNA-depleted and a 3' biotin-labeled adapter was ligated was added followed by partial digestion with RNase T1. RNA was then pulled down with streptavidin and underwent 5' phosphorylation. RNA was gel purified, underwent 5' adapter ligation and was converted to

cDNA by reverse transcription, PCR amplified and sequenced on a MiSeq sequencing system. Following mapping to the mouse genome (MM10), I determined the Poly(A) tail length by counting the number of A nucleotides (nt) starting just before the 3' adapter and continuing towards the gene body until I encountered 3 consecutive non-A nt at which time counting stopped and the total length recorded.

Results:

Nocturnin Expression is altered by nutrient status

The expression of *Nocturnin* mRNA (*Noc*) is known to cycle in the mouse across the circadian day (Wang et al., 2001, Gilbert et al., 2011), but its response to nutrient challenges such as fasting/refeeding has not been carefully examined. *Nocturnin* mRNA displays robust rhythmicity in the mouse liver with a peak phase occurring early in the dark phase (Metacycle, JTK Cycle ,FDR<0.001) (Figure 1A, i). I explored the effect of fasting/refeeding on *Noc* expression by collecting liver samples from mice either fed RC *Ad Lib* (ZT0, 10), fasted for 10h (ZT0-10 fast) or fasted and then refed for 1h (ZT0-10 fast, refed ZT10-11) (see experimental schematic in Figure 1A, ii). The circadian rise in *Nocturnin* expression can be seen in the *Ad Lib* samples and the rise at ZT10 is blunted in animals after a 10h fast (Figure 1A, iii). *Noc* expression is significantly elevated in the liver following 1h refeeding after a 10h fast (Figure 1A, iii) (One-way ANOVA, P<0.05).

Previous studies have shown *Noc* expression to be increased in adipose tissue over successive generations of Western-like HFD in mice (Massiera et al., 2010a). However these studies provide little to no information on possible temporal changes in *Noc* expression with HFD feeding and are limited to adipose tissue, where *Noc's* amplitude of expression is low (Gilbert et al., 2011). To explore this effect in a more rigorous manner, I exposed mice to a HFD for 3 weeks and then harvested liver samples around-the-clock to examine the effect of HFD on *Nocturnin's* rhythmic profile. *Noc's* rhythmicity is maintained, but the HFD feeding has a significant effect on its expression (Two-way ANOVA, P<0.05) (Figure 1B, i). Indeed, its peak

expression is significantly elevated over that from a standard diet at ZT12 (Two-way ANOVA, Multiple Comparisons P<0.001). I performed a similar fasting/refeeding paradigm on HFD fed mice, but conducted the fasting and refeeding during the dark phase, when Nocturnin protein (NOC) is normally high (Niu et al., 2011) (see experimental schematic in Figure 1B, ii). Again, a 10h fast (ZT12-22) caused blunted levels of *Noc* expression (Figure 1B, iii). Allowing animals to refeed for 4h following a 10h fast (Fast ZT12-22, refeed ZT22-2) significantly induced *Nocturnin* mRNA (Figure 1B, iii, Two-way ANOVA P<0.05).

Altered cholesterol metabolism with loss of Nocturnin

Due to the large upregulation of *Noc* expression with HFD feeding and its acute regulation by fasting/refeeding, I sought to examine the global expression of mRNA by performing mRNA-seq on liver lysates from HFD-fed WT and $Noc^{-/-}$ mice under different nutritional challenges. I used the *Ad Lib* (FED), 10h Fast (FAST) and 10h Fast + 4h Refed (REFED) samples from the HFD paradigm described in Figure 1B, ii and 2A, i for mRNA-seq (n=3 samples/genotype/condition). Given NOC's presumed role as a deadenylase, its targets could potentially have longer Poly(A) tails and thus greater mRNA stability and abundance in the $Noc^{-/-}$ samples. The precise relationship between Poly(A) tail length and mRNA abundance is complex (Kojima et al., 2012, Subtelny et al., 2014, Kojima et al., 2015, Park et al., 2016), but I used this reasoning to first focus on the upregulated genes in the $Noc^{-/-}$ liver. I performed Gene Ontology and Functional Annotation Clustering analysis using the DAVID bioinformatics database (Huang da et al., 2009b, Huang da et al., 2009a) on the genes (n=271) significantly

upregulated in the KO mice at ZT22 I the *Ad Lib*, Fed state. The top cluster contained terms associated with cholesterol metabolism (Figure 2A, ii). Many of the genes associated with these terms belong to the cholesterol biosynthetic pathway (Figure 2B, highlighted in red). Upregulation of cholesterol biosynthetic genes might predict an increase in overall levels of cholesterol in *Noc*$^{-/-}$ mice; however I found plasma and hepatic cholesterol levels to be similar between WT and KO mice (Figure 2, i and ii). Cholesterol can be metabolized into primary bile acids in the liver and I found that genes encoding two of the key bile acid regulatory enzymes, *Cyp7a1* and *Cyp7b1*, were also upregulated in the livers of *Noc*$^{-/-}$ mice (Figure 2B).

Nocturnin regulates bile acid metabolism under HFD conditions

As the *Noc*$^{-/-}$ mice have increased expression of bile acid and cholesterol synthesis genes, but no change in systemic cholesterol levels, the increase in cholesterol biosynthesis could be a compensation for altered bile acid metabolism or vice versa. I wanted to investigate the temporal dynamics of these processes further and so I compared the Fed and Fasted RNA-seq data from my HFD animals. This allowed me to compare genes that show changes under different nutrient conditions (Fed vs Fast) at similar circadian times (ZT22). I again focused on genes significantly upregulated in the KO as these could be potential targets of NOC's deadenylase activity. I found a large number of genes uniquely upregulated in the *Noc*$^{-/-}$ mice in the fasted vs. fed state (Figure 3A, ii). I performed gene ontology analysis with the genes from this KO-unique set and one of the top categories was termed "Bile Acid Biosynthetic Process" and contained *Cyp7a1*, the enzyme responsible for 75% of primary bile acid synthesis in the liver (Figure 3A, ii). *Cyp7a1*

and another bile acid synthesis gene, *Cyp7b1*, were identified in the gene ontology analysis from genes unique downregulated in the KO transitioning between the FAST and REFED state (Figure 3A, iii). Both *Cyp7a1* and *Cyp7b1* show increased expression in the FED and FAST state, though they return to WT levels after 4h refeeding (One-way ANOVA, $P<0.05$) (Figure 3B, i and ii). To examine the dynamics of *Cyp7a1* regulation in response to fasting and refeeding, I also measured its expression in WT and KO animals at 1h refeeding following a fast. The level of *Cyp7a1* remains significantly elevated above WT levels at 1h refeeding (One-way ANOVA, $P<0.001$) but shows similar expression to that of WT mice at 4h refeeding. These data demonstrate that mice lacking *Noc* have an impaired response of bile acid metabolism during the dynamic transition between different metabolic states (i.e. Fed/Fast/Refed) whereby they are overproducing bile acids in the fed and fasted states and show a slowed response to inhibiting bile acid production with refeeding following a fast.

Gallbladder volume is altered in mice lacking Nocturnin

Nocturnin clearly plays a role in cholesterol and bile acid metabolism under dietary-challenged conditions (HFD, Figure 2 and 3), possibly through regulation of bile acid and/or cholesterol synthesis gene expression. Primary bile acids are produced in the liver and stored in the gallbladder for release into the small intestine upon nutrient ingestion. With the upregulated expression of bile acid synthesis genes in *Noc*$^{-/-}$ mice, I predicted altered filling of the gallbladder as a phenotypic result. To test this, I examined gallbladder volumes of mice undergoing a fasting/refeeding protocol (food removed from ZT0-ZT10 and refeeding occurring from ZT10-

ZT11) on a HFD background and found that *Noc*$^{-/-}$ mice had significantly increased gallbladder volumes after 1h refeeding following a 10h fast (Figure 4A, i) (Student's t-test, ****, P<0.0001). The mean difference in gallbladder volume between the fasted and refed states for the WT and KO animals is only ~1uL (Figure 4A, ii), not enough to account for the ~5uL difference in the refed state. In order to determine whether this is a diet-specific effect I compared the gallbladder volumes of mice undergoing the fast/refeed paradigm after RC conditions as well. Similarly, *Noc*$^{-/-}$ animals on RC show increased gallbladder volumes following 1h refeeding after a fast (Figure 4B) (Student's t-test, *, P<0.05). Additionally, *Noc*$^{-/-}$ mice have significantly elevated gallbladder volumes at 10h fasting under RC feeding (Student's t-test, *, P<0.05) and a similar trend with HFD feeding. Again, the mean difference in gallbladder volumes between the fasted and refed states was nearly identical between WT and KO animals (Figure 4B, ii), indicating that *Noc*$^{-/-}$ animals are likely overfilling their gallbladders in the fasted state, rather than having impairments with bile acid release.

Loss of Nocturnin alters the temporal dynamics of bile acid production and Poly(A) tail length

Loss of *Nocturnin* appears to dramatically alter bile metabolism regardless of diet. An important component of bile acid synthesis underlying my fasting/refeeding paradigm is the time of day, or circadian phase, and so I examined whether circadian disruption might occur in bile acid synthesis in *Noc*$^{-/-}$ mice. To do this I harvested livers and gallbladders from WT and *Noc*$^{-/-}$ mice around-the-clock under *Ad Lib*, RC fed conditions. The gallbladder shows a robust rhythm in volume in WT and *Noc*$^{-/-}$ mice (Figure 5B, i) (Two-way ANOVA, effect of time P<0.001).

Noc$^{-/-}$ display a significantly altered rhythm in gallbladder volume (Two-way ANOVA, effect of genotype $P<0.05$) and consistently showed larger gallbladder volumes across the circadian cycle with the largest magnitude difference reaching significance at ZT9 (Two-way ANOVA, multiple comparisons $P<0.05$) (Figure 5B, i). As primary bile acids are synthesized from cholesterol in the liver, I also examined hepatic cholesterol levels. Cholesterol levels cycle in both WT and KO liver (Figure 5A, i) (Two-way ANOVA, effect of time $P<0.01$) but the overall profile is altered. Early in the light phase, when KO gallbladder volumes begin to rise above WT levels, the hepatic cholesterol levels in the KO dip below WT. They then show an increase in cholesterol that moderately overshoots WT levels late in the late phase, thus increasing the absolute amplitude of the KO cholesterol rhythm. Levels of cholesterol in the plasma were unchanged between WT and KO mice (Appendix I, Figure 1A).

Using mRNA-seq I examined the expression of both cholesterol and bile acid synthesis genes in WT and KO liver across the circadian cycle. *Farnesyl diphosphate synthase* (*Fdps*), which is involved in cholesterol synthesis, does not show cycling at the mRNA level in the WT liver but does have a peak in expression in the KO at ZT18 (Figure 5A, ii). Several other genes involved in cholesterol synthesis show altered expression patters in the KO liver. *HMG-CoA reductase* (*Hmgcr*) expression is shifted with a peak occurring at ZT18 and, similar to *Fdps*, *Squalene epoxidase* (*Sqle*) shows no cycling in the WT but has a sharp peak in expression at ZT18 in the KO (Appendix I, Figure 2A-C, i). CYP7A1, the protein encoded by the *Cyp7a1* gene, accounts for approximately 75% of the bile acid pool size and catalyzes the first and rate-limiting reaction of classical bile acid synthesis (Russell and Setchell, 1992, Schwarz et al.,

1996, Schwarz et al., 1998, Schwarz et al., 2001). *Cyp7a1* shows similar mRNA peak expression in WT and KO liver across the light:dark transition. There is an additional peak of expression in the KO late in the dark phase at ZT21 (Figure 5B, ii). Gene expression of additional members of the bile acid synthesis pathway is similar throughout the circadian cycle except for the late dark/early light phase where the expression is higher in the KOs (Appendix I, Figure 3A-C, i).

To explore whether these cholesterol and/or bile acid synthesis genes are potential targets of NOC via its deadenylase activity I collaborated with Dr. Peng Gao to perform TAIL-seq, which allows us to assess the Poly(A) tail length of mRNAs (Chang et al., 2014). I examined the Poly(A) tail length of *Fdps* and found that the long-tail Poly(A) forms (>100 nt) were specifically regulated between ZT12 and ZT0 in WT liver with a marked decrease in long-tail forms between ZT12 and ZT18 and an increase occurring between ZT18 and ZT0. In contrast, the *Fdps* Poly(A) species in KO liver lose the regulation between ZT12 and ZT18 and there is an increase in the long-tail Poly(A) forms in the KO at ZT18 (Figure 5A, iii). The KOs still show an increase in long-tail forms between ZT18 and ZT0 and this increase keeps the long-tail forms at a higher level than WTs at ZT0 and ZT6.

The length of the mRNA Poly(A) tail has long been thought to correspond to transcript stabilization and translation efficiency with longer Poly(A) tail lengths associated with increased stabilization and translation (Zhang et al., 2010b, Weill et al., 2012). The definitive cutoffs for absolute “long” and “short” designations as they relate to translation have been challenged recently (Subtelny et al., 2014, Park et al., 2016). To help address the relationship between the

temporal Poly(A) tail length dynamics that I measured and the corresponding translation efficiency, I examined publically available Ribo-seq and Total RNA-seq data sets (Janich et al., 2015, Janich et al., 2016). For *Fdps*, there is an increase in translation between ZT18 and ZT0 and this corresponds with the increased frequency of long Poly(A) tail length mRNA forms that I measure in the WT (Appendix I, Figure 2A, i-iii). This correlation then implies that the increased Poly(A) tail length of *Fdps* in the KO throughout the late dark/early light phase could result in greater *Fdps* translation and thus increased cholesterol synthesis. There also appears to be regulation of *Hmgcr* and *Sqle* Poly(A) tail lengths across the circadian cycle, however the time resolution of the TAIL-seq data makes it less clear how these changes relate to the observed phasing of translation (Appendix I, Figure 2B-C, i-iii).

When I analyzed the Poly(A) tail length of *Cyp7a1* in WT liver I found a progressive increase in the long-tail forms (Poly(A) >100nt) during the light phase with a peak at ZT12 (Figure 5B, iii), corresponding to the peak in mRNA expression (Figure 5B, ii) and translation (Appendix I, Figure 3A, i-iii). While the KO *Cyp7a1* mRNA levels maintained a similar profile to WTs early in the light phase, the peak in long-tail Poly(A) species at ZT12 was decreased. An increase in the long-tail Poly(A) species was observed at ZT18 and ZT0 in the KOs. *Cyp7b1* in WT liver also has a peak in translation at ZT12 and this also correlates with its maximal frequency in long Poly(A) tail forms (Appendix I, Figure 3B, i-iii). *Cyp8b1*, which has a near anti-phasic expression compared to Cyp7a1, also has long Poly(A) tail length rhythm that is opposite that of *Cyp7a1* in WTs. For the *Cyp8b1* mRNAs, the frequency of long Poly(A) tail forms peaks between ZT18 and 0 and this correlates with maximal translation (Appendix I,

Figure 3C, i-iii). While a peak in long Poly(A) tail frequencies still occurs between ZT18 and ZT0 for *Cyp8b1* in KOs, the frequency is much lower at ZT18, creating a large absolute amplitude change between these timepoints.

I examined other components of the enterohepatic feedback system that regulate bile synthesis. *Nr1h4* (*Fxr*) and *Nr0b2* (*Shp*) are both involved in the negative regulation of bile acid synthesis as hepatic bile acids act as ligands for farnesoid X-receptor (FXR) and increase *Shp* expression which in turn inhibits *Cyp7a1* expression (Russell, 2003). *Fxr* and *Shp* show similar patterns of expression in both WT and KO liver (Appendix I, Figure 4A-B, i), though ileal *Fxr* may be more critical for regulation of *Cyp7a1* (Kim et al., 2007). Regardless, they each show changes in Poly(A) tail length across the circadian cycle in the liver and the regulation throughout the light phase is similar in both WT and KO. While the TAIL-seq data only covers the liver, I wanted to examine Fgf15 expression in the liver as it is a key factor in regulation bile acid synthesis (Inagaki et al., 2005). I measured *Fgf15* mRNA expression in the ileum of WT and KO mice by qPCR and the general phasing was again similar between genotypes (Appendix I, Figure 4C, i). KO animals do show a small increase in *Fgf15* expression late in the dark phase (ZT18-21) which persists into the early portion of the light phase (ZT0). Interestingly, while *Noc* is expressed in the ileum, it does not show over rhythmicity (Appendix I, Figure 4D). Gallbladder filling is stimulated in part by activation of the G-protein-couple cell surface receptor TGR5 (Li et al., 2011), but I found no change in the expression level of *Tgr5* mRNA in the gallbladders of WT and KO mice at ZT9 (Appendix I, Figure 4E), the timepoint when gallbladder volume is at its maximum in KO mice (Figure 5B, i).

Discussion

Synchrony between an organism's internal and external environment is vital to maximize energy utilization and storage. Coordination of internal metabolic processes is important when nutrient availability is dependent on time-of-day. The molecular machinery of the circadian system works well for this, employing myriad mechanisms to maintain proper regulation of metabolic flux. My studies bring a new mechanistic gear to this machinery through Nocturnin's temporal regulation of Poly(A) tail length dynamics.

I first demonstrated that *Noc's* circadian expression can be modified by nutrient status in liver tissue (Figure 1A, B). *Noc* functions as an immediate early gene (Garbarino-Pico et al., 2007) and belongs to a select few genes that are able to maintain rhythmicity in the liver when the core clock within hepatocytes is disrupted (Kornmann et al., 2007). My data is consistent with this and demonstrates that *Noc* can show both acute and temporal responses to nutrient influx. My data further define a metabolic window in which NOC expression may be necessary. It was previously reported that *Nocturnin* mRNA expression in the liver was not altered by a fast or refeeding Regular Chow (Gilbert et al., 2011). This study used a fasting paradigm that was slightly more extreme by fasting animals overnight and refeeding them for 2 h during the early portion of the light phase. My paradigm mimicked the more natural fasting period during the light phase and examined the ability of *Nocturnin* to be induced beyond its normal circadian levels. My results show that *Noc* mRNA levels are induced above their circadian threshold in the RC state after just 1 h refeeding Regular Chow (Figure 1A, iii). If I challenged the mice first with HFD feeding and then fasted them throughout the night and refed them at a time of the circadian cycle when *Nocturnin* mRNA expression is normally low (late dark phase), I again

observed an induction of *Nocturnin* (Figure 1B, iii). These data point towards a complex, yet important, regulatory process whereby Nocturnin is responsive to nutrient in a temporal and nutrient-specific manner. As NOC is a deadenylase, an important mechanistic step in determining its metabolic function is identifying its targets.

High fat diet has a profound effect on *Nocturnin* expression (Figure 1B, i and iii) and it is known that loss of Nocturnin can confer resistance to diet-induced obesity and hepatic steatosis (Green et al., 2007). I therefore wanted to search for potential targets of NOC in a temporal and nutrient-specific condition where NOC function may be most important. I chose to look at the hepatic transcriptome in WT and $Noc^{-/-}$ mice by mRNA-seq in the HFD condition and in a normal and nutrient-challenged state (Fed/Fast/Refed). Given Nocturnin's normal expression profile, and the large induction with HFD feeding, I harvested livers from WT and $Noc^{-/-}$ mice during the dark phase when NOC protein is high (Niu et al., 2011). I found a large upregulation of mRNAs involved in cholesterol biosynthesis (Figure 2A, B). However, when I examined plasma and hepatic levels of cholesterol, I found no change in their levels between WT and KO animals (Figure 2C). I hypothesized that cholesterol synthesis could be upregulated as a compensatory mechanism if cholesterol were being pulled out by another pathway.

In the liver, cholesterol is used to produce primary bile acids and my RNA-seq data revealed that the rate limiting enzyme for bile acid synthesis, *Cyp7a1* (Schwarz et al., 1998, Russell, 2003), was indeed upregulated as well (Figure 2B). This led me to focus on bile acid synthesis and I explored my RNA-seq data further by comparing genes upregulated in the Fed and Fast states between WT and $Noc^{-/-}$ mice. From this I was able to identify a large class of uniquely upregulated genes in KO animals transitioning between the Fed and Fast states (Figure

3A, ii). Contained in this group was *Cyp7a1*. I also examined the gene changes between the Fast and Refed states and found a large category of uniquely downregulated genes in the KO liver. *Cyp7a1* and *Cyp7b1* both appeared in this group (Figure 3A, iii) and showed altered dynamics in response to the metabolic transitions occurring between Fed → Fast → Refed (Figure 3B), namely increased expression in the fasting condition and unique downregulation with 4h refeeding. This altered regulation in *Noc*$^{-/-}$ mice is especially obvious when looking at *Cyp7a1* levels in the intermediate 1h and 4h Refed periods (Figure 3C). Whereas WT mice show little responsiveness of *Cyp7a1* to the refeeding, *Noc*$^{-/-}$ mice show an elevation in *Cyp7a1* that takes 4h of refeeding to return to WT levels. It is within this dynamic metabolic transition that NOC, via its deadenylase activity, could be functionally important.

Because CYP7A1 accounts for the majority of bile acid synthesis, it's increased expression in *Noc*$^{-/-}$ mice could result in greater bile acid production and storage in the gallbladder. I measured the gallbladder volumes of *Noc*$^{-/-}$ mice and found significantly elevated volumes in the Refed state following a Fast after HFD feeding (Figure 4A, i). The same phenotype exists on a regular chow background and the volume is significantly elevated in the fasted state as well (Figure 4B, i). If I calculate the gallbladder volume "release" as a difference between the Fast and Refed volumes for each genotype, the WT and KO volume "release" is similar (Figure 4A, ii and Figure 4B, ii). This would indicate that the volume difference is coming through increased bile acid production during the fasting period, rather than a deficit in bile acid release upon feeding.

Underlying the gallbladder filling in this Fast/Refed protocol is the normal circadian cycling of cholesterol and bile acid metabolism. WT and *Noc*$^{-/-}$ mice have hepatic cholesterol

levels that cycle throughout the circadian day though the KO profile has some notable temporal alterations (Figure 5A, i). In the *Noc*$^{-/-}$ liver the cholesterol levels begin to dip below that of WT early in the light phase. In the middle/late light phase the KO levels appear to increase above WT and this may be a compensatory upregulation in cholesterol synthesis. In the early portion of the light phase the levels between the WT and KO mice are similar before the KOs again begin to show a decrease late in the dark phase. Alterations in cholesterol metabolism appear to be happening locally within the liver as plasma cholesterol is similar in WT and *Noc*$^{-/-}$ mice (Appendix I, Figure 1A).

An explanation for this pattern in the KO can be explained in part by comparing cholesterol cycling with the temporal profile of gallbladder filling and release. Similar to the increased gallbladder volumes *Noc*$^{-/-}$ mice display with acute fasting (Figure 4), *Noc*$^{-/-}$ mice also have increased gallbladder volumes throughout the light phase (Figure 5B, i). As primary bile acids are synthesized from cholesterol in the liver, the dip in cholesterol levels early in the light phase could be coming from increased bile acid synthesis and gallbladder filling. To compensate, the KOs may increase cholesterol synthesis and this could produce the small increase in cholesterol that occurs late in the light phase. Feeding triggers a release of bile acid from the gallbladder into the proximal small intestine and those bile acids are recycled in the distal small intestine where they can return to the liver and inhibit bile acid synthesis. As the animals begin to feed early in the dark phase both cholesterol and gallbladder volumes are similar in WT and *Noc*$^{-/-}$ mice. Late in the light phase KO mice again show a dip in cholesterol levels at ZT21, preceding the increase in gallbladder volume that is observed.

In order to determine whether any of the key genes involved in cholesterol and bile acid metabolism are targets of NOC, I measured their overall transcriptional changes via mRNA-seq and their Poly(A) tail length via TAIL-seq. Many of the genes involved in cholesterol synthesis exhibit altered phasing in *Noc*$^{-/-}$ liver with peaks in mRNA expression late in the dark phase at ZT18 (Figure 5A, ii and Appendix 1 Figure 2A-C). In the *Noc*$^{-/-}$ liver, more *Fdps* mRNAs maintain long Poly(A) tails at ZT18-ZT0 and this keeps the frequency of those long-tailed forms elevated in *Noc*$^{-/-}$ liver over WT levels throughout the early light phase. As longer Poly(A) tails has been associated with increased translation (Zhang et al., 2010b, Weill et al., 2012, Kojima et al., 2012), then this might be an mechanistic explanation for the disrupted cholesterol metabolism that *Noc*$^{-/-}$ mice display.

NOC could be acting specifically on cholesterol synthesis targets and/or bile acid synthesis targets and so I examined the major bile acid synthesis genes as well. While the mRNA abundance of *Cyp7a1*, *Cyp7b1* and *Cyp8b1* was generally similar across the circadian day in both WT and KO liver, there was a strikingly consistent alteration of Poly(A) tail length in the KOs (Figure 5B and Appendix I, Figure 3A-B). All of these genes had elevated frequencies of the long Poly(A) forms in the ZT18-ZT0 range. This loss of regulation of the Poly(A) tail length corresponds with the peak in NOC expression (Niu et al., 2011). This dramatic change in Poly(A) tail length dynamics of the bile acid synthesis genes, combined with the lack of change in any of the components of the negative feedback machinery mediating this process (Appendix I Figure 4A-E), point towards a mechanism whereby NOC regulates bile acid synthesis rather than inhibition.

My work has helped elucidate a role for Nocturnin in mediating metabolic regulation in times of nutrient flux. In the normal *Ad Lib*, Fed, conditions Noc expression peaks during the dark phase as they are experiencing a metabolic transition from catabolism to anabolism. If I acutely fast and refeed mice, I see a similar pattern of *Nocturnin* expression where *Noc* is lower with nutrient deprivation (fasting) and higher or induced with nutrient influx (refeeding). In searching out potential targets of NOC, I have identified a new metabolic phenotype in $Noc^{-/-}$ mice whereby they have significantly elevated gallbladder volumes throughout the light phase. This is preceded by changes in Poly(A) tail length of mRNAs encoding key metabolic regulators of bile acid and cholesterol synthesis, namely *Cyp7a1* and *Fdps*, respectively which could be direct targets of NOC. It will be worthwhile to explore this phenotype further by reintroducing a *Nocturnin* transgene to $Noc^{-/-}$ animals specifically in the liver to see whether the increase in gallbladder volume that animals lacking Nocturnin display can be reversed. Additionally, it will be important to utilize tissue-specific KO mice to see if loss of Nocturnin specifically within the liver produces the same changes in Poly(A) tail length of metabolic regulators such as *Cyp7a1* that the global $Noc^{-/-}$ display. Bile acids are increasingly seen as important intracellular signaling molecules, for instance through acting as ligands for FXR in the liver (Kuipers et al., 2014). The bile acid pool is known to oscillate both in size and composition (Zhang et al., 2011), and so understanding how Nocturnin regulates the synthesis and regulation of bile acids in temporal and nutrient-challenged conditions will help understand how organisms maintain metabolic synchrony.

Chapter II Figures

Figure 1

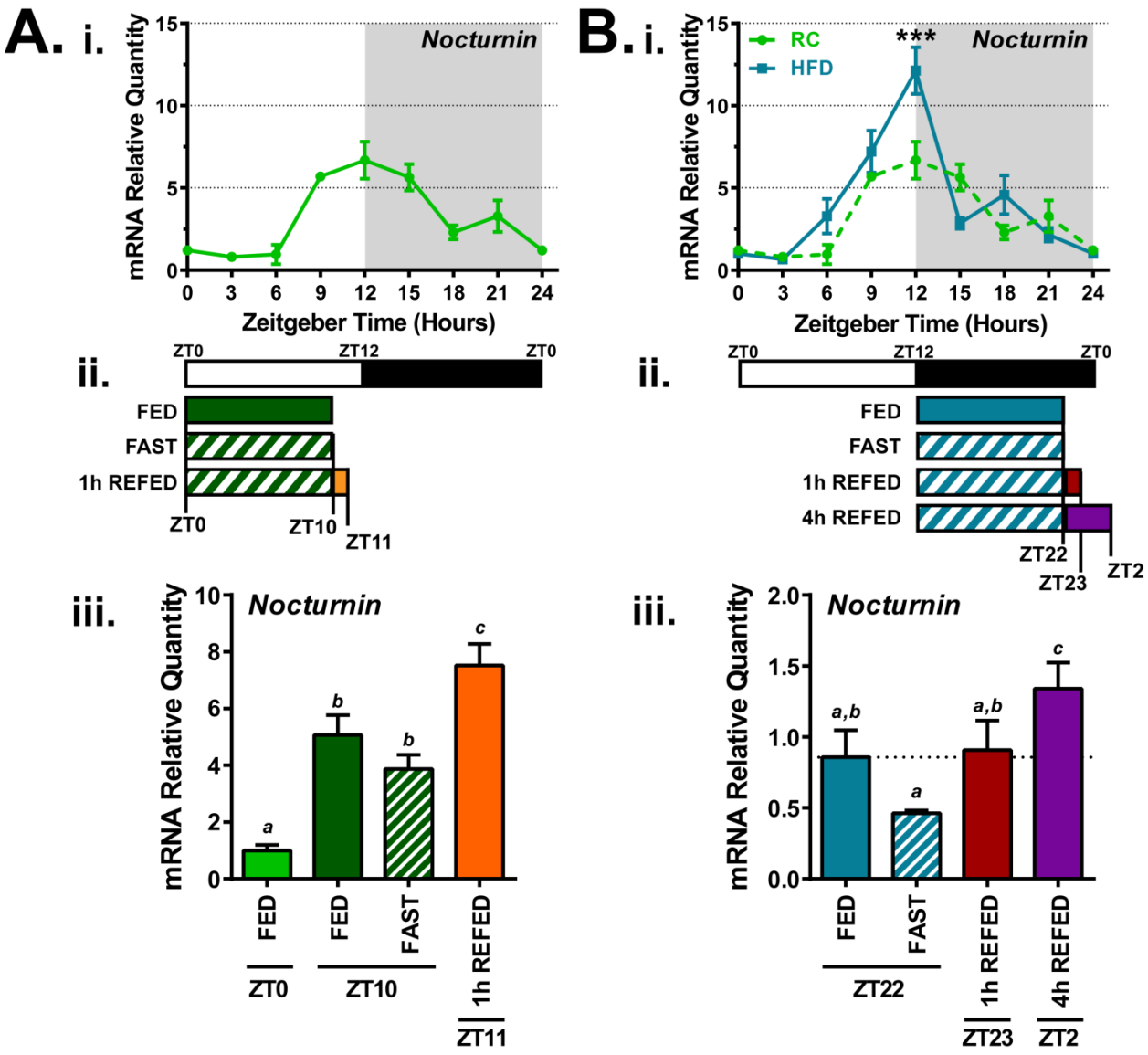

Figure 1. Hepatic expression of *Nocturnin* is altered by nutrient status
Hepatic *Nocturnin* mRNA (*Noc*) expression is modified by diet and the Fed/Fast/Refed states. Data points represent mean +/- SEM. Unless otherwise noted, statistical comparisons were made with One-way ANOVA and multiple comparison with different letters indicating statistically significant values at $P<0.05$. (A, i) Hepatic *Noc* expression from wildtype (WT) mice that were fed regular chow (RC) diet and had livers harvested at 3h intervals around the clock starting at

ZT0 (n=3-4/timepoint). The ZT0 timepoint has been double-plotted as both ZT0 and ZT24 for clarity. (A, ii) Schematic of the Fed/Fast/Refed paradigm used for animals on RC diet. Fasted animals were fasted for 10h with RC food removed at ZT0. 1h Refed animals were fasted for 10h with RC food removed at ZT0 and replaced at ZT10 for 1h. (A, iii) *Nocturnin* mRNA expression at different circadian times in either the Fed, Fast or 1h Refed state. (B, i) *Noc* expression from the RC condition is replotted from (A, i) and shown as a dashed line. *Noc* from WT animals fed a high fat diet (HFD) (Research Diets, D12492i, 60% kcal from fat) for 3 weeks and livers harvested at 3h intervals around the clock starting at ZT0 (n=4/timepoint). The ZT0 timepoint has been double-plotted as both ZT0 and ZT24 for clarity. *Noc* expression at ZT12 on HFD is significantly increased over ZT12 on RC (Two-way ANOVA, multiple comparisons $P<0.001$). (B, ii) Schematic of the Fed/Fast/Refed paradigm used for animals on HFD diet. Fasted animals were fasted for 10h with HFD food removed at ZT12. Refed animals were fasted for 10h with HFD food removed at ZT12 and replaced at ZT22 for either 1h (1h Refed) or 4h (4h Refed). (B, iii) *Noc* expression at different circadian times in either the Fed, Fast, 1h Refed or 4h Refed state.

Figure 2

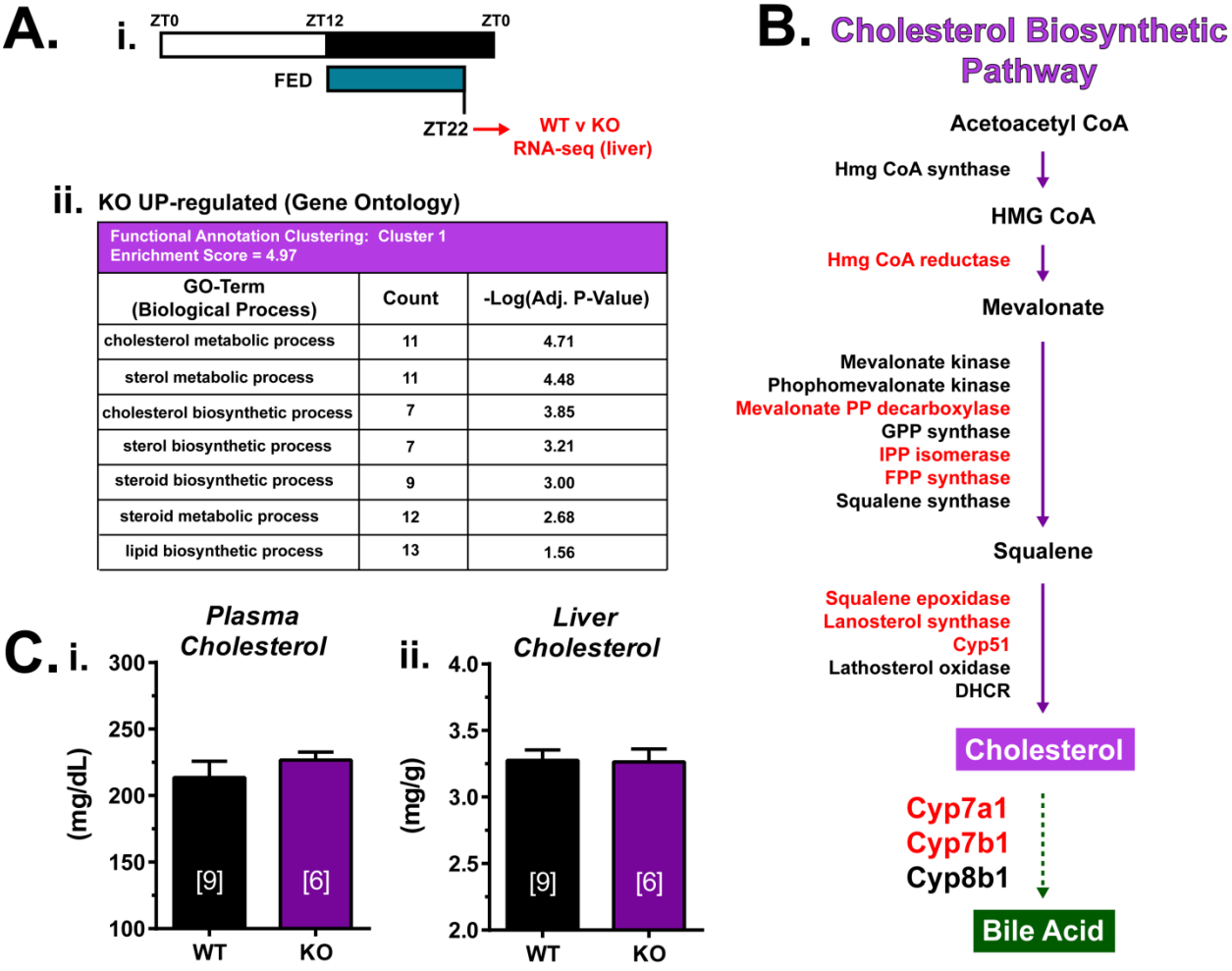

Figure 2. Altered expression of cholesterol and bile acid synthesis genes in *Noc*$^{-/-}$ mice
mRNA-seq from livers of WT and *Noc*$^{-/-}$ (KO) animals on a HFD revealed upregulation of genes associated with cholesterol biosynthesis, but did not change plasma or hepatic levels of cholesterol. Genes associated with bile acid synthesis were also upregulated in KO livers. (A, i) Schematic showing that livers were harvested from WT and KO animals on HFD at ZT22 (n=3/genotype) for mRNA-seq analysis. (A, ii) Genes significantly upregulated in KO samples were examined by Functional Annotation Clustering using the DAVID Bioinformatic Resources based on Biological Process terms. (B) Genes appearing in the Functional Annotation Clustering from (A, ii) are highlighted in red and shown in the cholesterol biosynthetic and bile acid pathways. (C, i-ii) Plasma and liver cholesterol levels were measured in WT (n=9) and KO (n=6) mice at ZT22 on HFD. Bars represent the mean +/- SEM.

Figure 3

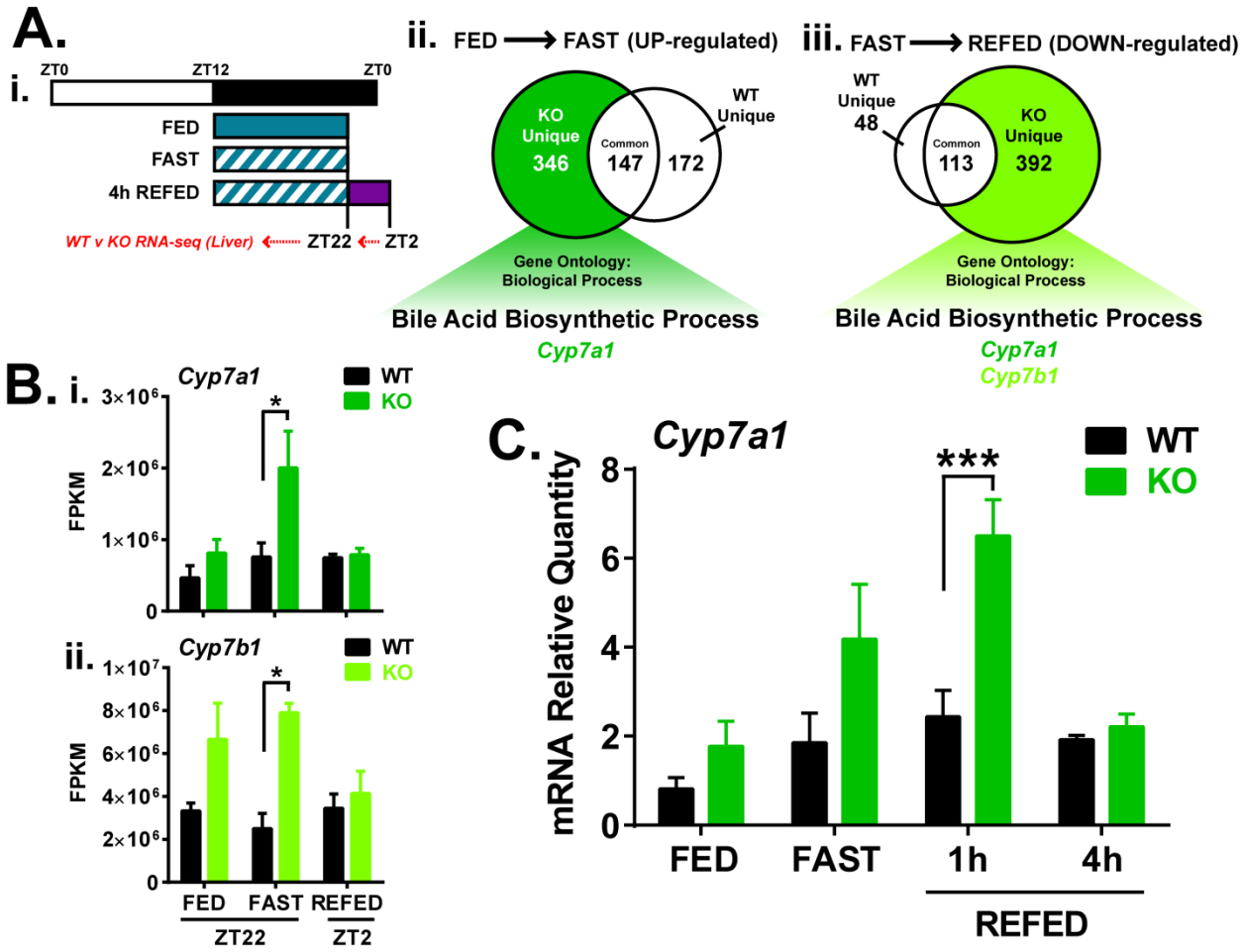

Figure 3. Increased expression of bile acid synthesis genes in mice lacking *Nocturnin*
Gene expression changes during the metabolic transition from the Fed to Fast state was measured by performing mRNA-seq on livers from WT and *Noc*$^{-/-}$ (KO) animals after 3 weeks HFD in either the *Ad Lib* (Fed), 10h Fast (Fast), or 4h Refed (Refed) state. (A, i) Schematic showing when tissues were collected in relation to the light:dark cycle and feeding condition. (A, ii-iii) Genes either up or downregulated in WT or KO liver were compared to see both common and unique regulation. Gene ontology based on Biological Process terms was performed on the KO unique genes and the term "Bile Acid Biosynthetic Process" appeared in both groups. (B, i-ii) The expression of Cyp7a1 and Cypb1 genes is shown as the Fragments Per Kilobase of Exon Per Million Mapped Reads (FPKM) mean +/- SEM in the Fed, Fast and Refed conditions. (C) qPCR was performed to examine *Cyp7a1* expression in the liver from the samples collected for mRNA-seq (Fed, Fast, 4h Refed) and the 1h Refed condition was examined as well (n=3-5/timepoint/genotype). Bars represent Mean +/- SEM.

Figure 4

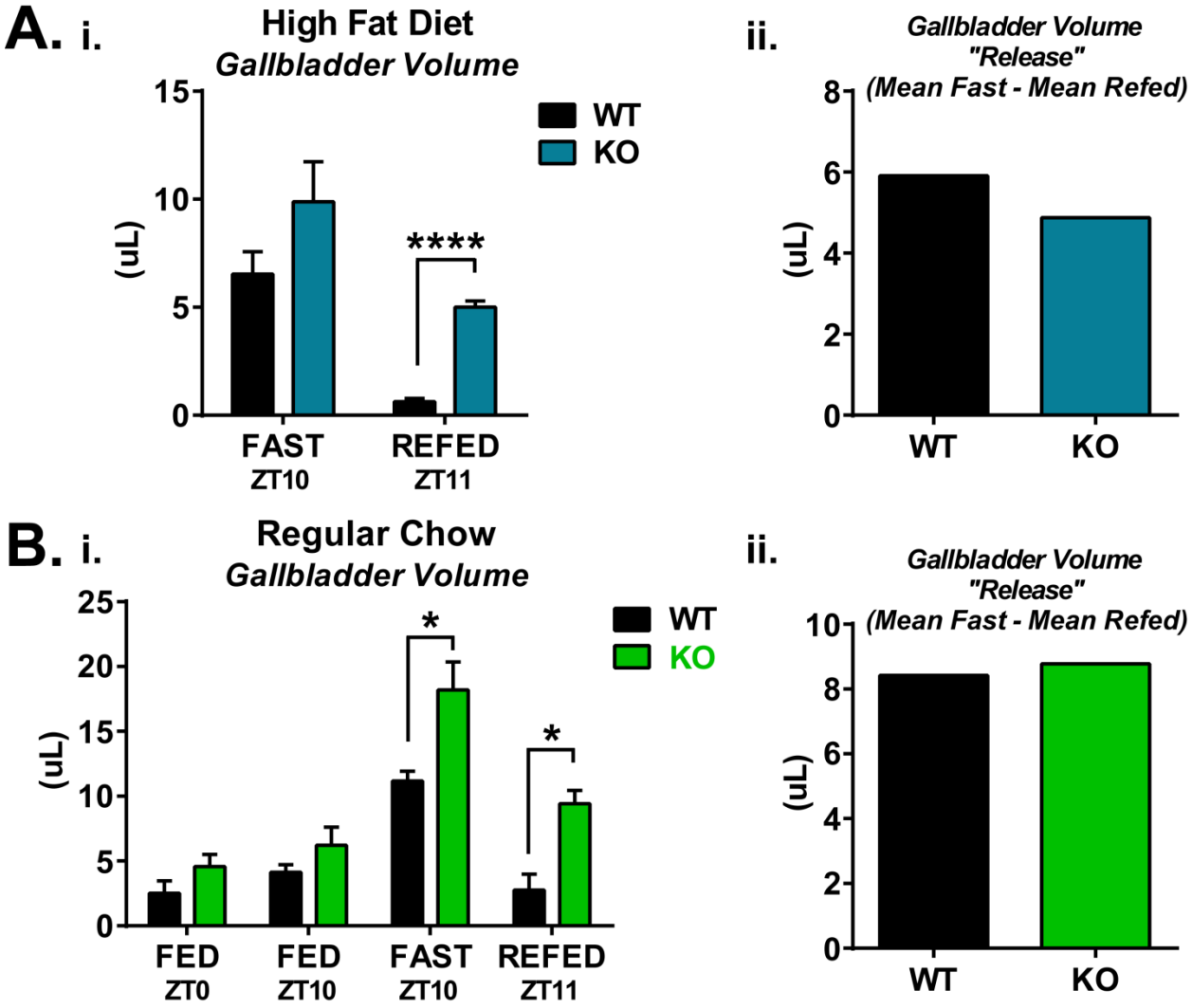

Figure 4. ***Noc*$^{-/-}$ mice have increased gallbladder volumes with fasting**
Mice lacking *Nocturnin* (*Noc*$^{-/-}$, KO), when subjected to a 10h fast, have increased gallbladder volumes and this increase persists through 1h refeeding following the fast. (A, i). WT and KO mice were fed a HFD for 3 weeks and fasted for 10h starting at ZT0. Gallbladders were collected and volume measured at ZT10 in the fasted condition (n=4-7 mice/genotype) or were Refed for 1h following a 10h fast (n=3-4/genotype). Bars represent Mean +/- SEM. (B, i) Gallbladders were harvested and volume measured as in (A) but animals (n=3-10/genotype/condition) were on regular chow background. Bars represent Mean +/- SEM (A, ii and B, ii) Gallbladder release was determined by subtracting the Mean of the Refed condition from the Mean of Fast condition for each genotype.

Figure 5

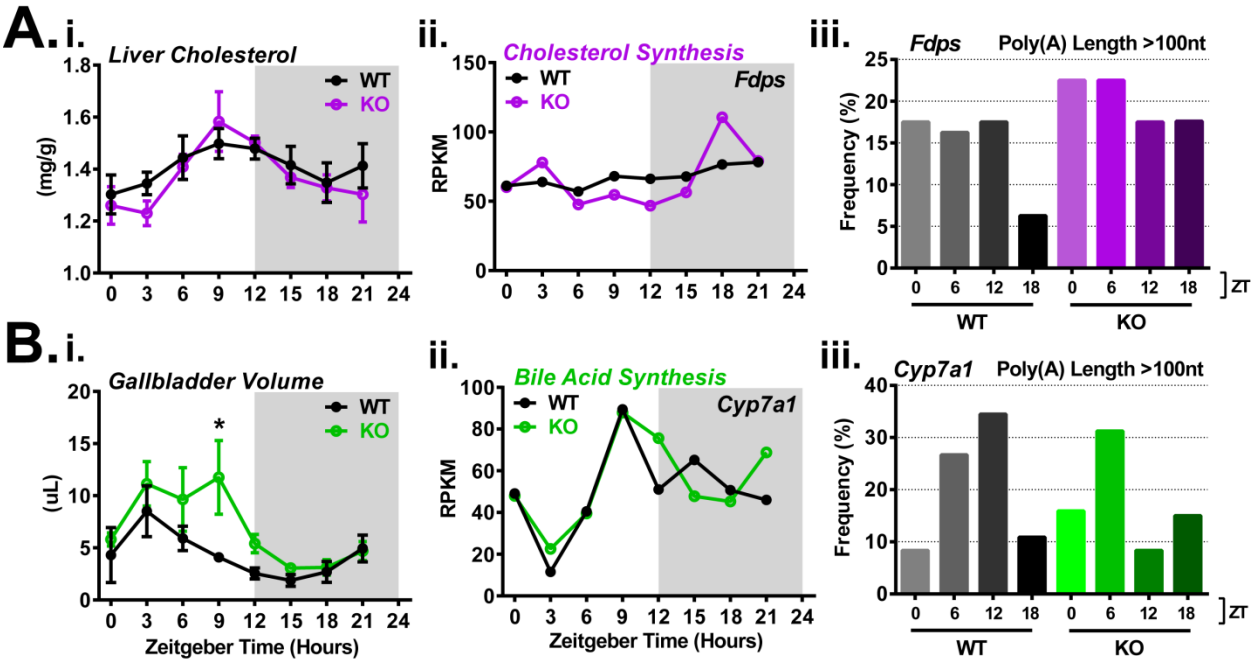

Figure 5. Loss of *Nocturnin* alters temporal dynamics of cholesterol and bile acid metabolism

Mice lacking *Nocturnin* (*Noc*$^{-/-}$, KO) have increased gallbladder volumes during the light phase of the circadian cycle. KO mice also have disrupted phasing of cholesterol synthesis genes and this may in part be due to altered Poly(A) tail length of genes involved in cholesterol and bile acid synthesis. (A, i and B, i) Liver and gallbladder were collected from WT and KO mice and liver cholesterol and gallbladder volume quantified (n=4-5/genotype/timepoint). Data points represent Mean +/- SEM. (A, ii and B, ii) mRNA-seq was performed on liver mRNA from WT and KO animals (n=2/genotype/timepoint). Normalized Reads Per Kilobase Per Million Mapped Reads (RPKM) is shown for *Fdps* and *Cyp7a1* genes. Data points are the Mean of two biological replicates at each timepoint for each genotype. (A, iii and B, iii) TAIL-seq was formed on liver mRNAs (n=1/genotype/timepoint) and plotted as the Frequency (%) of transcripts for each gene that were quantified as having a Poly(A) tail length greater than 100 nucleotides (>100 nt). For *Fdps*, 80-160 transcripts were counted per genotype at each timepoint. For *Cyp7a1* n=18-46 transcripts per genotype were counted at each timepoint.

Chapter III: Loss of the circadian deadenylase Nocturnin results in insulin resistance

Introduction

Nutrient availability in a cyclic environment necessitates a partitioning of metabolic processes into distinct temporal windows. Organisms have developed a circadian system to predict and anticipate these rhythmic changes through coordination of their internal environment with their external surroundings. Existing in nearly every cell of the body, the mammalian circadian clock consists of a series of interlocked transcription/translation feedback loops whose molecular outputs generate ~24h rhythms in physiology and behavior. The master clock is located in a region of the hypothalamus called the Suprachiasmatic Nucleus (SCN) which sits above the optic chiasm and receives light information from the eyes via the retino-hypothalamic tract (reviewed in (Ko and Takahashi, 2006)). Through chemical and hormonal outputs, cells of the SCN are able to synchronize the circadian machinery in cells of the periphery.

The importance of the circadian clock in maintaining metabolic synchrony has been shown through a variety of genetic manipulations in which disruption of the core clock leads to altered lipid and glucose metabolism leading to conditions such as obesity and diabetes (Turek et al., 2005, Lamia et al., 2008, Marcheva et al., 2010, Lamia et al., 2011). It is therefore necessary to understand the different mechanisms by which the circadian system interacts with and regulates peripheral metabolic rhythms. The core clock transcription factors CLOCK and BMAL have been found to bind to and regulate rhythmic expression of a wide variety of metabolic pathways in the liver (Koike et al., 2012, Le Martelot et al., 2012, Vollmers et al.,

2012). The mechanisms behind rhythm generation are complex as it is estimated that up to ~10% of the transcriptome in liver is rhythmic (Panda et al., 2002, Storch et al., 2002, Koike et al., 2012, Le Martelot et al., 2012, Menet et al., 2012, Vollmers et al., 2012) whereas ~20% of the hepatic proteome displays circadian cycling (Reddy et al., 2006, Robles et al., 2014). The contribution of posttranscriptional and posttranslational rhythms is emerging as an important contributor to molecular cycling (Kojima et al., 2012) and thus needs to be studied to help understand how the circadian coordination of metabolism takes places.

One form of posttranscriptional modification that is under circadian control is deadenylation (Kojima et al., 2011, Kojima et al., 2012). The 3' UTR of mRNAs is co-transcriptionally modified to contain adenosine residues constituting a Poly(A) tail which helps facilitate translation initiation (Zhang et al., 2010b, Weill et al., 2012). The Poly(A) tail length is tightly regulated and one class of enzymes that can modulate Poly(A) tails are deadenylases which are exonucleases that remove adenosine residues from the 3' UTR of mRNAs. *Nocturnin* (*Noc*, official gene symbols *Noct, Ccrn4l*) encodes a protein (NOC) which belongs to this class of deadenylase family members and has exonuclease activity and can remove Poly(A) tails (Green and Besharse, 1996, Baggs and Green, 2003, Garbarino-Pico et al., 2007). *Nocturnin* expression cycles with a peak in mRNA at the light:dark transition in the early dark phase and a protein peak in the mid-late dark phase (Niu et al., 2011). Specific targets of NOC have not been identified, though NOC has been implicated in a variety of metabolic processes such as lipid and glucose metabolism, adipogenesis and osteogenesis (Stubblefield et al., 2012).

Mice lacking *Nocturnin* (*Noc*$^{-/-}$, KO) are resistant to diet-induced obesity (DIO) and hepatic steatosis (Green et al., 2007). This phenotype is due in part to reduced lipid trafficking through enterocytes of the small intestine (Douris et al., 2011). It was also reported that *Noc*$^{-/-}$ have altered glucose tolerance and insulin sensitivity (Green et al., 2007), though a precise mechanism by which NOC contributes to glucose/insulin metabolism has not been rigorously investigated. I chose to explore this phenotype further by performing hyperinsulinemic-euglycemic clamps in WT and *Noc*$^{-/-}$ mice to definitively assess insulin sensitivity in KO animals. I combined this with fasting/refeeding paradigms to mimic the natural metabolic transitions that the animals may undergo throughout the circadian cycle. Finally, I utilized both mRNA-seq and a new method called TAIL-seq (Chang et al., 2014) to identify potential targets of NOC. With the TAIL-seq data I examined Poly(A) tail length changes in WT and *Noc*$^{-/-}$ mice to determine a possible molecular mechanism whereby NOC can regulate glucose/insulin metabolism and flux through control of the Poly(A) tail length of metabolic targets genes.

Methods

Mice: Male C57BL/6 WT and *Noc*$^{-/-}$ (KO) mice were generated by *Noc*$^{+/-}$ x *Noc*$^{+/-}$ heterozygous breeding to generate littermates for all experiments. Unless otherwise noted, mice used for experimentation were 9-12 weeks of age. Regular chow (RC) diet was Harlan Teklad diet 2918. High Fat Diet was Research Diets D12492i (60% kcal fat). Mice were individually housed in cages in environmental chambers under Light:Dark (LD) 12:12 conditions under Green LED lights where time of lights on was defined as Zeitgeber Time (ZT) 0 and time of lights off defined as ZT12. For HFD experiments, mice began feeding at 6-9 weeks of age for a total of 3 weeks. Mice were sacrificed by decapitation for blood and tissue collection. For mouse transgenic (TG) studies *ROSA26-rtTA x TRE-NocWT x WT*, *ROSA26-rtTA x TRE-NocWT x KO*, *ROSA26-rtTA x NocE193A x WT* and *ROSA26-rtTA x NocE193A x KO* were maintained as homozygous for both transgenes and homozygous on either the WT or KO background. Transgenic animals were either fed RC diet (TG OFF) or Harlan Teklad 2918 supplemented with 2 g/kg Doxycycline (TD.09751) (TG ON). To induce ubiquitous and maximal expression of the TG, TG ON animals were fed the Dox-supplemented diet for a minimum of 2 weeks prior to experimental manipulation.

Hyperinsulinemic-euglycemic clamp: The clamp procedure was conducted in collaboration with Dr. Gerald I. Shulman at Yale University. The procedure details were as described in (Kim, 2009). Briefly, mice received surgical implantation of an intravenous, bifurcated catheter allowing for the simultaneous infusion of glucose and insulin. Mice were allowed to recover from surgery for 4-5 days prior to the clamp procedure. For the clamp procedure, mice were

fasted overnight and an initial 2h baseline period of radio-labeled glucose [3-^{3}H] was infused. After this baseline period, microdialysis pumps infuse both glucose and insulin. 2-deoxy-D-[1-^{14}C] glucose (2-DOG) (10 uCi per mouse) was used to measure glucose uptake in muscle (gastrocnemius) and white adipose tissue (WAT) at the end of the clamp.

Tissue Metabolites: Following an overnight fast, WT and KO mice (n=5-8/genotype) were sacrificed and muscle (gastrocnemius) and liver immediately dissected and flash-frozen in liquid nitrogen for downstream measurement of triacylglycerol (TAG) or Total diacylglycerol (DAG).

Glucose and Insulin Tolerance Tests: Mice were administered either an oral glucose tolerance test (oGTT) or intraperitoneal glucose tolerance test (ipGTT) at either ZT6 or ZT18 following an 18h fast. Animals were fasted by being placed in a clean cage with woodchip bedding and water, but no food. For the ZT6 GTT, food was removed at ZT12 on the previous day. For the ZT18 GTT, food was removed at ZT0 on the day of the test. Glucose (1.5 g/kg D-glucose, Sigma) was either orally gavaged or given by intraperitoneal (IP) injection. Animals were weighed ~10 min. prior to dosing and blood glucose was monitored by tail vein puncture using a OneTouch Ultra Mini glucometer and associated glucose test strips. The ZT18 GTTs were administered under dim red light. The intraperitoneal insulin tolerance test (ipITT) was administered at either ZT7 or ZT17 following a 5h fast. For fasting, animals were placed in a clean cage with woodchip bedding and water, but no food. For the ZT7 ipITT, food was removed at ZT2 and for the ZT17 ipITT food was removed at ZT12.

Saline and Insulin Injection: WT and KO mice were fed a HFD (Research Diets, D12492i) for 3 weeks. At ZT0 on the day of injection, mice were placed in a fresh cage without food and fasted for 18h (ZT0-ZT18). At ZT18 mice received an intraperitoneal (IP) injection of either 0.9% saline or 0.75 U/kg Insulin (Humulin R, Eli Lilly) (n=3-4 mice/genotype/condition). Mice were sacrificed by decapitation 15 min after injection for tissue and blood collection. Liver tissue was removed and immediately flash-frozen in liquid nitrogen. Frozen tissue was stored at -80˚C until downstream processing.

Western Blotting: Frozen liver tissue was ground into a powder using a mortar and pestle under liquid nitrogen. Liver tissue powder (50-100 mg) was then homogenized with a Polytron mechanical homogenizer in 1 mL protein homogenization solution (20 mM HEPES, pH 7.5; 100 mM NaCl; 0.05% Triton X-100; 1 mM DTT; 5 mM sodium β-glycerophosphate; 0.5 mM Na_3VO_4; 1 mM EDTA; 0.5 mM PMSF; 1X protease inhibitor cocktail, Sigma Cat# P8340); 5 mM NaF). Protein concentration was determined with Bio-Rad Protein Assay Dye Reagent Concentrate (Cat#500-0006) according to the manufacturer's instructions. For each sample, 30 ug protein was run a 10% polyacrylamide gel and transferred to a PVDF membrane. Membranes were blocked for 1h in BLOTTO (0.05% w/v powdered milk; 0.5% TBS; 0.005% Tween-20) and then incubated with P-Akt(Ser473) 1˚ antibody (Cell Signaling #9271) in 5% BSA overnight. Membranes were washed in 0.1% v/v TBS-Tween and incubated for 30 min with an α-Rabbit IgG HRP 2˚ antibody. Membranes were then incubated with ECL substrate (GE) according to the manufacturer's instructions and the membranes were visualized with the STORM imaging system (Molecular Dynamics). Membranes were stripped with Re-Blot

Western Blot Recycling reagent (Millipore) according to the manufacturer's instructions. The membranes were then re-probed with Akt(Total) Antibody (Cell Signaling #9272) and visualized using the same procedure as that listed above for P-Akt(Ser473). Optical density of the resulting images was obtained using ImageJ software.

mRNA-seq: mRNA-seq libraries were created according to procedures outlined in (Takahashi et al., 2015) and sequenced on a HiSeq Sequencing System (Illumina) in the UT Southwestern Medical Center McDermett NGS Core. For mRNA-seq of HFD samples, the average read depth for all samples was 40 million reads. On average, 90% of the raw reads were mapped to the mouse genome (MM9). After QC filtering, an average of 28 million reads for each sample remained and of these, 77% were mapped to the MM9 genome and used for statistical comparisons by differential expression analsysis. For mRNA-seq of RC samples, a total of 16 samples was pooled (n=1/genotype/timepoint) and went through two rounds of sequencing. Each round yielding an average sequencing depth of 14 million reads per sample and the two rounds of sequencing were combined for each sample to achieve and average read depth of 28 million reads per sample. A second set of biological replicates (n=1/genotype/timepoint) was sequenced in a similar manner. An average of 97% of the total 28 million reads per sample was mapped to the mouse genome (MM10).

TAIL-seq and Poly(A) tail length quantitation: TAIL-seq was performed by Dr. Peng Gao in my lab according the methodology outlined by V. Narry Kim and colleagues (Chang et al., 2014). Briefly, Total RNA was isolated from flash-frozen liver samples using TRIzol. Total

RNA was rRNA-depleted and a 3’ biotin-labeled adapter was ligated was added followed by partial digestion with RNase T1. RNA was then pulled down with streptavidin and underwent 5’ phosphorylation. RNA was gel purified, underwent 5’ adapter ligation and was converted to cDNA by reverse transcription, PCR amplified and sequenced on a MiSeq sequencing system. Following mapping to the mouse genome (MM10), I determined the Poly(A) tail length by counting the number of A nucleotides (nt) starting just before the 3’ adapter and continuing towards the gene body until I encountered 3 consecutive non-A nt at which time counting stopped and the total length recorded.

Results

Nocturnin KO mice are insulin resistant following HFD feeding

Members of Dr. Gerald Shulman's lab at Yale University performed hyperinsulinemic-euglycemic clamps on WT and *Noc*$^{-/-}$ mice on either a RC or 3 week HFD background. WT and *Noc*$^{-/-}$ mice exhibit similar insulin sensitivity on a RC background as assessed by a similar glucose infusion rate (GIR) throughout the clamp (Figure 1A, i and ii). WT animals fed a HFD for 3 weeks display insulin resistance compared to RC-fed WT animals. Although the KO animals also display insulin resistance compared to KOs in the RC condition, the level of insulin resistance in the HFD KOs is more severe than that of the HFD WTs, i.e the GIR needed to maintain euglycemia in the KOs throughout the clamp is significantly reduced (Figure 1A, i and ii). Whole-body glucose turnover (Rd) is also significantly reduced in HFD KOs compared to HFD WTs (T-test, *P<0.0.5) (Figure 1A, iii). The decreased GIR and Rd exhibited by the KOs is due in part to enhanced gluconeogenesis in the insulin-stimulated, clamped state. While basal endogenous glucose production (BEGP) does not differ between genotypes on either diet (Figure B, i), *Noc*$^{-/-}$ mice have significantly increased clamp endogenous glucose production (CEGP) (Figure 1B, ii) (T-test, *P<0.05). HFD-fed *Noc*$^{-/-}$ mice also lose the ability to suppress endogenous glucose production (EGP) in the clamped state. Both WT and KO mice completely suppress EGP on a RC background, but HFD impairs this ability to some degree in HFD-fed WTs and even more severely in HFD-fed KOs (Figure 1B, iii) (T-test, P<0.01). *Noc*$^{-/-}$ mice in fact fail to suppress EGP to any degree and still exhibit glucose production, i.e. gluconeogenesis, in the clamped state. HFD-fed KO mice also have reduced 2-Deoxyglucose (2-DOG) uptake in insulin-stimulated muscle (gastrocnemius), but not white adipose tissue (WAT) (Figure 1B, iv)

(T-test, *P<0.05). It is interesting to note that, while *Noc* gene expression is significantly upregulated in liver with 3 weeks HFD feeding and responsive to fasting/refeeding (Chapter II, Figure 1B, i and iii), the expression of *Noc* in muscle (quad) is not altered by 3 weeks HFD feeding nor responsive to fasting/refeeding (Appendix II, Figure 2A-B). *Noc* also has a delayed peak expression in muscle (ZT15) as compared to liver (ZT12) (See Appendix II, Figure 2A vs Chapter II, Figure 1A-B, i). Levels of different lipids species do not differ between HFD-fed WT and KO muscle and liver tissue (Appendix II, Figure 1A-B). Triacylglycerol (TAG) levels in both muscle and liver tissue do not differ between WT and $Noc^{-/-}$ mice and total diacylglycerol (DAG) in HFD-fed WT and KO liver tissue is similar.

Temporal glucose metabolism is altered in $Noc^{-/-}$ mice with HFD feeding

While the hyperinsulinemic-euglycemic clamps demonstrated insulin-resistance in HFD-fed KO mice, I wanted to assess changes that might occur due to the circadian cycle and loss of *Nocturnin*. I administered an oral glucose tolerance test (oGTT) to WT and KO mice at two different times in the circadian cycle (ZT6 and ZT18 with ZT0 defined as the time of lights on and ZT12 the time of lights off) after 3 weeks of HFD feeding. WT and KO mice have similar oGTT responses during the light phase at ZT6, however $Noc^{-/-}$ mice have significantly impaired glucose tolerance during the dark phase at ZT18 (Figure 2A, i-iii) (Two-way ANOVA, repeated measures, P<0.05). One possibility for the decreased glucose tolerance and insulin resistance in KO mice could be a deficit in insulin signaling. Upon insulin stimulation, hepatic Akt becomes phosphorylated at Ser473. This phosphorylation activates Akt and P-Akt(473) can downregulate transcription of gluconeogenic genes (e.g. *Pepck*) and thus regulate glucose production. I fasted

HFD-fed WT and KO animals for 18h (food removed at ZT0) and gave them an intraperitoneal (IP) injection of either 0.9% saline or 0.75 U/kg insulin at ZT18 (Figure 2B, i). I harvested liver tissue 15 min after the IP injection and isolated liver lysates for Western blotting of P-Akt(Ser473) or Total-Akt (Figure 2B, ii). Both WT and KO animals have an increased P-Akt/Total-Akt ratio following insulin injection (One-way ANOVA, multiple comparisons, $P<0.05$) (Figure 2B, iii). KOs have a significantly larger P-Akt/Total-Akt ratio than WTs at 15 min post-insulin injection (One-way ANOVA, multiple comparisons, $**P<0.01$) (Figure 2B, iii). This would indicate that the glucose intolerance that *Noc*$^{-/-}$ exhibit at ZT18 is either downstream of Akt or part of another arm of the insulin-signaling pathway.

Dysregulation of gluconeogenic gene expression in Noc$^{-/-}$ mice

I have established that *Noc*$^{-/-}$ are insulin resistant with hyperinsulinemic-euglycemic clamps and glucose intolerant following an oral gavage of glucose during the dark phase. But these challenged conditions rely on exogenous administration of either insulin and/or glucose. I wanted to examine glucose metabolism in WT and KO mice in a basal and fast/refed state to see what role NOC may be playing in these more natural metabolic conditions. HFD-fed WT and *Noc*$^{-/-}$ both show a cycling of blood glucose (Two-way ANOVA, repeated measures, $P<0.0001$) which peaks during the light phase. This phasing of blood glucose has been previously reported for WT mice fed a HFD and is likely a reflection of the increased food intake during the light phase that mice fed a HFD exhibit (Kohsaka et al., 2007). When I challenge WT and KO mice with fasting and refeeding throughout the dark phase, a dysregulation of glucose metabolism in the KOs emerges. In the basal, Fed state at ZT22 the blood glucose levels do not differ between

WT and KO mice (Figure 3A, ii). However, if I fast the animals for 10h from ZT12-ZT22 and then refeed them for either 1h or 4h, the *Noc*$^{-/-}$ have higher blood glucose values after 10h fasting and their early response to 1h refeeding overshoots the basal level that WT mice achieve. By 4h refeeding, WT and KO levels are both similar to that basal, Fed state.

To determine what processes might be dysregulated in the *Noc*$^{-/-}$ liver during this metabolic transition from the Fed to Fast state I performed transcriptome analysis by mRNA-seq on liver mRNAs from WT and KO mice at ZT22 in either the *Ad Lib*, Fed or 10h Fast (Fast) state (Figure 3B, i). There were a number of genes upregulated to a similar degree in both WT and KO liver (n=147 genes) as well as large groups unique to either WT (n=172 genes) or KO (n=346 genes) (Figure 3B, ii). Because I am trying to determine potential targets of NOC, I focused on the genes uniquely upregulated in the KO liver with the reasoning that these genes may lose the regulation of their Poly(A) tail that NOC may normally exert and would thus be more stable and have a higher expression in the KOs. When I performed gene ontology on these KO-unique genes I found a category associated with gluconeogenesis that contained *Pepck*, one of the rate limiting enzymes in hepatic glucose production. The significant upregulation of *Pepck* mRNA in the KO following a 10h fast becomes comparable to WT levels again after 4h (Figure C, i-ii) (Two-way ANOVA, multiple comparisons, **P<0.01).

Temporal insulin resistance and altered Pepck Poly(A) tail length in Noc$^{-/-}$ mice

While *Noc*$^{-/-}$ mice display insulin resistance and disrupted glucose metabolism on a HFD-fed background, I wanted to determine whether regulation of glucose/insulin metabolism is a general function of NOC, regardless of diet. I performed an IP insulin tolerance test (ipITT) at

either ZT7 or ZT17 in mice on an RC-background and found that KO mice exhibit temporal insulin resistance with a significantly altered response to the ipITT at ZT17 (reduced drop in blood glucose) but not ZT7 as compared to WT mice (Figure 4A, i-ii) (Two-way ANOVA, repeated measures, $P<0.05$).

To examine glucose metabolism in an unchallenged condition I measured the blood glucose in WT and KO mice throughout the LD cycle in the *Ad Lib*, Fed state. WT mice maintain a relatively constant blood glucose level with a small dip early in the light phase and a small increase throughout the dark phase. In contrast, KO animals have swings in blood glucose with levels above that of WTs (ZT0, 3, 15) followed by dips below WT levels (ZT9, 12, 18, 21) (Figure 4B).

HFD-fed *Noc*$^{-/-}$ mice have increased *Pepck* mRNA expression with a fast and so I measured *Pepck* expression on the RC-fed background as well. I performed mRNA-seq from liver samples of WT and KO mice collected at different circadian times. Both WT and KO mice show a rise in *Pepck* mRNA in the mid-late light phase with a sharp drop early in the dark phase as the animals begin eating and reduce gluconeogenesis (Figure 4C, i). The rise in *Pepck* during the light:dark transition is significantly increased in the KO liver (ZT12), followed by a decrease below WT levels (ZT15-ZT18). The increased *Pepck* expression at ZT12 in *Noc*$^{-/-}$ could explain the subsequent spike in blood glucose at ZT15 and the reduced expression in KOs at ZT15 and ZT18 could explain the dip in blood glucose below WT levels at ZT18 and ZT21.

Altered *Pepck* expression in both RC and HFD-fed *Noc*$^{-/-}$ mice points toward *Pepck* as a potential target of NOC and its deadenylase function. I worked with Dr. Peng Gao in my laboratory to perform TAIL-seq in liver samples from WT and *Noc*$^{-/-}$ collected at different

circadian times in order to measure changes in Poly(A) tail length. *Pepck* in *Noc*$^{-/-}$ liver has a significantly increased frequency of long Poly(A) forms (>100nt) at ZT0 and ZT6. The largest difference in long Poly(A) forms for *Pepck* occurs at ZT0 with a frequency of 5% in WT versus 30% in KO liver (Figure 4C, ii). This dramatic increase in long Poly(A) tail frequency occurs specifically when NOC would normally be at its maximal expression in WT mice. I used publically available Ribo-seq and Total RNA-seq data (Janich et al., 2015, Janich et al., 2016) to compare the temporal patterning of Poly(A) tail length and translation for *Pepck* (Appendix II, Figure 3A, i-iii). The frequency of long Poly(A) tail *Pepck* mRNAs does not dramatically change in WT liver, but there is a small increase between ZT0-ZT6 that correlates with a small increase in translation. There is another increase in frequency of long Poly(A) tail mRNAs at ZT18 and this precedes a second increase in *Pepck* translation late in the dark phase (Appendix II, Figure 3A, iii).

I measured the glucose tolerance in WT and KO mice with a drug-inducible, ubiquitously-expressed functional WT *Nocturnin* transgene (*TG-NocWT*) or a catalytically dead *Nocturnin* transgene (*TG-NocE193A*). The *TG-NocE193* has an alanine (A) to glutamic acid (E) point mutation at position 193 of the NOC sequence which renders NOC unable to bind Mg^{2+} and prevents its deadenylase activity (Garbarino-Pico et al., 2007). RC-fed WT and KO mice with the transgene off have similar glucose tolerance following a oGTT administered at ZT6 (Appendix II, Figure 4A-b, i). Overexpression of the *TG-NocWT* improves glucose tolerance slightly during the peak response phase on a WT background (Figure 3A, ii). Overexpression of the *TG-NocWT* on a KO background significantly improves the entire glucose tolerance response (Two-way ANOVA, repeated measures, $P<0.05$). Overexpression of the catalytically-dead *TG-*

NocE193A fails to improve glucose tolerance on either the WT or KO background (Figure 4B, ii-iii).

Discussion

Nocturnin was previously thought to exert some form of control over glucose/insulin metabolism, though a precise mechanism was not known (Green et al., 2007). My studies have revealed that NOC is necessary for regulation of the dynamic transitions that occur as metabolic programs switch from energy utilization (catabolism) to storage (anabolism). In the context of glucose/insulin regulation, these metabolic transitions involve a dynamic flux of nutrients requiring precise temporal control to prevent disorders such as diabetes or obesity. *Noc* gene expression was known to be partially controlled by the core clock and potentially also through other nutrient and/or hormonal signals that arise through the daily partitioning of food intake (Oishi et al., 2003, Kornmann et al., 2007).

Noc can be acutely induced following a fast (Chapter II, Figure 1A-b, iii) and nutrient excess, such as HFD feeding, can significantly increase *Noc's* cyclic amplitude in the liver (Chapter II, Figure 1B). Loss of NOC is beneficial with HFD feeding in that $Noc^{-/-}$ are resistant to DIO and hepatic steatosis (Green et al., 2007), but I have now reported that $Noc^{-/-}$ are not protected from all aspects of DIO. $Noc^{-/-}$ display more severe insulin resistance that WT mice with HFD feeding (Figure 1A). Insulin resistance with HFD feeding can occur through increased intracellular lipid accumulation (Samuel et al., 2010, Samuel and Shulman, 2012). In the hyperinsulinemic-euglycemic clamp studies WT and KO mice had intracellular TAG and DAG levels that were similar in liver and muscle (Appendix II, Figure 1A-B). $Noc^{-/-}$ did have a small, though significant reduction in glucose uptake by muscle tissue (Figure 1B, iv), but NOC's function in muscle has not been rigorously explored. *Noc* expression does cycle in

muscle (Appendix II, Figure 2A), though *Noc* does not appear to respond to nutrient status in the same way as in liver tissue (compare Chapter II, Figure 1B and Appendix II, Figure 2A-B).

Given Nocturnin's rhythmic expression profile, the mechanism by which NOC regulates glucose and insulin metabolism is likely to have a temporal component. The hyperinsulinemic-euglycemic clamps were performed during the light phase (following an overnight fast) and *Noc*$^{-/-}$ mice did not show a difference in insulin sensitivity on the RC-fed background. Consistent with this, if I performed an ipITT on RC-fed WT and KO mice during the light phase, they had similar responses (Figure 4A, i). However, if I performed the ipITT during the dark phase, *Noc*$^{-/-}$ mice had a reduced % change in blood glucose, indicating insulin resistance (Figure 4A, ii). This insulin resistance could be a result of impairments in insulin signaling. I examined the insulin signaling pathway in WT and KO mice and found that they were both able to activate Akt (via Ser473 phosphorylation) following an injection of insulin (Figure 2B, i-iii). Thus, *Noc*$^{-/-}$ mice either do not have a deficit in hepatic insulin signaling per se, or the deficit exists downstream of Akt or in another tissue (i.e. muscle).

The insulin resistance in *Noc*$^{-/-}$ appears to manifest itself mostly when the KO mice are given a metabolic challenge such as glucose/insulin injection or fasting/refeeding. Indeed, basal glucose levels in the *Ad Lib*, fed state do not show significant differences (Figure 3A, i and Figure 4B). If *Noc*$^{-/-}$ are fasted and/or fasted and refed, their glucose levels are increased compared to WTs (Figure 3A, ii). *Noc*$^{-/-}$ have a failure to suppress endogenous glucose production (gluconeogenesis) (Figure 1B, i-iii) and this is associated with increased *Pepck* gene expression 3B-C). *Pepck* expression is not just increased in the challenged state in KO animals, but its rhythmic profile is also altered showing swings of both high and low expression in the late

light/early dark phase as compared to WTs (Figure 4C, i). By TAIL-seq analysis, I showed that the regulation of *Pepck's* Poly(A) tail length is altered in *Noc*$^{-/-}$ mouse liver (Figure 4C, ii). Whereas WT mice decrease the frequency of long Poly(A) tail *Pepck* mRNAs between ZT18 and ZT0, KO animals lose this regulation and instead have a dramatic increase in long Poly(A) tail *Pepck* forms. As the Poly(A) tail length of *Pepck* is associated with translation late in the dark phase (Appendix II, Figure 3), this large increase in long Poly(A) tail *Pepck* mRNAs in the KO liver could result in increased gluconeogenesis. Increased glucose production late in dark phase would then explain the higher glucose production in KOs early in the light phase that sets in motion the altered blood glucose flux (high to low swings) seen in *Noc*$^{-/-}$ across the circadian cycle (Figure 4B).

Establishing *Pepck* as a potential target of NOC now provides a mechanism for the nutrient-challenged insulin resistance of *Noc*$^{-/-}$ mice. As *Pepck* is dynamically regulated with fasting/refeeding, it is necessary to have tight control over its expression so that blood glucose levels are properly maintained. Posttranscriptional regulation of *Pepck* has previously been reported (Hajarnis et al., 2005, Dhakras et al., 2006, Mufti et al., 2011, Gummadi et al., 2012), but the circadian component and Poly(A) tail length has not been explored. Poly(A) tail length and translation are often correlated (Zhang et al., 2010b, Weill et al., 2012), thus it would be necessary to not only regulate the mRNA expression of temporally controlled genes, but also their Poly(A) tail. *Noc*$^{-/-}$ mice exhibit swings in blood glucose that could result from a failure to efficiently regulate the Poly(A) tail length of *Pepck*. The rhythmic peak of *Pepck's* Poly(A) tail length overlaps with NOC's peak expression. Because *Noc* can be acutely induced by refeeding

following a fast, it could be that this induction of NOC is necessary to properly regulate the Poly(A) tail of metabolic targets such as *Pepck*.

These findings place Nocturnin in a unique role for metabolic regulation. I have identified *Pepck* as a potential target of NOC, though there may be others. The altered glucose production exhibited by $Noc^{-/-}$ both basally and in the challenged state are evidence of NOC's role in regulating metabolic flux. Further identification of NOC's targets both in the liver and other tissues will aid in the understanding of how metabolic homeostasis is achieved across the circadian cycle and in response to the various nutrient challenges organisms encounter in their rhythmic environment.

Chapter III Figures

Figure 1

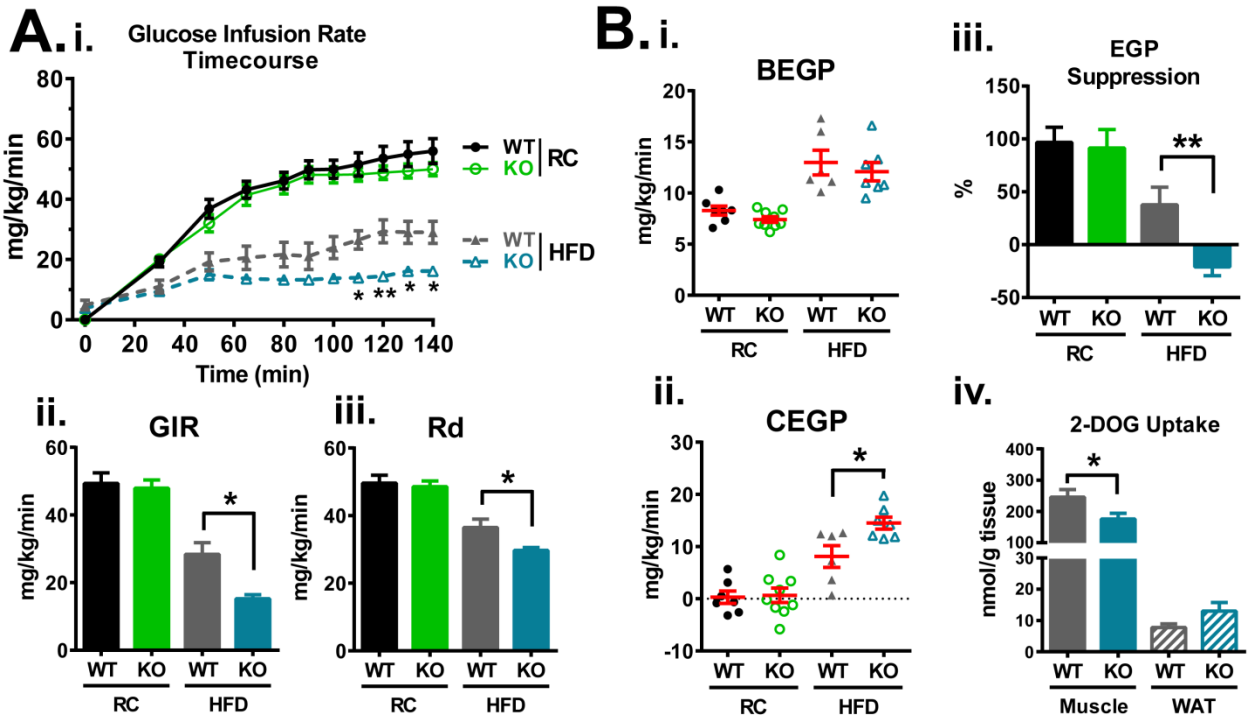

Figure 1. Hyperinsulinemic-euglycemic clamps in WT and KO mice
Mice lacking *Nocturnin* (*Noc*$^{-/-}$, KO) are insulin resistant after 3 weeks of High Fat Diet (HFD) feeding. KO animals display increased endogenous glucose production under clamped conditions and have reduced muscle uptake of 2-Deoxyglucose (2-DOG) in the insulin-stimulated state. Hyperinsulinemic-euglycemic clamps were performed as outlined in (Kim, 2009) *Abbreviations:* Glucose Infusion Rate (GIR), Whole body glucose turnover (Rd), Basal endogenous glucose production (BEGP), Clamp endogenous glucose production (CEGP), Endogenous glucose production (EGP), White adipose tissue (WAT). (A, i) Glucose infusion rate (GIR) timecourse following an overnight fast on mice from a regular chow (RC) (n=8-9/genotype) or 3 weeks HFD (n=6-7/genotype) background. Data points represent the Mean +/- SEM. Two-way ANOVA, repeated measures with multiple comparisons *P<0.05, **P<0.01. (A, ii) GIR summary over the final 40 min of the clamp procedure. Data represents the Mean +/- SEM with T-test *P<0.05. (A, iii) Rd summary expressed as Mean +/- SEM with T-test *P<0.05. (B, i-ii) BEGP and CEGP are shown with red bars indicating the Mean +/- SEM. Test *P<0.05. (B, iii) EGP suppression expressed as Mean +/- SEM. T-test **P<0.01. (B, iv) 2-DOG uptake was assessed is muscle (gastrocnemius) or WAT at the end of the clamp procedure. T-test P<0.05.

Figure 2

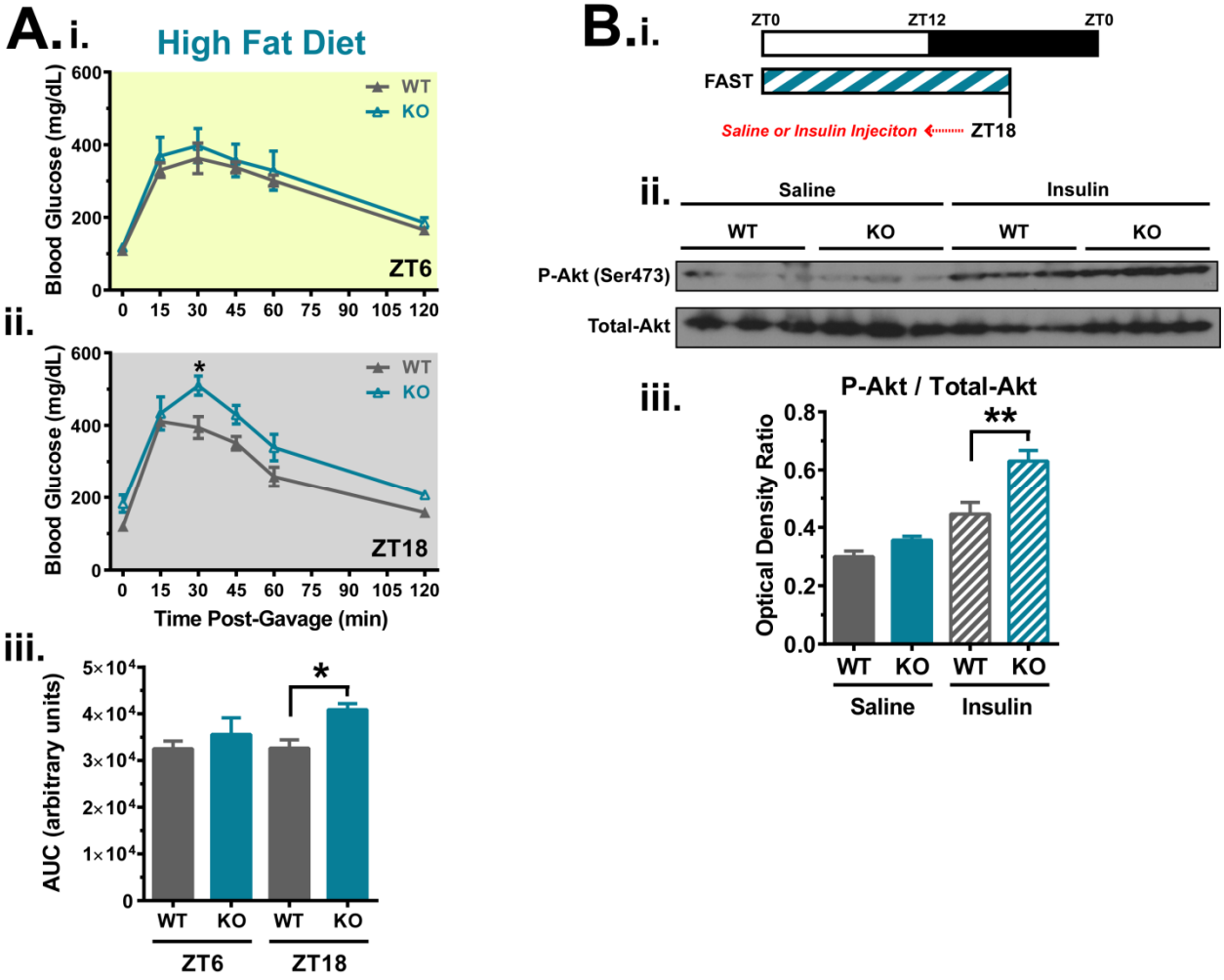

Figure 2. *Noc*$^{-/-}$ mice have altered glucose tolerance in the dark phase yet retain insulin-stimulated Akt activation

Mice lacking Nocturnin (*Noc*$^{-/-}$, KO) have decreased glucose tolerance during the dark phase following a fast on a HFD background. Insulin injection during the dark phase following a fast is able to activate Akt via phosphorylation at Ser473 in KO liver. (A, i-iii) WT and KO mice were fasted for 18 h prior to receiving an oral glucose tolerance test (oGTT). For the oGTT at ZT6, food was removed the previous night at ZT12 and animals were placed in a fresh cage. For the ZT18 oGTT food was removed at ZT0 on the day of the oGTT and mice were placed in a fresh cage. Mice were administered 1.5 g/kg D-glucose via oral gavage and blood glucose was monitored via tail vein puncture. Data points represent the Mean +/- SEM. Glucose tolerance was similar between WT and KO mice at ZT6, but *Noc*$^{-/-}$ exhibited decreased glucose tolerance at ZT18 (Two-way ANOVA, repeated measures, $P<0.05$) and the blood glucose of KO animals

was significantly elevated 30 minutes after the glucose gavage (Two-way ANOVA, multiple comparisons $P<0.05$). The area under the curve (AUC) was calculated for each glucose response curve for each genotype and, while there was no difference at ZT6, KOs were significantly increased at ZT18 (T-test, $P<0.05$). (B, i) Schematic of the paradigm used for insulin injection. Following 3 weeks of HFD feeding, WT and KO mice (n=3/genotype/condition) were fasted for 18 h (Food removed at ZT0) and then received an intraperitoneal injection of either 0.9% saline or 0.75 U/kg Insulin in 0.9% saline. Animals were sacrificed 15 min after saline or insulin injection and livers flash-frozen in liquid nitrogen. (B, ii) Western blot of P-Akt(Ser473) and Total-Akt levels in liver lysates from WT and KO mice injected with either saline or insulin. (B, iii) The optical density ratio of P-Akt / Total-Akt from the Western blot signal shown in (B, ii) was quantified for WT and KO samples. Bars are the Mean +/- SEM, One-way ANOVA, multiple comparisons, $**P<0.01$.

Figure 3

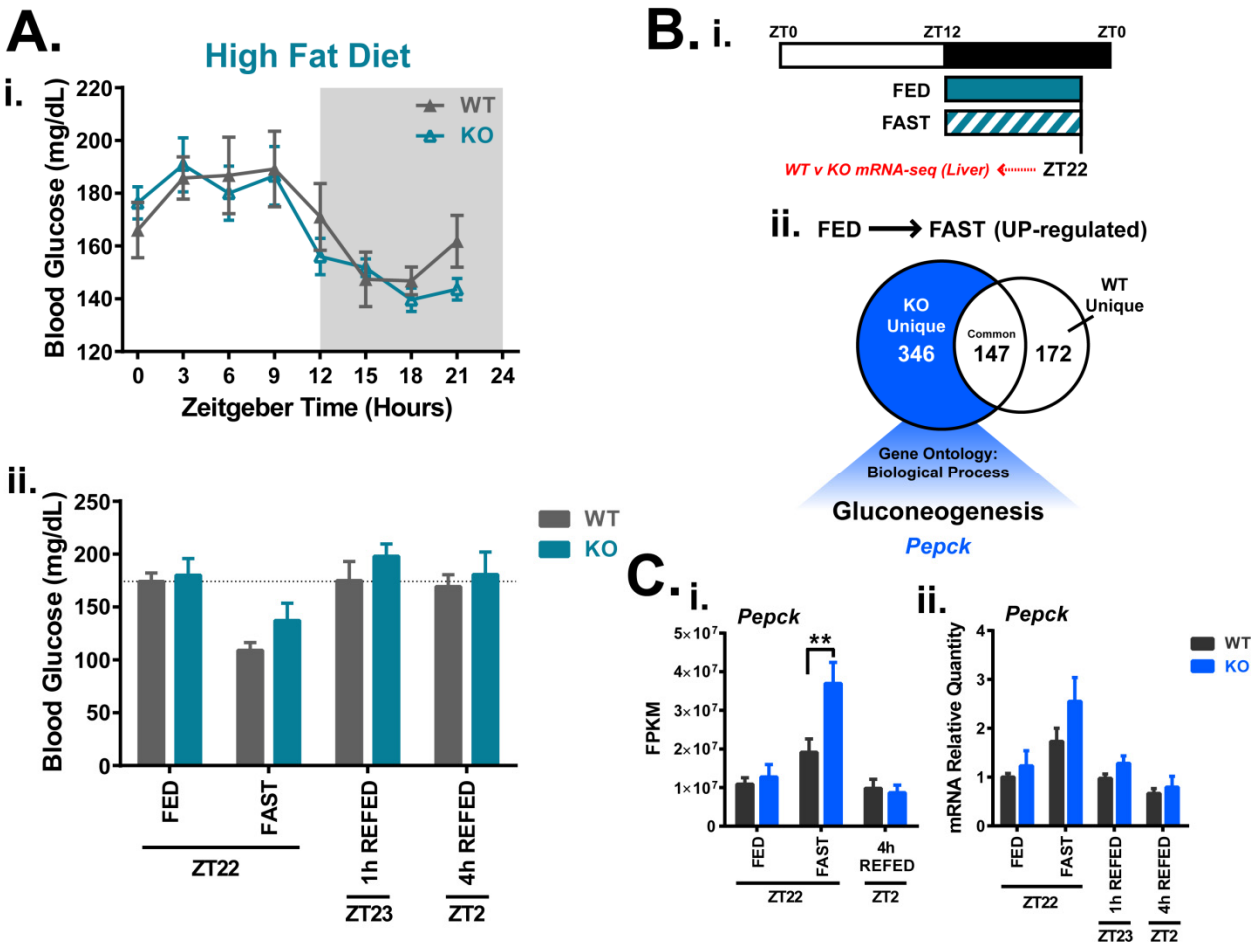

Figure 3. Altered glucose production in *Noc*$^{-/-}$ mice with fasting
Nocturnin KO mice (*Noc*$^{-/-}$, KO) have normal circadian cycling of blood glucose, but display increased gluconeogenesis with fasting and this is associated with increased *Pepck* gene expression. (A, i) Blood glucose was measured in WT and KO mice across the circadian cycle (n=5/genotype) after 3 weeks High Fat Diet (HFD) feeding. (A, ii) Blood glucose was measured in WT and KO mice after 3 weeks HFD in the Fed, Fast or Refed states. Fasted mice were fasted for 10h with HFD food removed at ZT12. Refed mice were fasted for 10h starting at ZT12 and HFD food was replaced at ZT22 for either 1h (1h Refed) or 4h (4h Refed). Bars represent the Mean +/- SEM. (B, i) Schematic describing tissue collection for mRNA-seq. Mice were fed a HFD for 3 weeks and liver tissue was harvested at ZT22 for mice in either the Ad lib, Fed condition or 10h fasted (Fast, food removed at ZT12) condition (n=3/genotype/condition). (B, ii) Genes that were significantly upregulated between the Fed and Fast state within each genotype were compared. KO animals had a large group of uniquely upregulated genes (346 total) and gene ontology revealed a category associated with gluconeogenesis. Contained within this

category was the *Pepck* gene. (C) Gene expression of *Pepck* expressed as FPKM from the mRNA-seq (C, i) or through qPCR (C, ii). Bars represent the Mean +/- SEM, Two-way ANOVA with multiple comparisons **P<0.01.

Figure 4

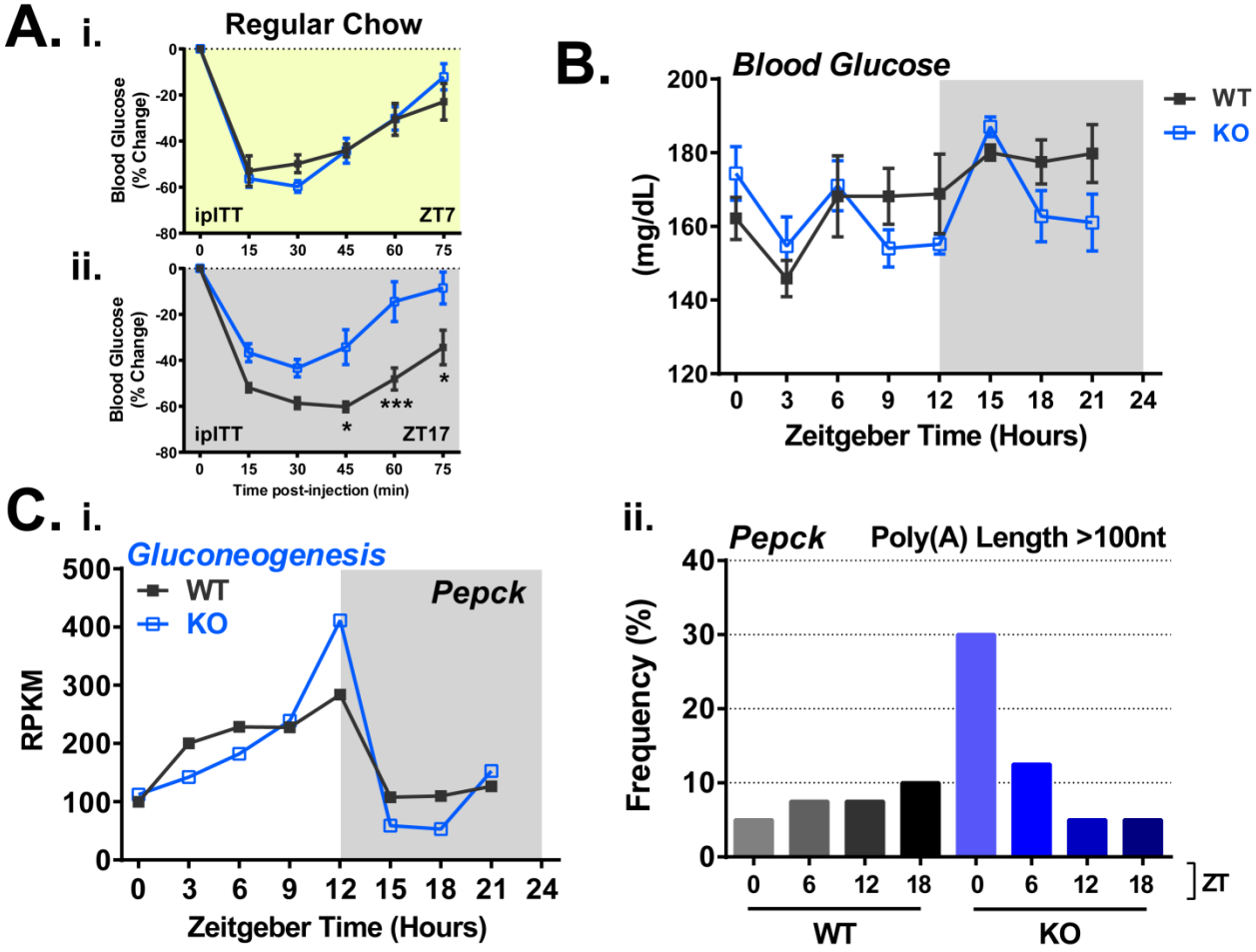

Figure 4. ***Noc*$^{-/-}$ mice display temporal insulin resistance and altered *Pepck* Poly(A) tail length**

Mice lacking Nocturnin (*Noc*$^{-/-}$, KO) display insulin resistance when given an insulin tolerance test during the dark phase (ZT17) but not the light phase (ZT7). Whole body glucose rhythms are not significantly altered, but *Pepck* mRNA expression is elevated at ZT12 in the KO liver and the *Pepck* mRNA also has an increased Poly(A) tail length at ZT0 and ZT6. (A, i-ii) WT and KO mice on a Regular Chow (RC) background were given an intraperitoneal (IP) injection of insulin (0.75 U/kg) at either ZT7 or ZT17 (n=7-10/genotype/condition) and blood glucose was monitored via tail vein puncture. Data points represent the mean +/- SEM. The change in blood glucose did not differ between WT and KO mice with the ipITT was administered at ZT6 (Two-way ANOVA, P=0.95) but the KO response was significantly altered (Two-way ANOVA P<0.05) and the change in blood glucose was significantly altered at 45, 60 and 75 min post-gavage (Two-way ANOVA, multiple comparisons, *P<0.05, ***P<0.001). (B) Blood glucose was measured from tail vein puncture of WT and KO mice throughout the circadian day (n=4-

5/genotype/timepoint. Data points represent the Mean +/- SEM. (C, i) Livers were harvested from WT and KO mice and mRNA-seq analysis performed (n=2/genotype/timepoint). Data points represent the mean of two biological replicates for each genotype at each timepoint. (C, ii) TAIL-seq on liver mRNAs was performed to measure Poly(A) tail length (n=1/genotype/timepoint). Bars represent the frequency of counted transcripts for the *Pepck* gene that had a Poly(A) tail length greater than 100 nucleotides (>100nt) (n=40 transcripts/genotype/timepoint).

Chapter IV: Discussion

When I started my graduate work, NOC had been implicated to function in a variety of metabolic conditions. NOC's molecular function was largely implied based on phenotypic observations in *Noc*$^{-/-}$ mice. My studies were able to further refine a metabolic role for NOC by combining mRNA-seq, TAIL-seq and phenotypic characterization across both 24h temporal and acute windows. I have discovered two novel pathways in which NOC is involved, namely the cholesterol and bile acid metabolic pathways. I have also shown that *Noc*$^{-/-}$ have temporal insulin resistance confined to the dark phase with RC feeding and develop severe insulin resistance with HFD feeding.

Identifying Targets of Nocturnin

My data show that in *Noc*$^{-/-}$ mice, there are significant changes in the Poly(A) tail length dynamics of genes associated with cholesterol, bile acid and glucose metabolism, namely *Fdps*, *Cyp7a1* and *Pepck*, respectively. The most strikingly common characteristic among the change in Poly(A) tail length of these genes is a loss of regulation in the late dark phase, when NOC expression is normally at its peak in WT mice. In this way, NOC appears to act as a sort of metabolic insulator, maintaining regulation of the ceiling of Poly(A) tail length for a variety of metabolic targets. When NOC is absent in *Noc*$^{-/-}$ mice, NOC targets overshoot their normal Poly(A) tail length frequency distributions and this sets in motion a change in metabolic flux mediated by the enzymes that these targets encode.

In some instances, the change in Poly(A) tail in the KOs is also associated with altered mRNA abundance. There have been many recent reports that show mRNA abundance and Poly(A) tail length do not have to be correlated. Indeed, there are classes of genes which do not show transcriptional rhythms or rhythms in mRNA abundance, but which show robust cycling in translation and/or Poly(A) tail length. This highlights the importance of posttranscriptional regulation within the clock network. Knowing what targets NOC may be regulating helps in the understanding of how and why *Noc* expression is regulated in different ways.

Regulation of Noc expression

The circadian clock does well to coordinate the anticipation of metabolic transitions. Many rate limiting enzymes for key metabolic pathways cycle. But one must consider that the cycling observed in controlled laboratory conditions reflect the ideal metabolic situation in which the animals are either able to feed freely (*Ad Lib*) or at least within well-defined time windows (temporal restricted feeding). In the wild, it is likely that organisms have to work for their food and meal timing, while relatively constrained to large time windows such as "light phase" or "dark phase," likely needs to retain some form of acute regulation. I believe that my work with Nocturnin has revealed it to be an important component of both the circadian and acute mechanisms of metabolic regulation. In the liver, *Noc* expression is able to cycle under both normal conditions (RC diet) and conditions of nutrient excess (HFD). It is important to note that amplitude of *Noc* expression is increased with 3 weeks of HFD feeding. This is in contrast to many of the core clock components which decease in amplitude with HFD feeding (Kohsaka et

al., 2007). *Noc* is also acutely induced by refeeding following a fast on both a RC and HFD-fed background. This, combined with the finding that *Noc* retains its hepatic rhythmicity when the liver clock is no longer functioning (Kornmann et al., 2007) suggests that in the HFD condition, when *Noc* may lose some of its input from the clock, its expression is driven towards a higher amplitude. It is not likely that the clock serves to dampen *Noc* expression per se, as $Clock^{\Delta 19}$ mutant mice have reduced *Noc* amplitude, though again *Noc* retains its ability to cycle (Oishi et al., 2003). With my data showing altered Poly(A) tail lengths of genes encoding key metabolic enzymes, it seems likely that *Noc* needs to retain both circadian and acute responsiveness in order to maintain regulation over nutrient flux.

Data supporting this hypothesis of NOC's necessity for maintaining metabolic flux are studies looking at temporal restricted feeding (tRF). tRF is able to uncouple peripheral and central oscillators, with core clock genes and genes encoding metabolic enzymes in peripheral tissues tracking food availability as well as the rest/wake cycle (Damiola et al., 2000, Vollmers et al., 2009, Hatori et al., 2012, Adamovich et al., 2014, Chaix et al., 2014). While many rhythmic genes show altered phasing with tRF, *Noc* expression also shifts its peak expression to the light phase when food is restricted to a 6h window in the middle of the light phase (Gilbert et al., 2011). Knowing that NOC may be regulating key enzymes involved in metabolic pathways acutely regulated by food intake, it makes sense that NOC would need to shift its expression along with food intake.

Nocturnin and Cholesterol/Bile Acid Metabolism

The necessity of NOC for proper cholesterol and bile acid metabolism is clear, as demonstrated by the significant increase in gallbladder volume throughout the light phase of the circadian cycle. Additionally, many of the cholesterol and bile acid biosynthetic enzymes are altered either in mRNA expression and/or Poly(A) tail length. The difficulty in interpreting these results comes from determining cause and effect. I see changes in the Poly(A) tail length dynamics of both cholesterol and bile acid synthesis genes. Additionally, *Noc*$^{-/-}$ mice have changes in both the phasing of hepatic cholesterol and gallbladder volume. It is possible that loss of regulation by NOC for one of these pathways leads to a compensatory change in the other. Bile acid and cholesterol synthesis both occur in the liver and so teasing apart the cause and effect with a tissue-specific loss of *Noc* would not help in this case. Instead, it could be possible to feed *Noc*$^{-/-}$ mice with particular BAs and observe how possible changes in their metabolism disrupt cholesterol metabolism.

Examination of bile acid metabolism must also take into account the entire enterohepatic network. This consists of the intestines, liver and gallbladder. *Noc* is rhythmically expressed in both the intestine and liver, so it will valuable to determine its expression level and rhythmicity in the gallbladder as well. A measurement of the composition of the entire bile acid pool in *Noc*$^{-/-}$ mice would also help determine whether bile acid synthesis in general is upregulated or whether the KO animals have altered production of certain BA species. As previously mentioned, different BA species have different affinity for FXR and can thus have varying effects on systemic metabolism. Determining possible changes in BA composition of *Noc*$^{-/-}$

could then help determine if the cholesterol/bile acid phenotype is related to any of the other metabolic phenotypes that these mice exhibit.

Nocturnin and Glucose/Insulin Metabolism

It was valuable to measure both the circadian cycling of metabolites and their acute response to nutritional challenges in *Noc*$^{-/-}$ mice. This revealed the altered temporal flux of blood glucose in the KO mice as well as the increased glucose production with fasting. The swings in blood glucose in *Noc*$^{-/-}$ mice are a classical indicator of diabetes, pointing toward the improper regulation of glucose metabolism. The KO data indicate a deficit in inhibition of glucose production as the main cause. The KO animals are unable to suppress gluconeogenesis in response to insulin and this failure is accompanied by a loss of *Pepck* mRNA regulation. *Noc*$^{-/-}$ have increased *Pepck* mRNA abundance when challenged by fasting and refeeding and the temporal profile is altered in the normal Fed state. My data showing that *Pepck* loses the strict regulation on its Poly(A) tail length in KOs appears to be a mechanistic link between the insulin resistance of *Noc*$^{-/-}$ mice and NOC function.

Moving forward, it will be important to examine other components of the gluconeogenic pathway such as *G6pc* and *FoxO1* to see whether NOC regulates glucose production broadly or at specific nodes throughout glucose production. Additionally, *Noc*$^{-/-}$ have reduced insulin-stimulated glucose uptake in the muscle. *Noc* normally cycles in the muscle but with altered phasing as compared to the liver. *Noc* also does not have the same responsiveness to nutrient in muscle. As many of the genes I have identified as potential targets of NOC have functions

specific to the liver, it will be necessary to examine whether NOC has specific gene targets or categories in different tissues.

Noc As a Therapeutic Target: The Good and the Bad of Knocking Out Noc

Prior to my studies, it would seem that loss of *Nocturnin* in mice was a relatively good thing. *Noc*$^{-/-}$ mice are resistant to DIO and hepatic steatosis, likely through altered lipid flux through the intestine (Green et al., 2007, Douris et al., 2011). *Noc*$^{-/-}$ mice are even protected from the severity of a lethal dose of the endotoxin lipopolysaccharide (LPS) (Niu et al., 2011). But the good rarely comes without some degree of bad. Whereas obesity and insulin resistance often occur hand-in-hand, *Noc*$^{-/-}$ mice have a dissociation of these phenotypes and develop severe insulin resistance upon HFD feeding. Even when fed a RC diet, *Noc*$^{-/-}$ have altered temporal insulin resistant during the dark (active) phase.

Identifying targets of NOC and temporal windows in which its function are critical will help in the potential inclusion of NOC as a therapeutic target. While loss of *Nocturnin* globally has both good and bad phenotypes, it may be possible to modulate *Noc* expression within specific tissues or for specific periods of time throughout the circadian cycle to confer beneficial effects. My results in transgenic mice overexpressing *Noc* highlight the potential benefits of modulating *Noc* expression. When I reintroduced NOC by overexpressing a WT *Nocturnin* transgene on a *Noc*$^{-/-}$ background I was able to improve glucose tolerance. This has implications for human patients with diabetes who develop insulin resistance and lose the ability to regulate blood glucose. Additionally, patients undergoing surgery to cholecystectomy (gallbladder

removal) have dramatically altered BA circulation through the enterohepatic system (Kimball et al., 1976, Malagelada et al., 1973). It may be possible to pharmacologically target NOC and modulate its expression or activity to help restore some of the natural regulation that this system requires.

Appendix I

Figure 1

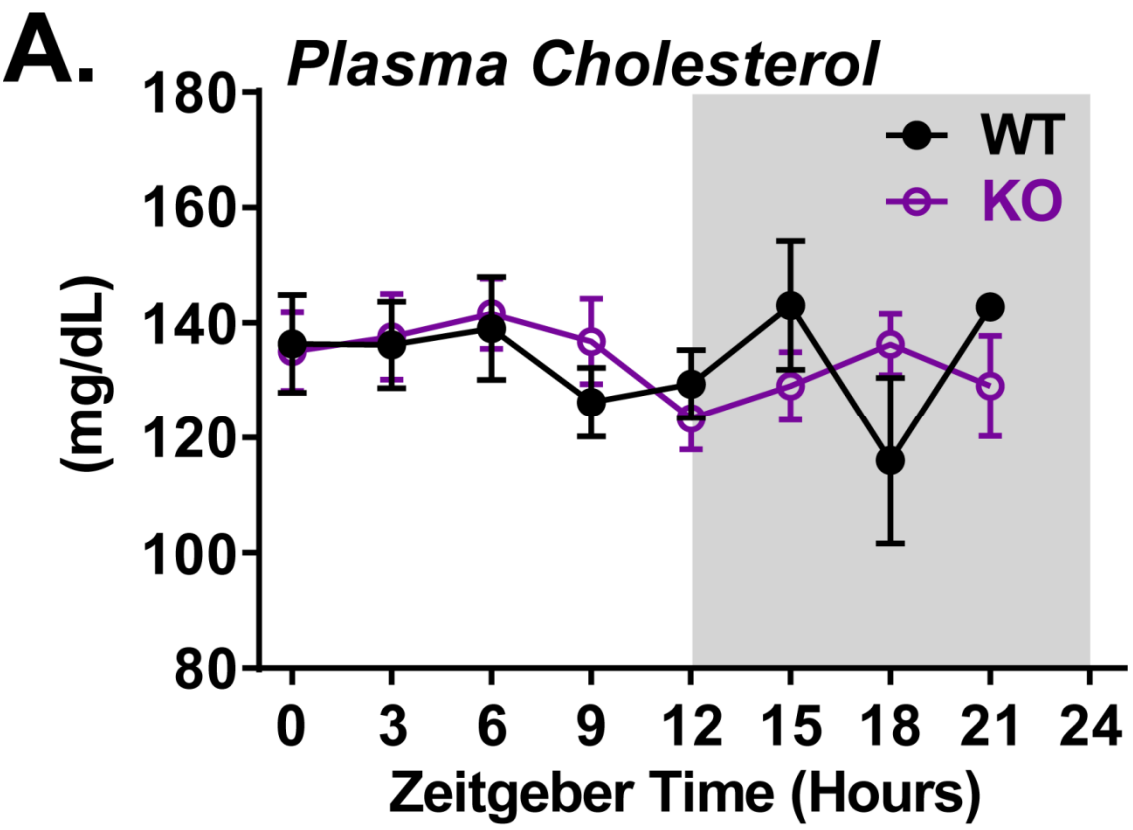

Figure 1. Plasma cholesterol levels in WT and *Noc*$^{-/-}$ mice across the circadian cycle
The temporal phasing and levels of cholesterol in the plasma of WT and *Noc*$^{-/-}$ (KO) mice is not changed. (A) Whole blood was collected from WT and KO mice (n=4-5/genotype/timepoint) into EDTA-coated tubes and placed on ice. Plasma was separated by centrifugation for 10 min at 4000 RCF and then cholesterol was quantified.

Figure 2

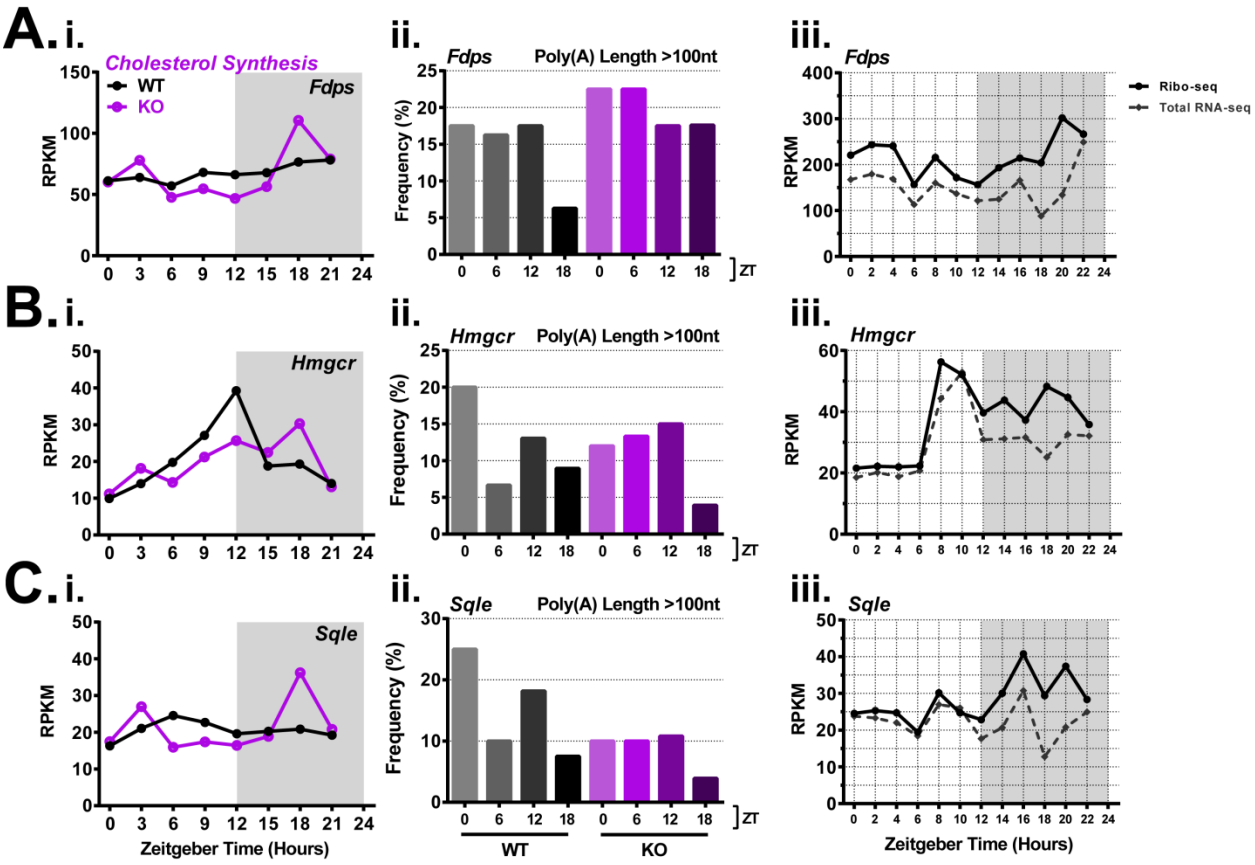

Figure 2. mRNA, Poly(A) tail length and translational rhythms in cholesterol synthesis components

Genes involved in cholesterol synthesis show altered hepatic expression and phasing in *Noc*$^{-/-}$ (KO) mice. Cholesterol synthesis genes exhibit temporal regulation of Poly(A) tail length and these temporal changes are correlated with mRNA and translation rhythms. *Noc*$^{-/-}$ mice have altered Poly(A) tail length regulation which could explain the change in mRNA expression. (A-C, i) mRNA-seq was performed on liver mRNA from WT and KO animals (n=2/genotype/timepoint). Normalized Reads Per Kilobase Per Million Mapped Reads (RPKM) are shown for *Fdps*, *Hmgcr*, and *Sqle* genes. Data points are the Mean of two biological replicates at each timepoint for each genotype. (A-C, ii) TAIL-seq was formed on liver mRNAs

(n=1/genotype/timepoint) and plotted as the Frequency (%) of transcripts for each gene that were quantified as having a Poly(A) tail length greater than 100 nucleotides (>100 nt). For *Fdps*, 80-160 transcripts were counted per genotype at each timepoint. For *Hmgcr* n=15-67 transcripts per genotype were counted at each timepoint. For *Sqle* n=10-51 transcripts per genotype were counted at each timepoint. (A-C, iii) Ribo-seq and Total RNA-seq from a publically available data set (Janich et al., 2015, Janich et al., 2016) is plotted as the Mean RPKM of 2 biological replicates at each timepoint.

Figure 3

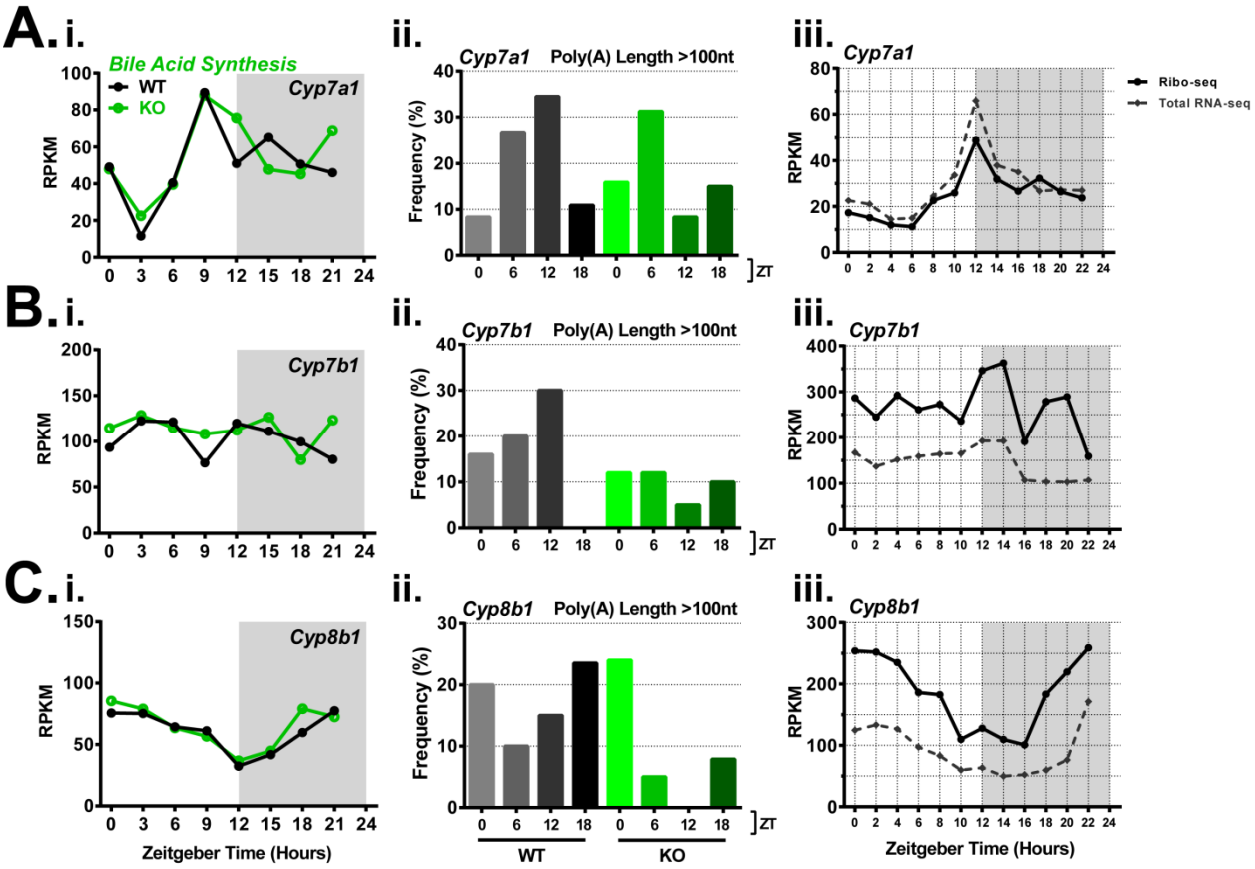

Figure 3. Bile acid synthesis genes show temporal changes in Poly(A) tail length and translation

Genes involved in bile acid synthesis show altered hepatic expression and phasing in *Noc*$^{-/-}$ (KO) mice. Bile acid synthesis genes exhibit temporal regulation of Poly(A) tail length and these temporal changes are correlated with mRNA and translation rhythms. *Noc*$^{-/-}$ mice have altered Poly(A) tail length regulation which could explain the change in mRNA expression. (A-C, i) mRNA-seq was performed on liver mRNA from WT and KO animals (n=2/genotype/timepoint). Normalized Reads Per Kilobase Per Million Mapped Reads (RPKM) are shown for *Cyp7a1*, *Cyp7b1*, and *Cyp8b1* genes. Data points are the Mean of two biological replicates at each timepoint for each genotype. (A-C, ii) TAIL-seq was formed on liver mRNAs (n=1/genotype/timepoint) and plotted as the Frequency (%) of transcripts for each gene that were quantified as having a Poly(A) tail length greater than 100 nucleotides (>100 nt). For *Cyp7a1*, n=18-46 transcripts were counted per genotype at each timepoint. For *Cyp7b1* n=20-25 transcripts per genotype were counted at each timepoint. For *Cyp8b1* n=20-75 transcripts per genotype were counted at each timepoint. (A-C, iii) Ribo-seq and Total RNA-seq from a

publically available data set (Janich et al., 2015, Janich et al., 2016) is plotted as the Mean RPKM of 2 biological replicates at each timepoint.

Figure 4

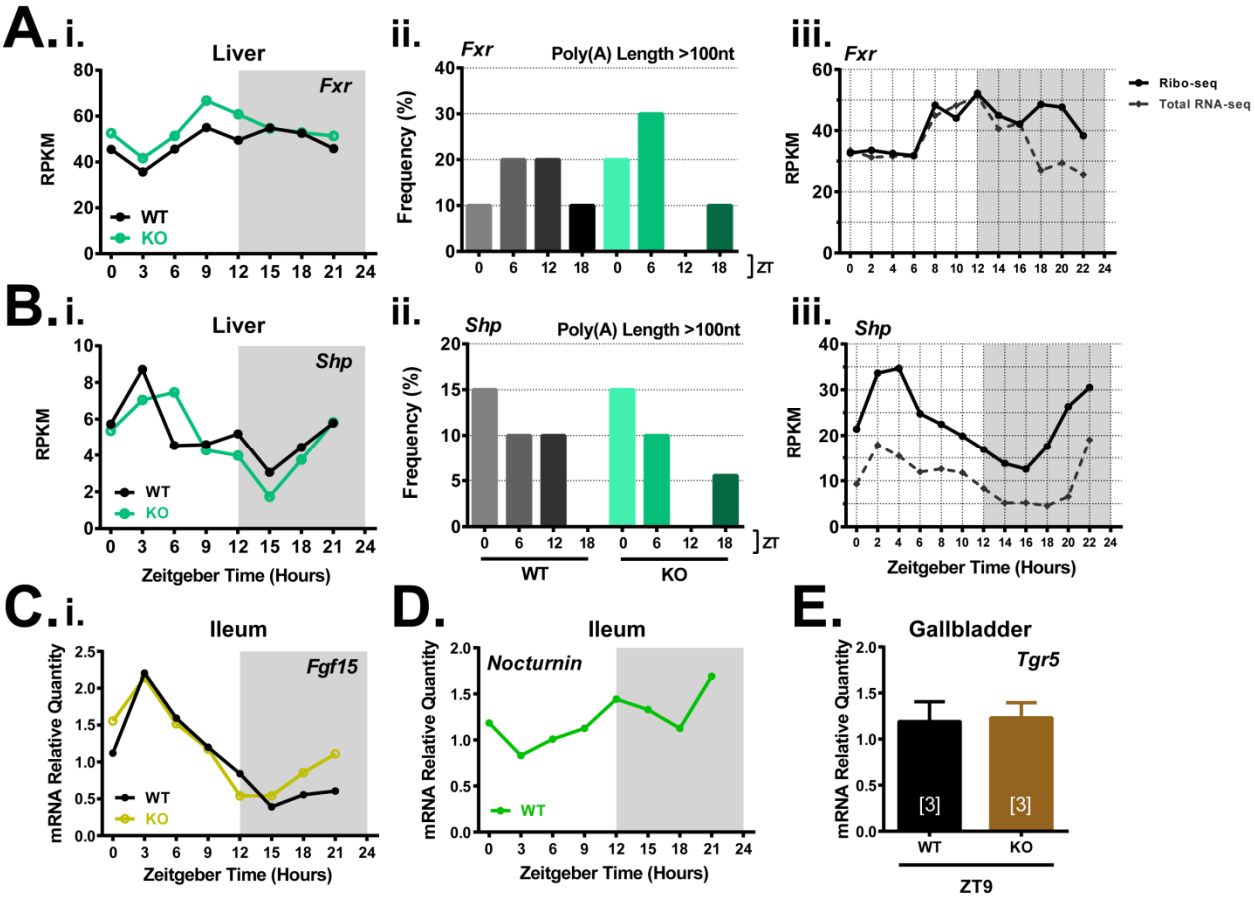

Figure 4. Components of the enterohepatic system regulating bile acid metabolism
Components of the enterohepatic system regulating bile acid metabolism show similar phasing patterns of expression (*Fxr*, *Shp*, *Fgf15*) in WT and *Noc*$^{-/-}$ (KO) mice. *Noc* does not cycle in the ileum. *Tgr5* expression during the light phase (ZT9) is similar between WT and KO gallbladder. (A-B, i) mRNA-seq was performed on liver mRNA from WT and KO animals (n=2/genotype/timepoint). Normalized Reads Per Kilobase Per Million Mapped Reads (RPKM) are shown for the *Fxr* and *Shp* genes. Data points are the Mean of two biological replicates at each timepoint for each genotype. (A-B, ii) TAIL-seq was formed on liver mRNAs (n=1/genotype/timepoint) and plotted as the Frequency (%) of transcripts for the *Fxr* or *Shp* gene that were quantified as having a Poly(A) tail length greater than 100 nucleotides (>100 nt). For *Fxr*, n=20 transcripts were counted per genotype per timepoint. For *Shp*, n=18-20 transcripts were counted per genotype at each timepoint. (A-B, iii) Ribo-seq and Total RNA-seq from a publically available data set (Janich et al., 2015, Janich et al., 2016) is plotted as the Mean RPKM of 2 biological replicates at each timepoint. (C) qPCR amplification of *Fgf15* gene

expression from WT and KO mice ileum (n=2-3/genotype/timepoint). Data points represent the Mean. (D) qPCR amplification of *Noc* gene expression from WT mouse ileum (n=2/timepoint). Data points represent the Mean. (E) qPCR amplification of *Tgr5* gene expression from WT and KO gallbladder harvested at ZT9 (n=3/genotype). Data represent the Mean +/- SEM.

Appendix II

Figure 1

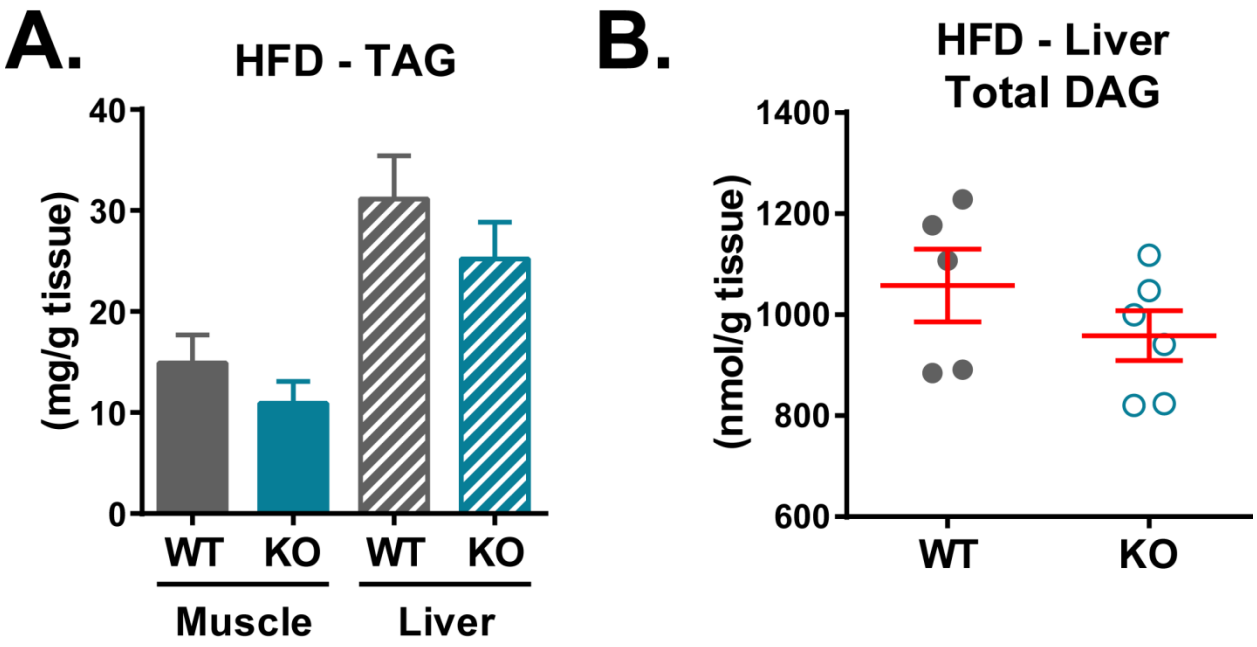

Figure 1. Lipid species in muscle and liver of HFD-fed, overnight fasted WT and *Noc*$^{-/-}$ mice

High Fat Diet (HFD)-fed WT and *Noc*$^{-/-}$ (KO) mice have similar triacyglycerol (TAG) levels in muscle (gastrocnemius) and liver after overnight fasting. Total diacylglycerol (DAG) in HFD-fed WT and KO mice livers are not changed after an overnight fast. (A-B) WT and KO mice (n=5-8) were fed a HFD diet for 3 weeks and then fasted overnight before tissue collection of muscle and liver. Bars and lines represent the Mean +/- SEM.

Figure 2

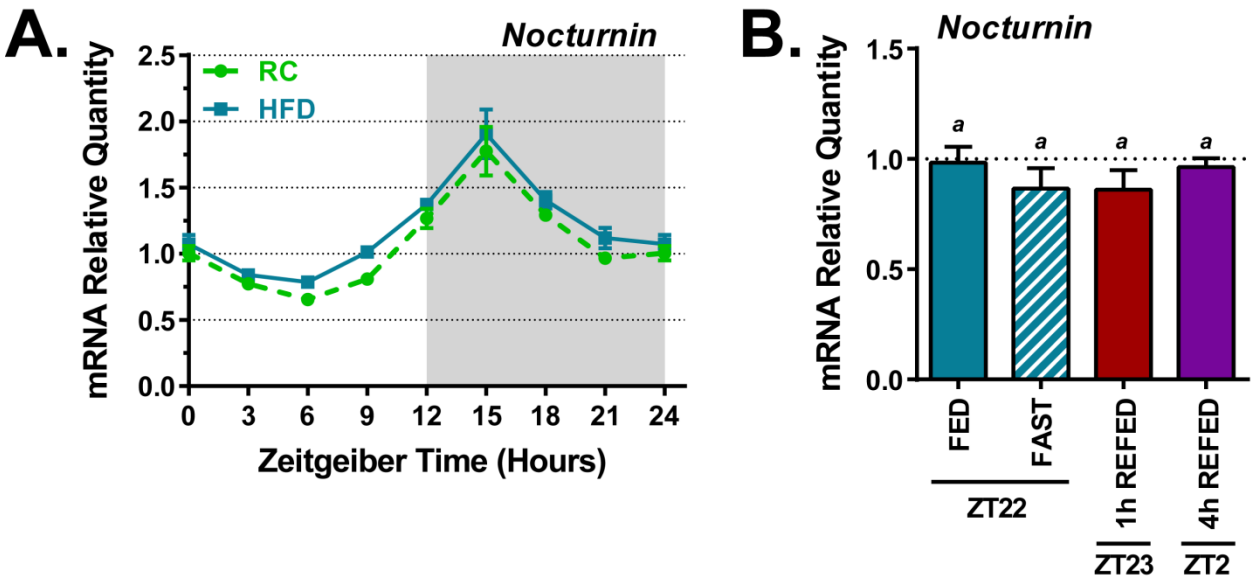

Figure 2. *Nocturnin* mRNA expression in muscle
Nocturnin mRNA (Noc) is rhythmically expressed in muscle (quadriceps) with a peak in expression at ZT15 under both Regular Chow (RC) and 3 weeks High fat Diet (HFD) feeding conditions. Noc expression does not respond to fasting/refeeding on a HFD background. (A) Muscle (quadriceps) was collected from WT mice at different times across the circadian cycle (n=3-4/timepoint). Data points represent Mean +/- SEM. *Noc* cycles in both diet conditions (Two-Way ANOVA, P<0.0001). (B) WT mice (n=3-4/condition) were fed a HFD for 3 weeks and then muscle tissue (quadriceps) was collected at ZT22 in the *Ad Libitum* (FED) condition or 10h Fast (FAST, food removed at ZT12). Additionally, muscle was collected at ZT23 in the 1h REFED or ZT2 in the 4h REFED condition. Refed animals were fasted for 10h from ZT12-ZT22 and HFD food replaced at ZT22 for either 1h (1h REFED) or 4h (4h REFED). Noc expression was measured by qPCR and bars represent Mean +/- SEM. Letters represent means that are not statistically significant (One-way ANOVA, multiple comparisons).

Figure 3

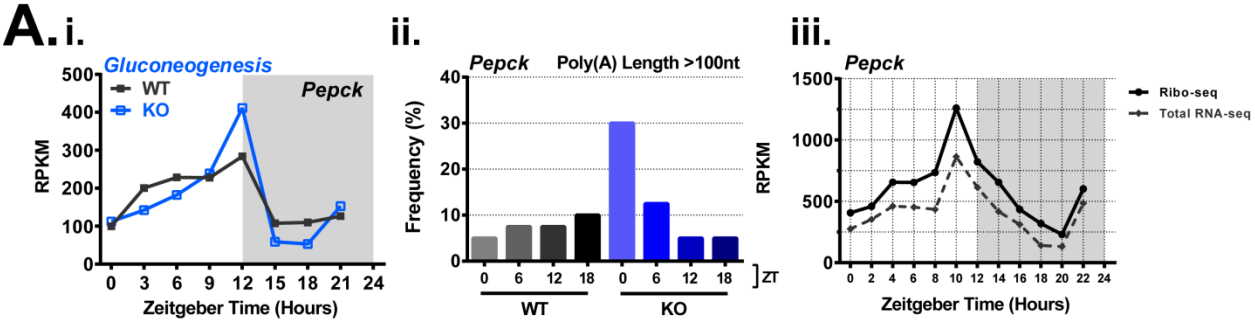

Figure 3. Temporal profiles of mRNA expression, Poly(A) tail length and translation for *Pepck*

The gluconeogenic gene *Pepck* has altered mRNA expression and Poly(A) tail length regulation in *Noc*$^{-/-}$ (KO) mice. (A, i) mRNA-seq was performed on liver mRNA from WT and KO animals (n=2/genotype/timepoint). Normalized Reads Per Kilobase Per Million Mapped Reads (RPKM) are shown. Data points are the Mean of two biological replicates at each timepoint for each genotype. (A, ii) TAIL-seq was formed on liver mRNAs (n=1/genotype/timepoint) and plotted as the Frequency (%) of transcripts that were quantified as having a Poly(A) tail length greater than 100 nucleotides (>100 nt). For *Pepck*, n=40 transcripts were counted per genotype per timepoint. (A, iii) Ribo-seq and Total RNA-seq from a publically available data set (Janich et al., 2015, Janich et al., 2016) is plotted as the Mean RPKM of 2 biological replicates at each timepoint.

Figure 4

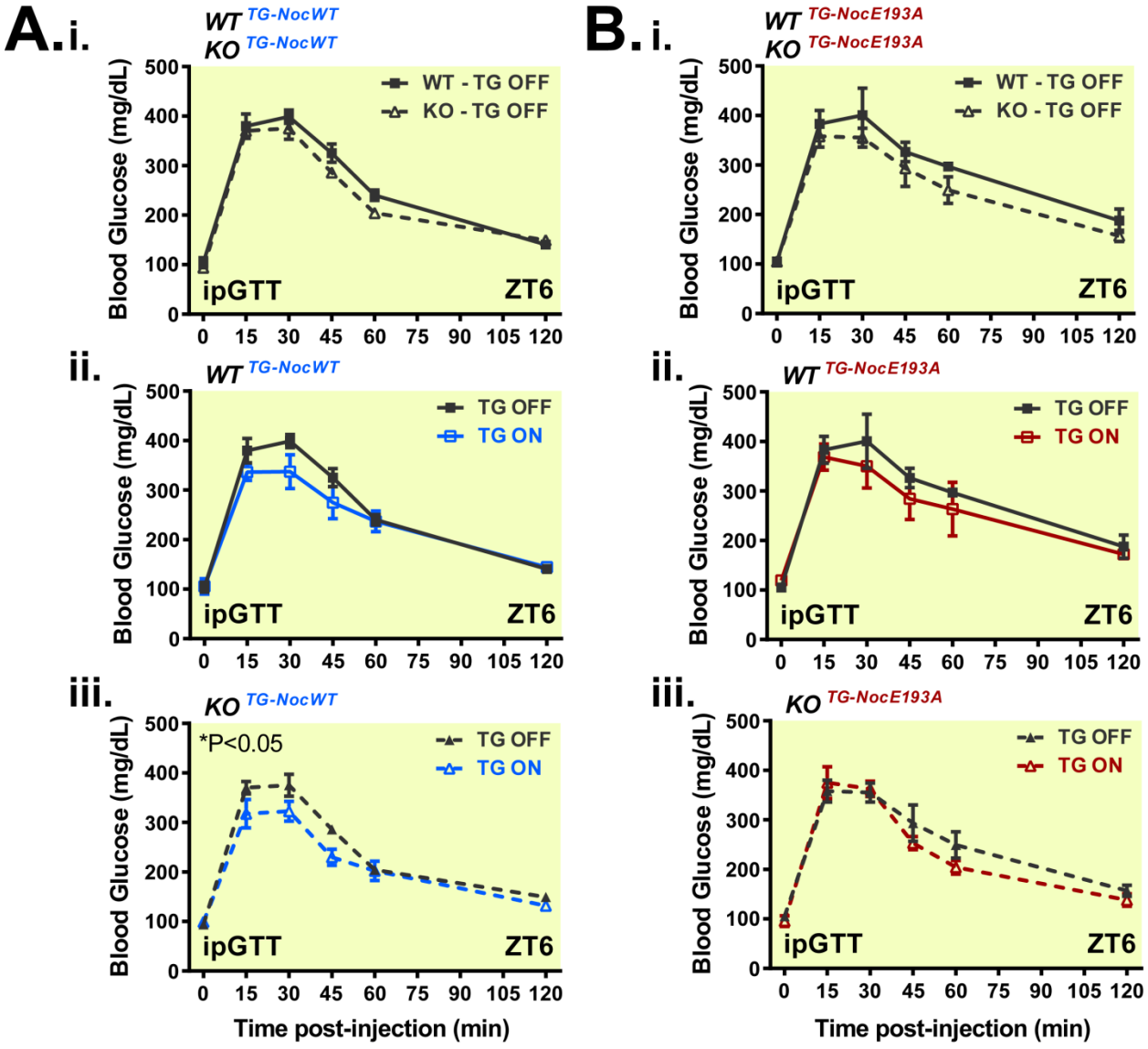

Figure 4. Overexpression of a *WT Nocturnin* transgene improves glucose tolerance in *Noc*$^{-/-}$ mice

Overexpressing a WT *Nocturnin* transgene (*TG-NocWT*) on a *Noc*$^{-/-}$ (KO) background improves glucose tolerance whereas overexpressing a catalytically dead mutant *Nocturnin* transgene (*TG-NocE193A*) does not. (A-B, i-iii) *ROSA26-rtTA x TRE-NocWT x WT*, *ROSA26-rtTA x TRE-NocWT x KO*, *ROSA26-rtTA x NocE193A x WT* and *ROSA26-rtTA x NocE193A x KO* were maintained as homozygous for both transgenes and homozygous on either the WT or KO background. Transgenic animals were either fed Regular Chow (RC) diet (TG OFF) or RC

supplemented with 2 g/kg Doxycycline (TG ON). To induce ubiquitous and maximal expression of the TG, TG ON animals were fed the Dox-supplemented diet for a minimum of 2 weeks prior to experimental manipulation. Mice (n=2-4/transgene/condition) were administered an intraperitoneal glucose tolerance test (ipGTT) at either ZT6 or ZT18 following an 18h fast. Animals were fasted by being placed in a clean cage with woodchip bedding and water, but no food. For the ZT6 GTT, food was removed at ZT12 on the previous day. For the ZT18 GTT, food was removed at ZT0 on the day of the test. Glucose (1.5 g/kg D-glucose, Sigma) was given by intraperitoneal (IP) injection. Blood glucose was monitored by tail vein puncture ZT18 ipGTTs were administered under dim red light. Data points represent the mean +/- SEM. Statistical analysis was Two-way ANOVA, repeated measures, *$P<0.05$)

References:

ADAMOVICH, Y., ROUSSO-NOORI, L., ZWIGHAFT, Z., NEUFELD-COHEN, A., GOLIK, M., KRAUT-COHEN, J., WANG, M., HAN, X. & ASHER, G. 2014. Circadian clocks and feeding time regulate the oscillations and levels of hepatic triglycerides. *Cell Metab,* 19**,** 319-30.

AKASHI, M. & TAKUMI, T. 2005. The orphan nuclear receptor RORalpha regulates circadian transcription of the mammalian core-clock Bmal1. *Nat Struct Mol Biol,* 12**,** 441-8.

ALTAREJOS, J. Y. & MONTMINY, M. 2011. CREB and the CRTC co-activators: sensors for hormonal and metabolic signals. *Nat Rev Mol Cell Biol,* 12**,** 141-51.

ASHER, G., GATFIELD, D., STRATMANN, M., REINKE, H., DIBNER, C., KREPPEL, F., MOSTOSLAVSKY, R., ALT, F. W. & SCHIBLER, U. 2008. SIRT1 regulates circadian clock gene expression through PER2 deacetylation. *Cell,* 134**,** 317-28.

ASHER, G., REINKE, H., ALTMEYER, M., GUTIERREZ-ARCELUS, M., HOTTIGER, M. O. & SCHIBLER, U. 2010. Poly(ADP-ribose) polymerase 1 participates in the phase entrainment of circadian clocks to feeding. *Cell,* 142**,** 943-53.

AYALA, J. E., SAMUEL, V. T., MORTON, G. J., OBICI, S., CRONIGER, C. M., SHULMAN, G. I., WASSERMAN, D. H. & MCGUINNESS, O. P. 2010. Standard operating procedures for describing and performing metabolic tests of glucose homeostasis in mice. *Dis Model Mech,* 3**,** 525-34.

BAE, K., JIN, X., MAYWOOD, E. S., HASTINGS, M. H., REPPERT, S. M. & WEAVER, D. R. 2001. Differential functions of mPer1, mPer2, and mPer3 in the SCN circadian clock. *Neuron,* 30**,** 525-36.

BAGGS, J. E. & GREEN, C. B. 2003. Nocturnin, a deadenylase in Xenopus laevis retina: a mechanism for posttranscriptional control of circadian-related mRNA. *Curr Biol,* 13**,** 189-98.

BALSALOBRE, A., BROWN, S. A., MARCACCI, L., TRONCHE, F., KELLENDONK, C., REICHARDT, H. M., SCHUTZ, G. & SCHIBLER, U. 2000a. Resetting of circadian time in peripheral tissues by glucocorticoid signaling. *Science,* 289**,** 2344-7.

BALSALOBRE, A., DAMIOLA, F. & SCHIBLER, U. 1998. A serum shock induces circadian gene expression in mammalian tissue culture cells. *Cell,* 93**,** 929-37.

BALSALOBRE, A., MARCACCI, L. & SCHIBLER, U. 2000b. Multiple signaling pathways elicit circadian gene expression in cultured Rat-1 fibroblasts. *Curr Biol,* 10**,** 1291-4.

BOOKOUT, A. L., DE GROOT, M. H., OWEN, B. M., LEE, S., GAUTRON, L., LAWRENCE, H. L., DING, X., ELMQUIST, J. K., TAKAHASHI, J. S., MANGELSDORF, D. J. & KLIEWER, S. A. 2013. FGF21 regulates metabolism and circadian behavior by acting on the nervous system. *Nat Med,* 19**,** 1147-52.

CANAPLE, L., RAMBAUD, J., DKHISSI-BENYAHYA, O., RAYET, B., TAN, N. S., MICHALIK, L., DELAUNAY, F., WAHLI, W. & LAUDET, V. 2006. Reciprocal regulation of brain and muscle Arnt-like protein 1 and peroxisome proliferator-activated

receptor alpha defines a novel positive feedback loop in the rodent liver circadian clock. *Mol Endocrinol,* 20**,** 1715-27.

CHAIX, A., ZARRINPAR, A., MIU, P. & PANDA, S. 2014. Time-restricted feeding is a preventative and therapeutic intervention against diverse nutritional challenges. *Cell Metab,* 20**,** 991-1005.

CHANG, H., LIM, J., HA, M. & KIM, V. N. 2014. TAIL-seq: genome-wide determination of poly(A) tail length and 3' end modifications. *Mol Cell,* 53**,** 1044-52.

CHEN, L., MAGLIANO, D. J. & ZIMMET, P. Z. 2012. The worldwide epidemiology of type 2 diabetes mellitus--present and future perspectives. *Nat Rev Endocrinol,* 8**,** 228-36.

CHO, H., ZHAO, X., HATORI, M., YU, R. T., BARISH, G. D., LAM, M. T., CHONG, L. W., DITACCHIO, L., ATKINS, A. R., GLASS, C. K., LIDDLE, C., AUWERX, J., DOWNES, M., PANDA, S. & EVANS, R. M. 2012. Regulation of circadian behaviour and metabolism by REV-ERB-alpha and REV-ERB-beta. *Nature,* 485**,** 123-7.

COTTER, D. G., SCHUGAR, R. C. & CRAWFORD, P. A. 2013. Ketone body metabolism and cardiovascular disease. *Am J Physiol Heart Circ Physiol,* 304**,** H1060-76.

DAMIOLA, F., LE MINH, N., PREITNER, N., KORNMANN, B., FLEURY-OLELA, F. & SCHIBLER, U. 2000. Restricted feeding uncouples circadian oscillators in peripheral tissues from the central pacemaker in the suprachiasmatic nucleus. *Genes Dev,* 14**,** 2950-61.

DE AGUIAR VALLIM, T. Q., TARLING, E. J. & EDWARDS, P. A. 2013. Pleiotropic roles of bile acids in metabolism. *Cell Metab,* 17**,** 657-69.

DHAKRAS, P. S., HAJARNIS, S., TAYLOR, L. & CURTHOYS, N. P. 2006. cAMP-dependent stabilization of phosphoenolpyruvate carboxykinase mRNA in LLC-PK1-F+ kidney cells. *Am J Physiol Renal Physiol,* 290**,** F313-8.

DOURIS, N., KOJIMA, S., PAN, X., LERCH-GAGGL, A. F., DUONG, S. Q., HUSSAIN, M. M. & GREEN, C. B. 2011. Nocturnin regulates circadian trafficking of dietary lipid in intestinal enterocytes. *Curr Biol,* 21**,** 1347-55.

DUPRESSOIR, A., BARBOT, W., LOIREAU, M. P. & HEIDMANN, T. 1999. Characterization of a mammalian gene related to the yeast CCR4 general transcription factor and revealed by transposon insertion. *J Biol Chem,* 274**,** 31068-75.

DUPRESSOIR, A., MOREL, A. P., BARBOT, W., LOIREAU, M. P., CORBO, L. & HEIDMANN, T. 2001. Identification of four families of yCCR4- and Mg2+-dependent endonuclease-related proteins in higher eukaryotes, and characterization of orthologs of yCCR4 with a conserved leucine-rich repeat essential for hCAF1/hPOP2 binding. *BMC Genomics,* 2**,** 9.

ECKEL-MAHAN, K. L., PATEL, V. R., DE MATEO, S., OROZCO-SOLIS, R., CEGLIA, N. J., SAHAR, S., DILAG-PENILLA, S. A., DYAR, K. A., BALDI, P. & SASSONE-CORSI, P. 2013. Reprogramming of the circadian clock by nutritional challenge. *Cell,* 155**,** 1464-78.

ECKEL-MAHAN, K. L., PATEL, V. R., MOHNEY, R. P., VIGNOLA, K. S., BALDI, P. & SASSONE-CORSI, P. 2012. Coordination of the transcriptome and metabolome by the circadian clock. *Proc Natl Acad Sci U S A,* 109**,** 5541-6.

EVANS, R. M., BARISH, G. D. & WANG, Y. X. 2004. PPARs and the complex journey to obesity. *Nat Med,* 10**,** 355-61.

GACHON, F., OLELA, F. F., SCHAAD, O., DESCOMBES, P. & SCHIBLER, U. 2006. The circadian PAR-domain basic leucine zipper transcription factors DBP, TEF, and HLF modulate basal and inducible xenobiotic detoxification. *Cell Metab,* 4**,** 25-36.

GARBARINO-PICO, E. & GREEN, C. B. 2007. Posttranscriptional regulation of mammalian circadian clock output. *Cold Spring Harb Symp Quant Biol,* 72**,** 145-56.

GARBARINO-PICO, E., NIU, S., ROLLAG, M. D., STRAYER, C. A., BESHARSE, J. C. & GREEN, C. B. 2007. Immediate early response of the circadian polyA ribonuclease nocturnin to two extracellular stimuli. *RNA,* 13**,** 745-55.

GILBERT, M. R., DOURIS, N., TONGJAI, S. & GREEN, C. B. 2011. Nocturnin expression is induced by fasting in the white adipose tissue of restricted fed mice. *PLoS One,* 6**,** e17051.

GREEN, C. B. & BESHARSE, J. C. 1996. Identification of a novel vertebrate circadian clock-regulated gene encoding the protein nocturnin. *Proc Natl Acad Sci U S A,* 93**,** 14884-8.

GREEN, C. B., BESHARSE, J. C. & ZATZ, M. 1996. Tryptophan hydroxylase mRNA levels are regulated by the circadian clock, temperature, and cAMP in chick pineal cells. *Brain Res,* 738**,** 1-7.

GREEN, C. B., DOURIS, N., KOJIMA, S., STRAYER, C. A., FOGERTY, J., LOURIM, D., KELLER, S. R. & BESHARSE, J. C. 2007. Loss of Nocturnin, a circadian deadenylase,

confers resistance to hepatic steatosis and diet-induced obesity. *Proc Natl Acad Sci U S A,* 104**,** 9888-93.

GRIMALDI, B., BELLET, M. M., KATADA, S., ASTARITA, G., HIRAYAMA, J., AMIN, R. H., GRANNEMAN, J. G., PIOMELLI, D., LEFF, T. & SASSONE-CORSI, P. 2010. PER2 controls lipid metabolism by direct regulation of PPARgamma. *Cell Metab,* 12**,** 509-20.

GUILLAUMOND, F., DARDENTE, H., GIGUERE, V. & CERMAKIAN, N. 2005. Differential control of Bmal1 circadian transcription by REV-ERB and ROR nuclear receptors. *J Biol Rhythms,* 20**,** 391-403.

GUMMADI, L., TAYLOR, L. & CURTHOYS, N. P. 2012. Concurrent binding and modifications of AUF1 and HuR mediate the pH-responsive stabilization of phosphoenolpyruvate carboxykinase mRNA in kidney cells. *Am J Physiol Renal Physiol,* 303**,** F1545-54.

HAEUSLER, R. A., PRATT-HYATT, M., WELCH, C. L., KLAASSEN, C. D. & ACCILI, D. 2012. Impaired generation of 12-hydroxylated bile acids links hepatic insulin signaling with dyslipidemia. *Cell Metab,* 15**,** 65-74.

HAJARNIS, S., SCHROEDER, J. M. & CURTHOYS, N. P. 2005. 3'-Untranslated region of phosphoenolpyruvate carboxykinase mRNA contains multiple instability elements that bind AUF1. *J Biol Chem,* 280**,** 28272-80.

HATORI, M., VOLLMERS, C., ZARRINPAR, A., DITACCHIO, L., BUSHONG, E. A., GILL, S., LEBLANC, M., CHAIX, A., JOENS, M., FITZPATRICK, J. A., ELLISMAN, M. H.

& PANDA, S. 2012. Time-restricted feeding without reducing caloric intake prevents metabolic diseases in mice fed a high-fat diet. *Cell Metab,* 15**,** 848-60.

HOOGERWERF, W. A., HELLMICH, H. L., CORNELISSEN, G., HALBERG, F., SHAHINIAN, V. B., BOSTWICK, J., SAVIDGE, T. C. & CASSONE, V. M. 2007. Clock gene expression in the murine gastrointestinal tract: endogenous rhythmicity and effects of a feeding regimen. *Gastroenterology,* 133**,** 1250-60.

HUANG DA, W., SHERMAN, B. T. & LEMPICKI, R. A. 2009a. Bioinformatics enrichment tools: paths toward the comprehensive functional analysis of large gene lists. *Nucleic Acids Res,* 37**,** 1-13.

HUANG DA, W., SHERMAN, B. T. & LEMPICKI, R. A. 2009b. Systematic and integrative analysis of large gene lists using DAVID bioinformatics resources. *Nat Protoc,* 4**,** 44-57.

INAGAKI, T., CHOI, M., MOSCHETTA, A., PENG, L., CUMMINS, C. L., MCDONALD, J. G., LUO, G., JONES, S. A., GOODWIN, B., RICHARDSON, J. A., GERARD, R. D., REPA, J. J., MANGELSDORF, D. J. & KLIEWER, S. A. 2005. Fibroblast growth factor 15 functions as an enterohepatic signal to regulate bile acid homeostasis. *Cell Metab,* 2**,** 217-25.

JANICH, P., ARPAT, A. B., CASTELO-SZEKELY, V. & GATFIELD, D. 2016. Analyzing the temporal regulation of translation efficiency in mouse liver. *Genom Data,* 8**,** 41-4.

JANICH, P., ARPAT, A. B., CASTELO-SZEKELY, V., LOPES, M. & GATFIELD, D. 2015. Ribosome profiling reveals the rhythmic liver translatome and circadian clock regulation by upstream open reading frames. *Genome Res,* 25**,** 1848-59.

KAASIK, K., KIVIMAE, S., ALLEN, J. J., CHALKLEY, R. J., HUANG, Y., BAER, K., KISSEL, H., BURLINGAME, A. L., SHOKAT, K. M., PTACEK, L. J. & FU, Y. H. 2013. Glucose sensor O-GlcNAcylation coordinates with phosphorylation to regulate circadian clock. *Cell Metab,* 17**,** 291-302.

KASUKAWA, T., SUGIMOTO, M., HIDA, A., MINAMI, Y., MORI, M., HONMA, S., HONMA, K., MISHIMA, K., SOGA, T. & UEDA, H. R. 2012. Human blood metabolite timetable indicates internal body time. *Proc Natl Acad Sci U S A,* 109**,** 15036-41.

KAWAI, M., GREEN, C. B., HOROWITZ, M., ACKERT-BICKNELL, C., LECKA-CZERNIK, B. & ROSEN, C. J. 2010a. Nocturnin: a circadian target of Pparg-induced adipogenesis. *Ann N Y Acad Sci,* 1192**,** 131-8.

KAWAI, M., GREEN, C. B., LECKA-CZERNIK, B., DOURIS, N., GILBERT, M. R., KOJIMA, S., ACKERT-BICKNELL, C., GARG, N., HOROWITZ, M. C., ADAMO, M. L., CLEMMONS, D. R. & ROSEN, C. J. 2010b. A circadian-regulated gene, Nocturnin, promotes adipogenesis by stimulating PPAR-gamma nuclear translocation. *Proc Natl Acad Sci U S A,* 107**,** 10508-13.

KAWAMATA, Y., FUJII, R., HOSOYA, M., HARADA, M., YOSHIDA, H., MIWA, M., FUKUSUMI, S., HABATA, Y., ITOH, T., SHINTANI, Y., HINUMA, S., FUJISAWA, Y. & FUJINO, M. 2003. A G protein-coupled receptor responsive to bile acids. *J Biol Chem,* 278**,** 9435-40.

KIM, I., AHN, S. H., INAGAKI, T., CHOI, M., ITO, S., GUO, G. L., KLIEWER, S. A. & GONZALEZ, F. J. 2007. Differential regulation of bile acid homeostasis by the farnesoid X receptor in liver and intestine. *J Lipid Res,* 48**,** 2664-72.

KIM, J. K. 2009. Hyperinsulinemic-euglycemic clamp to assess insulin sensitivity in vivo. *Methods Mol Biol,* 560**,** 221-38.

KIMBALL, A., PERTSEMLIDIS, D. & PANVELIWALLA, D. 1976. Composition of biliary lipids and kinetics of bile acids after cholecystectomy in man. *Am J Dig Dis,* 21**,** 776-81.

KO, C. H. & TAKAHASHI, J. S. 2006. Molecular components of the mammalian circadian clock. *Hum Mol Genet,* 15 Spec No 2**,** R271-7.

KOHSAKA, A., LAPOSKY, A. D., RAMSEY, K. M., ESTRADA, C., JOSHU, C., KOBAYASHI, Y., TUREK, F. W. & BASS, J. 2007. High-fat diet disrupts behavioral and molecular circadian rhythms in mice. *Cell Metab,* 6**,** 414-21.

KOIKE, N., YOO, S. H., HUANG, H. C., KUMAR, V., LEE, C., KIM, T. K. & TAKAHASHI, J. S. 2012. Transcriptional architecture and chromatin landscape of the core circadian clock in mammals. *Science,* 338**,** 349-54.

KOJIMA, S., GATFIELD, D., ESAU, C. C. & GREEN, C. B. 2010. MicroRNA-122 modulates the rhythmic expression profile of the circadian deadenylase Nocturnin in mouse liver. *PLoS One,* 5**,** e11264.

KOJIMA, S., GENDREAU, K. L., SHER-CHEN, E. L., GAO, P. & GREEN, C. B. 2015. Changes in poly(A) tail length dynamics from the loss of the circadian deadenylase Nocturnin. *Sci Rep,* 5**,** 17059.

KOJIMA, S., SHER-CHEN, E. L. & GREEN, C. B. 2012. Circadian control of mRNA polyadenylation dynamics regulates rhythmic protein expression. *Genes Dev,* 26**,** 2724-36.

KOJIMA, S., SHINGLE, D. L. & GREEN, C. B. 2011. Post-transcriptional control of circadian rhythms. *J Cell Sci,* 124**,** 311-20.

KORNMANN, B., SCHAAD, O., BUJARD, H., TAKAHASHI, J. S. & SCHIBLER, U. 2007. System-driven and oscillator-dependent circadian transcription in mice with a conditionally active liver clock. *PLoS Biol,* 5**,** e34.

KUBOTA, T., KUBOTA, N., KUMAGAI, H., YAMAGUCHI, S., KOZONO, H., TAKAHASHI, T., INOUE, M., ITOH, S., TAKAMOTO, I., SASAKO, T., KUMAGAI, K., KAWAI, T., HASHIMOTO, S., KOBAYASHI, T., SATO, M., TOKUYAMA, K., NISHIMURA, S., TSUNODA, M., IDE, T., MURAKAMI, K., YAMAZAKI, T., EZAKI, O., KAWAMURA, K., MASUDA, H., MOROI, M., SUGI, K., OIKE, Y., SHIMOKAWA, H., YANAGIHARA, N., TSUTSUI, M., TERAUCHI, Y., TOBE, K., NAGAI, R., KAMATA, K., INOUE, K., KODAMA, T., UEKI, K. & KADOWAKI, T. 2011. Impaired insulin signaling in endothelial cells reduces insulin-induced glucose uptake by skeletal muscle. *Cell Metab,* 13**,** 294-307.

KUIPERS, F., BLOKS, V. W. & GROEN, A. K. 2014. Beyond intestinal soap--bile acids in metabolic control. *Nat Rev Endocrinol,* 10**,** 488-98.

LAMIA, K. A., PAPP, S. J., YU, R. T., BARISH, G. D., UHLENHAUT, N. H., JONKER, J. W., DOWNES, M. & EVANS, R. M. 2011. Cryptochromes mediate rhythmic repression of the glucocorticoid receptor. *Nature,* 480**,** 552-6.

LAMIA, K. A., SACHDEVA, U. M., DITACCHIO, L., WILLIAMS, E. C., ALVAREZ, J. G., EGAN, D. F., VASQUEZ, D. S., JUGUILON, H., PANDA, S., SHAW, R. J., THOMPSON, C. B. & EVANS, R. M. 2009. AMPK regulates the circadian clock by cryptochrome phosphorylation and degradation. *Science,* 326**,** 437-40.

LAMIA, K. A., STORCH, K. F. & WEITZ, C. J. 2008. Physiological significance of a peripheral tissue circadian clock. *Proc Natl Acad Sci U S A,* 105**,** 15172-7.

LE MARTELOT, G., CANELLA, D., SYMUL, L., MIGLIAVACCA, E., GILARDI, F., LIECHTI, R., MARTIN, O., HARSHMAN, K., DELORENZI, M., DESVERGNE, B., HERR, W., DEPLANCKE, B., SCHIBLER, U., ROUGEMONT, J., GUEX, N., HERNANDEZ, N. & NAEF, F. 2012. Genome-wide RNA polymerase II profiles and RNA accumulation reveal kinetics of transcription and associated epigenetic changes during diurnal cycles. *PLoS Biol,* 10**,** e1001442.

LE MARTELOT, G., CLAUDEL, T., GATFIELD, D., SCHAAD, O., KORNMANN, B., LO SASSO, G., MOSCHETTA, A. & SCHIBLER, U. 2009. REV-ERBalpha participates in circadian SREBP signaling and bile acid homeostasis. *PLoS Biol,* 7**,** e1000181.

LE MINH, N., DAMIOLA, F., TRONCHE, F., SCHUTZ, G. & SCHIBLER, U. 2001. Glucocorticoid hormones inhibit food-induced phase-shifting of peripheral circadian oscillators. *EMBO J,* 20**,** 7128-36.

LI, M. D., RUAN, H. B., HUGHES, M. E., LEE, J. S., SINGH, J. P., JONES, S. P., NITABACH, M. N. & YANG, X. 2013. O-GlcNAc signaling entrains the circadian clock by inhibiting BMAL1/CLOCK ubiquitination. *Cell Metab,* 17**,** 303-10.

LI, R., YUE, J., ZHANG, Y., ZHOU, L., HAO, W., YUAN, J., QIANG, B., DING, J. M., PENG, X. & CAO, J. M. 2008. CLOCK/BMAL1 regulates human nocturnin transcription through binding to the E-box of nocturnin promoter. *Mol Cell Biochem,* 317**,** 169-77.

LI, T., HOLMSTROM, S. R., KIR, S., UMETANI, M., SCHMIDT, D. R., KLIEWER, S. A. & MANGELSDORF, D. J. 2011. The G protein-coupled bile acid receptor, TGR5, stimulates gallbladder filling. *Mol Endocrinol,* 25**,** 1066-71.

LIU, C., LI, S., LIU, T., BORJIGIN, J. & LIN, J. D. 2007. Transcriptional coactivator PGC-1alpha integrates the mammalian clock and energy metabolism. *Nature,* 447**,** 477-81.

MA, K., XIAO, R., TSENG, H. T., SHAN, L., FU, L. & MOORE, D. D. 2009. Circadian dysregulation disrupts bile acid homeostasis. *PLoS One,* 4**,** e6843.

MAKISHIMA, M., OKAMOTO, A. Y., REPA, J. J., TU, H., LEARNED, R. M., LUK, A., HULL, M. V., LUSTIG, K. D., MANGELSDORF, D. J. & SHAN, B. 1999. Identification of a nuclear receptor for bile acids. *Science,* 284**,** 1362-5.

MALAGELADA, J. R., GO, V. L., SUMMERSKILL, W. H. & GAMBLE, W. S. 1973. Bile acid secretion and biliary bile acid composition altered by cholecystectomy. *Am J Dig Dis,* 18**,** 455-9.

MARCHEVA, B., RAMSEY, K. M., BUHR, E. D., KOBAYASHI, Y., SU, H., KO, C. H., IVANOVA, G., OMURA, C., MO, S., VITATERNA, M. H., LOPEZ, J. P., PHILIPSON, L. H., BRADFIELD, C. A., CROSBY, S. D., JEBAILEY, L., WANG, X., TAKAHASHI, J. S. & BASS, J. 2010. Disruption of the clock components CLOCK and BMAL1 leads to hypoinsulinaemia and diabetes. *Nature,* 466**,** 627-31.

MARCHEVA, B., RAMSEY, K. M., PEEK, C. B., AFFINATI, A., MAURY, E. & BASS, J. 2013. Circadian clocks and metabolism. *Handb Exp Pharmacol***,** 127-55.

MARUYAMA, T., MIYAMOTO, Y., NAKAMURA, T., TAMAI, Y., OKADA, H., SUGIYAMA, E., ITADANI, H. & TANAKA, K. 2002. Identification of membrane-type receptor for bile acids (M-BAR). *Biochem Biophys Res Commun,* 298**,** 714-9.

MASSIERA, F., BARBRY, P., GUESNET, P., JOLY, A., LUQUET, S., MOREILHON-BREST, C., MOHSEN-KANSON, T., AMRI, E. Z. & AILHAUD, G. 2010a. A Western-like fat diet is sufficient to induce a gradual enhancement in fat mass over generations. *J Lipid Res,* 51**,** 2352-61.

MASSIERA, F., BARBRY, P., GUESNET, P., JOLY, A., LUQUET, S., MOREILHON BREST, C., MOHSEN-KANSON, T., AMRI, E. Z. & AILHAUD, G. P. 2010b. A Western-like fat diet is sufficient to induce a gradual enhancement in fat mass over generations. *Journal of Lipid Research*.

MCNAMARA, P., SEO, S. B., RUDIC, R. D., SEHGAL, A., CHAKRAVARTI, D. & FITZGERALD, G. A. 2001. Regulation of CLOCK and MOP4 by nuclear hormone

receptors in the vasculature: a humoral mechanism to reset a peripheral clock. *Cell,* 105**,** 877-89.

MENET, J. S., RODRIGUEZ, J., ABRUZZI, K. C. & ROSBASH, M. 2012. Nascent-Seq reveals novel features of mouse circadian transcriptional regulation. *Elife,* 1**,** e00011.

MINAMI, Y., KASUKAWA, T., KAKAZU, Y., IIGO, M., SUGIMOTO, M., IKEDA, S., YASUI, A., VAN DER HORST, G. T., SOGA, T. & UEDA, H. R. 2009. Measurement of internal body time by blood metabolomics. *Proc Natl Acad Sci U S A,* 106**,** 9890-5.

MOHAWK, J. A., GREEN, C. B. & TAKAHASHI, J. S. 2012. Central and peripheral circadian clocks in mammals. *Annu Rev Neurosci,* 35**,** 445-62.

MOHAWK, J. A. & TAKAHASHI, J. S. 2011. Cell autonomy and synchrony of suprachiasmatic nucleus circadian oscillators. *Trends Neurosci,* 34**,** 349-58.

MOORE, R. Y. 2013. The suprachiasmatic nucleus and the circadian timing system. *Prog Mol Biol Transl Sci,* 119**,** 1-28.

MUFTI, J., HAJARNIS, S., SHEPARDSON, K., GUMMADI, L., TAYLOR, L. & CURTHOYS, N. P. 2011. Role of AUF1 and HuR in the pH-responsive stabilization of phosphoenolpyruvate carboxykinase mRNA in LLC-PK(1)-F(+) cells. *Am J Physiol Renal Physiol,* 301**,** F1066-77.

NAKAHATA, Y., AKASHI, M., TRCKA, D., YASUDA, A. & TAKUMI, T. 2006. The in vitro real-time oscillation monitoring system identifies potential entrainment factors for circadian clocks. *BMC Mol Biol,* 7**,** 5.

NAKAHATA, Y., KALUZOVA, M., GRIMALDI, B., SAHAR, S., HIRAYAMA, J., CHEN, D., GUARENTE, L. P. & SASSONE-CORSI, P. 2008. The NAD+-dependent deacetylase SIRT1 modulates CLOCK-mediated chromatin remodeling and circadian control. *Cell,* 134**,** 329-40.

NAKAHATA, Y., SAHAR, S., ASTARITA, G., KALUZOVA, M. & SASSONE-CORSI, P. 2009. Circadian control of the NAD+ salvage pathway by CLOCK-SIRT1. *Science,* 324**,** 654-7.

NIU, S., SHINGLE, D. L., GARBARINO-PICO, E., KOJIMA, S., GILBERT, M. & GREEN, C. B. 2011. The circadian deadenylase Nocturnin is necessary for stabilization of the iNOS mRNA in mice. *PLoS One,* 6**,** e26954.

OISHI, K., ATSUMI, G., SUGIYAMA, S., KODOMARI, I., KASAMATSU, M., MACHIDA, K. & ISHIDA, N. 2006. Disrupted fat absorption attenuates obesity induced by a high-fat diet in Clock mutant mice. *FEBS Lett,* 580**,** 127-30.

OISHI, K., MIYAZAKI, K., KADOTA, K., KIKUNO, R., NAGASE, T., ATSUMI, G., OHKURA, N., AZAMA, T., MESAKI, M., YUKIMASA, S., KOBAYASHI, H., IITAKA, C., UMEHARA, T., HORIKOSHI, M., KUDO, T., SHIMIZU, Y., YANO, M., MONDEN, M., MACHIDA, K., MATSUDA, J., HORIE, S., TODO, T. & ISHIDA, N. 2003. Genome-wide expression analysis of mouse liver reveals CLOCK-regulated circadian output genes. *J Biol Chem,* 278**,** 41519-27.

OISHI, K., SHIRAI, H. & ISHIDA, N. 2005. CLOCK is involved in the circadian transactivation of peroxisome-proliferator-activated receptor alpha (PPARalpha) in mice. *Biochem J,* 386**,** 575-81.

OWEN, B. M., MANGELSDORF, D. J. & KLIEWER, S. A. 2015. Tissue-specific actions of the metabolic hormones FGF15/19 and FGF21. *Trends Endocrinol Metab,* 26**,** 22-9.

PAIK, J. H., KOLLIPARA, R., CHU, G., JI, H., XIAO, Y., DING, Z., MIAO, L., TOTHOVA, Z., HORNER, J. W., CARRASCO, D. R., JIANG, S., GILLILAND, D. G., CHIN, L., WONG, W. H., CASTRILLON, D. H. & DEPINHO, R. A. 2007. FoxOs are lineage-restricted redundant tumor suppressors and regulate endothelial cell homeostasis. *Cell,* 128**,** 309-23.

PAN, X. & HUSSAIN, M. M. 2007. Diurnal regulation of microsomal triglyceride transfer protein and plasma lipid levels. *J Biol Chem,* 282**,** 24707-19.

PAN, X. & HUSSAIN, M. M. 2009. Clock is important for food and circadian regulation of macronutrient absorption in mice. *J Lipid Res,* 50**,** 1800-13.

PAN, X., TERADA, T., IRIE, M., SAITO, H. & INUI, K. 2002. Diurnal rhythm of H+-peptide cotransporter in rat small intestine. *Am J Physiol Gastrointest Liver Physiol,* 283**,** G57-64.

PAN, X., TERADA, T., OKUDA, M. & INUI, K. 2004. The diurnal rhythm of the intestinal transporters SGLT1 and PEPT1 is regulated by the feeding conditions in rats. *J Nutr,* 134**,** 2211-5.

PANDA, S., ANTOCH, M. P., MILLER, B. H., SU, A. I., SCHOOK, A. B., STRAUME, M., SCHULTZ, P. G., KAY, S. A., TAKAHASHI, J. S. & HOGENESCH, J. B. 2002. Coordinated transcription of key pathways in the mouse by the circadian clock. *Cell,* 109**,** 307-20.

PARK, J. E., YI, H., KIM, Y., CHANG, H. & KIM, V. N. 2016. Regulation of Poly(A) Tail and Translation during the Somatic Cell Cycle. *Mol Cell,* 62**,** 462-71.

PARKS, D. J., BLANCHARD, S. G., BLEDSOE, R. K., CHANDRA, G., CONSLER, T. G., KLIEWER, S. A., STIMMEL, J. B., WILLSON, T. M., ZAVACKI, A. M., MOORE, D. D. & LEHMANN, J. M. 1999. Bile acids: natural ligands for an orphan nuclear receptor. *Science,* 284**,** 1365-8.

PEEK, C. B., AFFINATI, A. H., RAMSEY, K. M., KUO, H. Y., YU, W., SENA, L. A., ILKAYEVA, O., MARCHEVA, B., KOBAYASHI, Y., OMURA, C., LEVINE, D. C., BACSIK, D. J., GIUS, D., NEWGARD, C. B., GOETZMAN, E., CHANDEL, N. S., DENU, J. M., MRKSICH, M. & BASS, J. 2013. Circadian Clock NAD+ Cycle Drives Mitochondrial Oxidative Metabolism in Mice. *Science*.

PENDERGAST, J. S., BRANECKY, K. L., YANG, W., ELLACOTT, K. L., NISWENDER, K. D. & YAMAZAKI, S. 2013. High-fat diet acutely affects circadian organisation and eating behavior. *Eur J Neurosci,* 37**,** 1350-6.

POLONSKY, K. S., GIVEN, B. D., HIRSCH, L. J., TILLIL, H., SHAPIRO, E. T., BEEBE, C., FRANK, B. H., GALLOWAY, J. A. & VAN CAUTER, E. 1988. Abnormal patterns of insulin secretion in non-insulin-dependent diabetes mellitus. *N Engl J Med,* 318**,** 1231-9.

POTTHOFF, M. J., KLIEWER, S. A. & MANGELSDORF, D. J. 2012. Endocrine fibroblast growth factors 15/19 and 21: from feast to famine. *Genes Dev,* 26**,** 312-24.

PRASAI, M. J., MUGHAL, R. S., WHEATCROFT, S. B., KEARNEY, M. T., GRANT, P. J. & SCOTT, E. M. 2013. Diurnal variation in vascular and metabolic function in diet-induced obesity: divergence of insulin resistance and loss of clock rhythm. *Diabetes,* 62**,** 1981-9.

PREITNER, N., DAMIOLA, F., LOPEZ-MOLINA, L., ZAKANY, J., DUBOULE, D., ALBRECHT, U. & SCHIBLER, U. 2002. The orphan nuclear receptor REV-ERBalpha controls circadian transcription within the positive limb of the mammalian circadian oscillator. *Cell,* 110**,** 251-60.

PRENTKI, M. & MADIRAJU, S. R. 2008. Glycerolipid metabolism and signaling in health and disease. *Endocr Rev,* 29**,** 647-76.

PREVIS, S. F., BRUNENGRABER, D. Z. & BRUNENGRABER, H. 2009. Is there glucose production outside of the liver and kidney? *Annu Rev Nutr,* 29**,** 43-57.

RAMSEY, K. M., YOSHINO, J., BRACE, C. S., ABRASSART, D., KOBAYASHI, Y., MARCHEVA, B., HONG, H. K., CHONG, J. L., BUHR, E. D., LEE, C., TAKAHASHI, J. S., IMAI, S. & BASS, J. 2009. Circadian clock feedback cycle through NAMPT-mediated NAD+ biosynthesis. *Science,* 324**,** 651-4.

REDDY, A. B., KARP, N. A., MAYWOOD, E. S., SAGE, E. A., DEERY, M., O'NEILL, J. S., WONG, G. K., CHESHAM, J., ODELL, M., LILLEY, K. S., KYRIACOU, C. P. & HASTINGS, M. H. 2006. Circadian orchestration of the hepatic proteome. *Curr Biol,* 16**,** 1107-15.

REPPERT, S. M. & WEAVER, D. R. 2002. Coordination of circadian timing in mammals. *Nature,* 418**,** 935-41.

ROBLES, M. S., COX, J. & MANN, M. 2014. In-vivo quantitative proteomics reveals a key contribution of post-transcriptional mechanisms to the circadian regulation of liver metabolism. *PLoS Genet,* 10**,** e1004047.

RUDIC, R. D., MCNAMARA, P., CURTIS, A. M., BOSTON, R. C., PANDA, S., HOGENESCH, J. B. & FITZGERALD, G. A. 2004. BMAL1 and CLOCK, two essential components of the circadian clock, are involved in glucose homeostasis. *PLoS Biol,* 2**,** e377.

RUSSELL, D. W. 2003. The enzymes, regulation, and genetics of bile acid synthesis. *Annu Rev Biochem,* 72**,** 137-74.

RUSSELL, D. W. & SETCHELL, K. D. 1992. Bile acid biosynthesis. *Biochemistry,* 31**,** 4737-49.

RUTTER, J., REICK, M., WU, L. C. & MCKNIGHT, S. L. 2001. Regulation of clock and NPAS2 DNA binding by the redox state of NAD cofactors. *Science,* 293**,** 510-4.

SAHAR, S. & SASSONE-CORSI, P. 2012. Regulation of metabolism: the circadian clock dictates the time. *Trends Endocrinol Metab,* 23**,** 1-8.

SAMUEL, V. T., PETERSEN, K. F. & SHULMAN, G. I. 2010. Lipid-induced insulin resistance: unravelling the mechanism. *Lancet,* 375**,** 2267-77.

SAMUEL, V. T. & SHULMAN, G. I. 2012. Mechanisms for insulin resistance: common threads and missing links. *Cell,* 148**,** 852-71.

SATO, T. K., PANDA, S., MIRAGLIA, L. J., REYES, T. M., RUDIC, R. D., MCNAMARA, P., NAIK, K. A., FITZGERALD, G. A., KAY, S. A. & HOGENESCH, J. B. 2004. A functional genomics strategy reveals Rora as a component of the mammalian circadian clock. *Neuron,* 43**,** 527-37.

SCHEER, F. A., HILTON, M. F., MANTZOROS, C. S. & SHEA, S. A. 2009. Adverse metabolic and cardiovascular consequences of circadian misalignment. *Proc Natl Acad Sci U S A,* 106**,** 4453-8.

SCHWARZ, M., LUND, E. G., SETCHELL, K. D., KAYDEN, H. J., ZERWEKH, J. E., BJORKHEM, I., HERZ, J. & RUSSELL, D. W. 1996. Disruption of cholesterol 7alpha-hydroxylase gene in mice. II. Bile acid deficiency is overcome by induction of oxysterol 7alpha-hydroxylase. *J Biol Chem,* 271**,** 18024-31.

SCHWARZ, M., RUSSELL, D. W., DIETSCHY, J. M. & TURLEY, S. D. 1998. Marked reduction in bile acid synthesis in cholesterol 7alpha-hydroxylase-deficient mice does not lead to diminished tissue cholesterol turnover or to hypercholesterolemia. *J Lipid Res,* 39**,** 1833-43.

SCHWARZ, M., RUSSELL, D. W., DIETSCHY, J. M. & TURLEY, S. D. 2001. Alternate pathways of bile acid synthesis in the cholesterol 7alpha-hydroxylase knockout mouse are not upregulated by either cholesterol or cholestyramine feeding. *J Lipid Res,* 42**,** 1594-603.

STOKKAN, K. A., YAMAZAKI, S., TEI, H., SAKAKI, Y. & MENAKER, M. 2001. Entrainment of the circadian clock in the liver by feeding. *Science,* 291**,** 490-3.

STORCH, K. F., LIPAN, O., LEYKIN, I., VISWANATHAN, N., DAVIS, F. C., WONG, W. H. & WEITZ, C. J. 2002. Extensive and divergent circadian gene expression in liver and heart. *Nature,* 417**,** 78-83.

STUBBLEFIELD, J. J., TERRIEN, J. & GREEN, C. B. 2012. Nocturnin: at the crossroads of clocks and metabolism. *Trends Endocrinol Metab,* 23**,** 326-33.

SUBTELNY, A. O., EICHHORN, S. W., CHEN, G. R., SIVE, H. & BARTEL, D. P. 2014. Poly(A)-tail profiling reveals an embryonic switch in translational control. *Nature,* 508**,** 66-71.

TAKAHASHI, J. S., KUMAR, V., NAKASHE, P., KOIKE, N., HUANG, H. C., GREEN, C. B. & KIM, T. K. 2015. ChIP-seq and RNA-seq methods to study circadian control of transcription in mammals. *Methods Enzymol,* 551**,** 285-321.

TOH, K. L., JONES, C. R., HE, Y., EIDE, E. J., HINZ, W. A., VIRSHUP, D. M., PTACEK, L. J. & FU, Y. H. 2001. An hPer2 phosphorylation site mutation in familial advanced sleep phase syndrome. *Science,* 291**,** 1040-3.

TONTONOZ, P. & SPIEGELMAN, B. M. 2008. Fat and beyond: the diverse biology of PPARgamma. *Annu Rev Biochem,* 77**,** 289-312.

TSUCHIYA, Y., AKASHI, M. & NISHIDA, E. 2003. Temperature compensation and temperature resetting of circadian rhythms in mammalian cultured fibroblasts. *Genes Cells,* 8**,** 713-20.

TUREK, F. W., JOSHU, C., KOHSAKA, A., LIN, E., IVANOVA, G., MCDEARMON, E., LAPOSKY, A., LOSEE-OLSON, S., EASTON, A., JENSEN, D. R., ECKEL, R. H.,

TAKAHASHI, J. S. & BASS, J. 2005. Obesity and metabolic syndrome in circadian Clock mutant mice. *Science,* 308**,** 1043-5.

UM, J. H., PENDERGAST, J. S., SPRINGER, D. A., FORETZ, M., VIOLLET, B., BROWN, A., KIM, M. K., YAMAZAKI, S. & CHUNG, J. H. 2011. AMPK regulates circadian rhythms in a tissue- and isoform-specific manner. *PLoS One,* 6**,** e18450.

VOLLMERS, C., GILL, S., DITACCHIO, L., PULIVARTHY, S. R., LE, H. D. & PANDA, S. 2009. Time of feeding and the intrinsic circadian clock drive rhythms in hepatic gene expression. *Proc Natl Acad Sci U S A,* 106**,** 21453-8.

VOLLMERS, C., SCHMITZ, R. J., NATHANSON, J., YEO, G., ECKER, J. R. & PANDA, S. 2012. Circadian oscillations of protein-coding and regulatory RNAs in a highly dynamic mammalian liver epigenome. *Cell Metab,* 16**,** 833-45.

WANG, Y., OSTERBUR, D. L., MEGAW, P. L., TOSINI, G., FUKUHARA, C., GREEN, C. B. & BESHARSE, J. C. 2001. Rhythmic expression of Nocturnin mRNA in multiple tissues of the mouse. *BMC Dev Biol,* 1**,** 9.

WEILL, L., BELLOC, E., BAVA, F. A. & MENDEZ, R. 2012. Translational control by changes in poly(A) tail length: recycling mRNAs. *Nat Struct Mol Biol,* 19**,** 577-85.

YAMAZAKI, S., NUMANO, R., ABE, M., HIDA, A., TAKAHASHI, R., UEDA, M., BLOCK, G. D., SAKAKI, Y., MENAKER, M. & TEI, H. 2000. Resetting central and peripheral circadian oscillators in transgenic rats. *Science,* 288**,** 682-5.

YANG, X., DOWNES, M., YU, R. T., BOOKOUT, A. L., HE, W., STRAUME, M., MANGELSDORF, D. J. & EVANS, R. M. 2006. Nuclear receptor expression links the circadian clock to metabolism. *Cell,* 126**,** 801-10.

YOO, S. H., YAMAZAKI, S., LOWREY, P. L., SHIMOMURA, K., KO, C. H., BUHR, E. D., SIEPKA, S. M., HONG, H. K., OH, W. J., YOO, O. J., MENAKER, M. & TAKAHASHI, J. S. 2004. PERIOD2::LUCIFERASE real-time reporting of circadian dynamics reveals persistent circadian oscillations in mouse peripheral tissues. *Proc Natl Acad Sci U S A,* 101**,** 5339-46.

ZHANG, E. E., LIU, Y., DENTIN, R., PONGSAWAKUL, P. Y., LIU, A. C., HIROTA, T., NUSINOW, D. A., SUN, X., LANDAIS, S., KODAMA, Y., BRENNER, D. A., MONTMINY, M. & KAY, S. A. 2010a. Cryptochrome mediates circadian regulation of cAMP signaling and hepatic gluconeogenesis. *Nat Med,* 16**,** 1152-6.

ZHANG, X., VIRTANEN, A. & KLEIMAN, F. E. 2010b. To polyadenylate or to deadenylate: that is the question. *Cell Cycle,* 9**,** 4437-49.

ZHANG, Y. K., GUO, G. L. & KLAASSEN, C. D. 2011. Diurnal variations of mouse plasma and hepatic bile acid concentrations as well as expression of biosynthetic enzymes and transporters. *PLoS One,* 6**,** e16683.